

ANNUAL SUMMARY REPORT

Project Title: P10 Asphalt Fatigue at Queensland Temperatures:
Literature Review and Experiment Design
(Year 1 2013/14)

Project No: 007160

Author/s: Dr Erik Denneman, Jonathon Griffin, Dr Khar Yean
Khoo, Andrew Beecroft, Dr Jeffrey Lee and Dr Laszlo
Petho

Client: Queensland Department of Transport and Main Roads

Date: 25 June 2014

SUMMARY

The literature survey performed as part of Year 1 of this study confirmed the need to improve the models for the prediction of fatigue in asphalt pavements at elevated temperatures. Current fatigue models predict the fastest accumulation of fatigue damage at higher temperatures, while available field data shows that most fatigue damage accumulates in cooler winter months. The analysis of a Federal Highway Administration (FHWA) Accelerated Loading Facility study also indicated that the current Austroads fatigue prediction model may be more conservative at elevated temperatures compared to low and medium temperatures.

The four-point bending test is the standard test for the characterisation of the fatigue performance of asphalt mixes in Australia. The literature review found that the four-point bending test is a suitable test method to characterise the fatigue behaviour of asphalt over a range of temperatures, although there were mixed reports on the suitability of the tests at temperatures over 30 °C. No alternative method was identified that provides significant advantages over the four-point bending test. The proposed test program will therefore be based on four-point bending testing.

The literature review indicated that the low rate of fatigue damage accumulation in asphalt at high temperatures observed in the field and in the laboratory may be due to a number of factors, including slower crack growth due to lower stresses and stiffness and healing of the material. Healing is a function of the number and duration of rest periods, the viscosity of binder and temperature. The literature further indicated that there is at present no well-established method to characterise fatigue and healing properties based on binder testing only. The development of such a method would require a fundamental research program and it would be unlikely to yield results that would be implementable in the short to medium term.

Although the Report is believed to be correct at the time of publication, ARRB, to the extent lawful, excludes all liability for loss (whether arising under contract, tort, statute or otherwise) arising from the contents of the Report or from its use. Where such liability cannot be excluded, it is reduced to the full extent lawful. Without limiting the foregoing, people should apply their own skill and judgement when using the information contained in the Report.

Queensland Department of Transport and Main Roads Disclaimer

While every care has been taken in preparing this publication, the State of Queensland accepts no responsibility for decisions or actions taken as a result of any data, information, statement or advice, expressed or implied, contained within. To the best of our knowledge, the content was correct at the time of publishing.

This page is intentionally left blank

CONTENTS

1	INTRODUCTION	1
1.1	Problem statement	2
1.2	Objectives of the NACOE Project	2
1.3	Structure of the report	2
2	PREDICTING FATIGUE OF ASPHALT PAVEMENTS	3
2.1	Austrroads fatigue prediction model	3
2.1.1	<i>Shell fatigue equation</i>	3
2.1.2	<i>Shift factors in the SPDM</i>	3
2.1.3	<i>Shift factors in the AGPT</i>	5
2.1.4	<i>Design temperature in the AGPT</i>	5
2.2	Mechanistic empirical design guide	7
2.2.1	<i>Design temperature in MEPDG</i>	9
2.3	French pavement design method	10
2.3.1	<i>Asphalt Base Layer</i>	10
2.3.2	<i>Equivalent (design) temperature in the French pavement design method</i>	12
2.4	California Mechanistic Empirical design method	14
2.4.1	<i>Design temperature in CalME</i>	15
2.4.2	<i>Shift factor in CalME</i>	16
2.5	Predictive performance of the fatigue transfer functions	17
3	HIGH TEMPERATURE FATIGUE TESTING OF HOTMIX ASPHALT	18
3.1	Fatigue in asphalt	18
3.1.1	<i>Contributing factors</i>	18
3.1.2	<i>Temperature and strain magnitude</i>	19
3.2	Conventional fatigue characterisation	20
3.2.1	<i>Testing conditions</i>	20
3.2.2	<i>Bending beam</i>	21
3.2.3	<i>Rotating cantilever</i>	21
3.2.4	<i>Indirect tensile</i>	22
3.2.5	<i>Wheel-tracking</i>	22
3.2.6	<i>Direct tensile</i>	23
3.3	High temperature fatigue characterisation	23
3.3.1	<i>Four-point bending</i>	23
3.3.2	<i>Rotating cantilever</i>	27
3.3.3	<i>Indirect tensile</i>	28
3.3.4	<i>Wheel-tracking</i>	29
3.3.5	<i>Comparison of methods</i>	30
3.4	Using dissipated energy to predict pavement fatigue performance	30
3.5	Methods for endurance limit estimation	33
4	ACCELERATED PAVEMENT FATIGUE TESTING	38

4.1	FHWA ALF fatigue study	39
4.2	Pavement material properties – FHWA ALF trial	41
4.2.1	Asphalt.....	41
4.2.2	Crushed granular base.....	42
4.2.3	Prepared subgrade	43
4.3	Back calculation of pavement modulus – FHWA ALF trial.....	43
4.4	Analysis of the FHWA ALF trial results using different methods	44
4.4.1	Analysis A	46
4.4.2	Analysis B.....	48
4.5	Discussion	49
5	HEALING AND REST PERIODS.....	52
5.1	Damage and healing mechanisms	52
5.2	Interaction between rest periods and healing	53
5.2.1	Asphalt properties which affect healing	53
5.3	Consideration of healing parameters in asphalt pavement design.....	54
5.3.1	Rest periods.....	54
5.3.2	Optimum rest period duration	55
5.3.3	Rest period duration and temperature	55
5.3.4	Binder type and healing time	57
5.3.5	Binder ageing and temperature	58
5.3.6	Binder ageing and rest period duration and number.....	61
5.3.7	Damage level at rest period introduction	61
5.3.8	Effect of temperature on surface crack healing.....	62
5.3.9	Effect of filler size	63
6	PROPOSED RESEARCH PROGRAM	64
6.1	Research findings	64
6.2	Hypothesis.....	65
6.3	Methodology	65
6.3.1	Phase 1: Improved characterisation of fatigue at different temperatures: proof of concept	66
6.3.2	Phase 2: testing for general model development.....	67
	REFERENCES	70

TABLES

Table 2.1:	Factors correcting for the combination of intermittent loading, lateral distribution of wheel loads and temperature gradients in the asphalt layer	4
Table 2.2:	Suggested reliability factors (RF) for asphalt fatigue	5
Table 2.3:	Coefficient k_c , adjustment between model and in situ performance	11
Table 2.4:	Standard deviation of the layer thickness	12
Table 2.5:	Coefficient k_s , adjustment to the lack of uniformity of the formation	12
Table 2.6:	Example calculation of the equivalent temperature	14
Table 4.1:	Asphalt volumetric data extracted from FHWA ALF trial.....	42
Table 4.2:	Laboratory combined aggregate specific gravities and per cent absorption	42
Table 4.3:	Moduli of asphalt mixtures from the ITT	42
Table 4.4:	Moduli of unbound granular and prepared subgrade.....	43
Table 4.5:	Calculated tensile strains based on the back calculated moduli	44
Table 4.6:	Pavement configuration for FHWA ALF trial.....	44
Table 4.7:	Summary of analysis A	46
Table 4.8:	Interpolated upper limit to top sublayer of normal granular base	46
Table 4.9:	Material properties used in Analysis A and the calculated tensile strain at the bottom of the asphalt layer.....	47
Table 4.10:	Summary of analysis B	48
Table 4.11:	Tensile strains calculated for the bottom of the asphalt layer	49
Table 5.1:	Effect of healing on three binders as affected by ageing (RTFO and PAV) and temperature	58
Table 6.1:	Preliminary test matrix	68

FIGURES

Figure 1.1:	Load repetitions to failure at different design temperatures	1
Figure 2.1:	Chart for calculation of weighting factor	6
Figure 2.2:	Chart for weighted average temperature of the asphalt mix in the pavement	6
Figure 2.3:	Comparison between fatigue relationships in Shell and MS-1 pavement design methods	8
Figure 2.4:	Temperature distribution for a given analysis period	10
Figure 3.1:	Photograph of a four point bending fatigue testing equipment.....	24
Figure 3.2:	Schematic plots of conventional and modified flexural fatigue test setups.....	24
Figure 3.3:	Fatigue test results at different temperatures	26
Figure 3.4:	Strain-fatigue relationship for asphalt at different temperatures.....	26
Figure 3.5:	ITT setup	28
Figure 3.6:	MMLS3 test equipment at NCAT test track	29
Figure 3.7:	Fatigue life prediction using RDEC approach.....	33
Figure 3.8:	Traditional fatigue representation with low strain behaviour extrapolated.....	34
Figure 3.9:	Determination of the endurance limit using the single-stage Weibull function.....	35
Figure 3.10:	Typical extrapolation to estimate SR (with rest period) at $N_{f w/o RP}$ (PG 64–22, 40F, 4.2% AC, 4.5% Va, 200 microstrain).....	36
Figure 3.11:	SR vs strain at different values of rest period, stiffness, and number of load repetitions.	37
Figure 4.1:	FHWA ALF.....	38
Figure 4.2:	Super single wheel configuration in the FHWA ALF study.....	39
Figure 4.3:	Asphalt pavement structures tested in the FHWA ALF trial (1993–2001)	39
Figure 4.4:	Load passes for cracks to appear at surface of 100 mm thick asphalt sections	40
Figure 4.5:	Load passes for cracks to appear at surface of 200 mm thick asphalt sections	41

Figure 4.6:	Reported number of cycles to failure (crack length of 50 m) during FHWA ALF trial (100 mm asphalt and 560 mm crushed rock section)	45
Figure 4.7:	Reported number of cycles to failure (crack length of 50 m) during FHWA ALF trial (200 mm asphalt and 460 mm crushed rock section)	45
Figure 4.8:	Ratio between the predicted cycles to failure in Analysis A and the fatigue cycles from the FHWA ALF trial	47
Figure 4.9:	Ratio between the tensile strain at the bottom of asphalt obtained from Analysis A and the values reported in the research paper.....	48
Figure 4.10:	Ratio between the predicted cycles to failure in analysis B and the number of cycles to failure from the FHWA ALF trial.....	49
Figure 4.11:	Comparison of the computed number of cycles to failure (Analysis A – AGPT method) and the number of cycles to failure determined from FHWA ALF trial	50
Figure 4.12:	Comparison of the calculated tensile strain at the bottom of the asphalt layer between analysis A and FHWA ALF trial.....	51
Figure 4.13:	Comparison of the calculated tensile strain at the bottom of the asphalt layer between analysis B and FHWA ALF trial.....	51
Figure 5.1:	Example of effect of loading cycle (with and without rest period) on SR.....	55
Figure 5.2:	BOEF setup	56
Figure 5.3:	Example of crack (crack level of 0.9 mm) formation and closure with 3 h rest period at 5 °C: (a) before loading; (b) loading until crack of 0.9 mm achieved; (c) unloading; (d) reloading unit crack of 1.5 mm.....	56
Figure 5.4:	Hypothesis of cracking and healing process: cohesive zone model (CZM)	57
Figure 5.5:	Changes of the intrinsic healing function (R(t)) with time for five SHRP binders (denoted as AAB, AAD, AAM, ABD and AAF) tested in DSR at 25 °C, 10 rad/s and constant strain amplitude of 0.001%.....	58
Figure 5.6:	Comparison of the effect of healing (%) on three binders (PG 64-22, PG 70-22 and PG 76-22) as affected by two ageing conditions (RTFO and PAV) and temperature	60
Figure 5.7:	Effect of healing (%) on three binders (PG 64-22, PG 70-22 and PG 76-22) as affected by temperature and two ageing conditions: (a) RTFO; (b) PAV.....	61
Figure 5.8:	Effect of traverse temperature on flexural strength of asphalt test specimen.....	62
Figure 5.9:	Effect of traverse temperature on healing of asphalt test specimen at outdoor exposure of one month	63
Figure 5.10:	Typical effect of two fillers on stiffness recovery for asphalt specimen over two-hour rest period	63

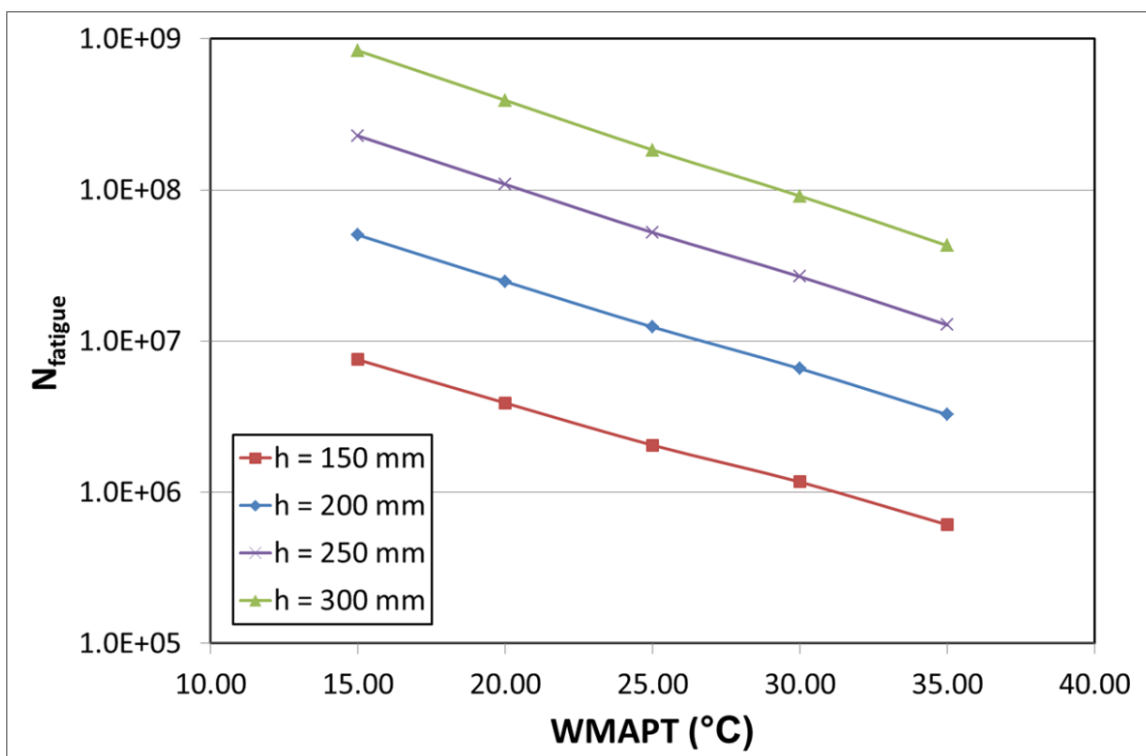
1 INTRODUCTION

Full depth asphalt pavement thicknesses in excess of 400 mm have been used for heavily-trafficked urban road applications in Queensland for many years. One of the reasons for the large thickness is that current pavement design models predict an increased rate of fatigue damage accumulation at high temperatures. This is a consequence of the higher strain levels generated in the pavement at elevated temperatures and the associated exponential reduction in asphalt modulus with temperature. However, this negative correlation between pavement temperature and fatigue resistance does not agree with historical in-service observations.

The issue is illustrated in Figure 1.1, which compares the predicted number of passes of the 80 kN Standard Axle load to fatigue failure ($N_{fatigue}$) with the weighted mean annual pavement temperature (WMAPT) for asphalt pavements of various thicknesses. The fatigue life was calculated using the model in Part 2 of the Austroads Guide to Pavement Technology (AGPT) (Austroads 2012) assuming a subgrade modulus of 70 MPa and a full depth asphalt pavement. The asphalt moduli values were typical of size 14 asphalt with Class 320 bitumen at 25 °C presented in Table 6.13 of the AGPT adjusted for different temperatures using Figure 6.7 in the AGPT.

Figure 1.1 shows that, for a WMAPT of 32 °C (Brisbane), the pavement thickness needs to be approximately 50 mm greater than a pavement in Melbourne (WMAPT of 24 °C) for the same design traffic loading if the AGPT fatigue models are adopted.

Figure 1.1: Load repetitions to failure at different design temperatures



Data from accelerated pavement testing (APT) studies overseas seems to indicate that, in contrast to what the current fatigue models predict, the majority of fatigue damage accumulation occurs at low temperatures rather than at elevated temperatures (Mateos et al. 2012; Pellinen et al. 2004; Stuart, Mogawer & Romero 2002). Factors at play may include the healing of surface cracking and the increased elasticity of the binder at elevated temperatures.

1.1 Problem statement

There is a need to examine whether current pavement design models accurately reflect the nature of fatigue damage accumulation in thick asphalt pavements in Queensland. The development of improved models for predicting the fatigue life of asphalt pavements which better reflect operating conditions in Queensland could result in a significant reduction in the thickness of full depth asphalt pavements. There is also a need to improve the laboratory characterisation of asphalt fatigue at elevated temperatures. It may be necessary for Australia to play a leading role in this research, as fatigue prediction at elevated pavement temperatures is less of a priority in the USA and Europe.

1.2 Objectives of the NACOE Project

In response to these needs, Queensland Department of Transport and Main Roads (TMR) commissioned a project 'Characterisation of Asphalt Fatigue at Queensland Pavement Temperatures' to be conducted by ARRB under the National Asset Centre of Excellence (NACOE) research and development program. This research is fundamental to TMR because of the higher operating temperatures compared to most other Australian States. The successful conduct of this project could also result in significant reductions in the initial cost of asphalt pavements.

The objectives of the first year of this multi-year project are:

- Review the literature and assemble available published data on the laboratory characterisation of the fatigue properties of asphalt mixes at elevated temperatures and the results of field trials, including accelerated loading trials.
- Assess the suitability of the laboratory beam fatigue test at high temperatures (>30°C).
- Assess the influence of rest periods and healing on fatigue.
- Identify possible alternative laboratory test methods.
- Assess the outcomes of the US Federal Highway Administration (FHWA) accelerated loading trials conducted at temperatures of 4°C, 19°C and 28°C.
- Develop hypotheses on how the fatigue prediction models could be improved, this work to be conducted in subsequent years of this project.
- Recommend a laboratory test method for characterisation of fatigue in asphalt mixes at high temperatures
- Prepare a status report on 2013/14 activities, and the proposed program for work to be conducted in 2014/15.

1.3 Structure of the report

This introductory section is followed by an overview of fatigue prediction models for asphalt pavements in Section 2. A discussion of the various available configurations for laboratory fatigue testing is provided in Section 3. The outcomes of accelerated loading trials conducted at different temperatures is discussed in Section 4. The influence of healing and rest periods on fatigue performance is discussed in Section 5. Based on the findings of year one of the study, hypotheses are proposed in Section 6 to be tested in the following years. This section also includes the proposed experimental plan.

2 PREDICTING FATIGUE OF ASPHALT PAVEMENTS

In most conventional flexible pavement design methods fatigue cracking in asphalt is assumed to initiate at the bottom of the asphalt layer. The critical location is where the traffic load-induced horizontal tensile strain is the highest. Models to predict the rate of fatigue damage propagation are typically developed based on laboratory experiments on asphalt specimens subjected to cyclic loading. A shift factor (SF) is applied to relate the results of the laboratory models to field conditions.

This section provides background to a number of fatigue prediction models for asphalt pavements reported in the literature. The incorporation of the effect of temperature in the design methods is discussed to some detail. Finally, published information on the relationship between the predicted fatigue life and observed life under accelerated loading is presented.

2.1 Austroads fatigue prediction model

The fatigue model in the AGPT is based on the relationship in the Shell *Pavement Design Manual* (SPDM) (Shell International Petroleum Company 1978). The Shell models are one of the oldest and most widely used methods to predict the fatigue resistance of asphalt pavements (Pellinen et al. 2004). In this section, background on the development of the SPDM model and its use in the AGPT is provided.

2.1.1 Shell fatigue equation

The SPDM equation was developed based on the results of two and three-point, sinusoidal, displacement controlled, bending tests on 13 mixes (Van Dijk and Visser 1977). The SPDM relationship for fatigue performance of asphalt in laboratory tests is shown in Equation 1. It was proposed in the SPDM, that this equation would be used to calculate the permissible strain in the asphalt (ϵ_{fat}) having a given binder content (V_b) [%] and mix stiffness (S_{mix}) [N/m²] to yield the number of fatigue cycles (N_{fat}) to failure.

$$\epsilon_{fat} = (0.856 \cdot V_b + 1.08) S_{mix}^{-0.36} \cdot N_{fat}^{-0.2} \quad 1$$

The predictive model for asphalt fatigue damage currently contained in the AGPT is shown as Equation 2. The SPDM equation was rewritten to yield the number of allowable load repetitions (N) as a function of the volume of binder (V_b) [%] in the asphalt mix, the modulus (E) [MPa] of the asphalt and the tensile strain ($\mu\epsilon$) at the bottom of the asphalt layer.

$$N = RF \left[\frac{6918 (0.856 V_b + 1.08)}{E^{0.36} \mu\epsilon} \right]^5 \quad 2$$

A reliability factor (RF) is used in the AGPT to relate the laboratory-determined fatigue life prediction model to the predicted in-service fatigue life. In a similar manner to the fatigue models, the RF value incorporates a SF to take account of the differences between laboratory and field conditions as well as a design reliability factor. The SPDM also suggests that a shift function should be used to adjust the results of the laboratory testing to field conditions. This is discussed in the following section of this report.

2.1.2 Shift factors in the SPDM

The SPDM states that the fatigue data obtained in the laboratory cannot be applied directly to thickness design in the field, due to the effect of:

- random load pulses and strain distribution

- intermittent loading with rest periods in between load pulses
- lateral wander of loading
- healing in the asphalt surfacing
- temperature variations in the asphalt layer.

For these reasons, correction factors were introduced to relate the laboratory models to field performance as follows.

- Effect of healing and intermittent loading: the effective fatigue life is increased by a factor of 2-10. The correction factor for open-graded or lean mixes would be on the low side of the range, while the high side of the range would be applied to dense, rich mixes.
- Effect of transverse wander: the effective fatigue life is increased by a factor of about 2.5.
- Effect of temperature distribution in the asphalt pavement: the effective fatigue life is reduced by a factor of 1-3. The lower range of this correction factor is relevant to low-moderate temperature regions and/or thin asphalt pavements. The higher range, on the other hand, is relevant to thick pavements in warm climates.

The ultimate total correction factor was expected to be in the range of 10–20.

The influence of temperature and thickness on the correction factor in the SPDM was subsequently quantified more clearly by Gerritsen and Koole (1987). The correction factors proposed by Gerritsen and Koole are shown in Table 2.1. In the SPDM, mixes were categorised in terms of stiffness, with S1 representing dense basecourses and S2 open-graded mixes. In terms of fatigue performance, F1 represents mixes with moderate bitumen and air void contents and F2 represents mixes with high air void content. It is not known how this categorisation of the mixes applies to asphalt mixes currently used in Australia. The values in Table 2.1 show that the influence of temperature, represented in the table by the weighted mean annual air temperature (wMAAT), on expected fatigue life is greater for thin asphalt pavements than for thick pavements.

Table 2.1: Factors correcting for the combination of intermittent loading, lateral distribution of wheel loads and temperature gradients in the asphalt layer

Thickness of asphalt layer	wMAAT	Mix code			
		S1-F1	S2-F1	S1-F2	S2-F2
mm	°C				
$h_1 < 100$	4	15	15	10	5
	12	20	20	15	10
	20	20	20	15	10
	28	25	25	20	15
$100 < h_1 < 200$	4	15	15	10	5
	12	15	15	10	10
	20	15	15	15	10
	28	15	15	15	10
$h_1 > 200$	4	10	10	10	5
	12	10	10	10	5
	20	10	10	10	5
	28	10	10	10	5

Source: Gerritsen and Koole (1987).

2.1.3 Shift factors in the AGPT

When the SPDM fatigue equation was first included in the AGPT in 1987, no factor was included to correct for the differences between laboratory and field performance. At the time, it was not appreciated that the equation was developed to predict the laboratory fatigue life of asphalt from mix properties and that SFs in the order of 10-20 were proposed by Shell to relate the predicted values to field performance (Austroads 2008).

The fact that the SF had been omitted in the AGPT came to light at some point between the publication of the 1992 Guide, and the draft of the 2001 edition. The need to include a SF was assessed by Jameson (1999). Based on the report by Jameson, the Working Group decided to include a SF of five in a 2001 draft version of the AGPT (Austroads 2008). However, due to concerns that the total thickness of thick asphalt pavements would be significantly reduced through the introduction of the SF, a decision was made to exclude the SF from the 2004 edition of the AGPT. Instead, it was stated in the 2004 edition that the use of a SF of 1.0 would result in a reliability of 95% of the asphalt outlasting the design traffic load. The reliability factor (RF) concept as shown in Equation 2 was introduced. The RF values as contained in the 2012 version of the AGPT (Austroads 2012) are shown in Table 2.2. Note that, as the laboratory model is based on the mean of laboratory result (i.e. a 50% reliability level), an RF of 1.0 does therefore represent a substantial shift in life prediction between laboratory and field.

Table 2.2: Suggested reliability factors (RF) for asphalt fatigue

Desired project reliability				
80%	85%	90%	95%	97.5%
2.5	2.0	1.5	1.0	0.67

Source: Austroads (2012).

2.1.4 Design temperature in the AGPT

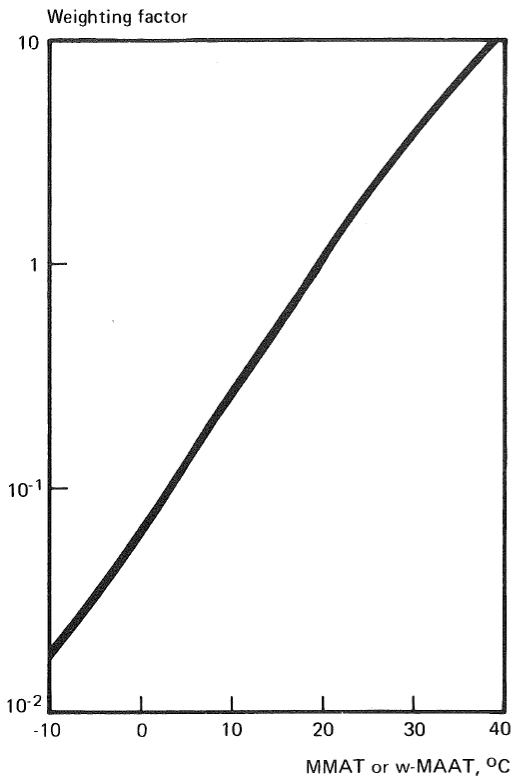
In the AGPT, the temperature regime in asphalt pavements is characterised using the WMAPT. The WMAPT calculation procedure in the AGPT originated from the SPDM (Shell 1978). The WMAPT is used to predict the field modulus and the fatigue life of asphalt pavements. It is a representative temperature value that takes into account the daily and monthly variations in pavement temperature.

The procedure to calculate the WMAPT includes obtaining mean monthly air temperature (MMAT) from a nearby weather station for every month of the year. From the MMAT, a monthly weighting factor is determined using the chart shown in Figure 2.1. The average monthly weighting factors for the year are used in the calculation of the WMAAT using the same chart. In the Shell method different weighting factors are used for the procedures to calculate modulus and fatigue life than for the prediction of permanent deformation. Finally, the temperature of the asphalt in the pavement (WMAPT) is obtained from Figure 2.2. The temperature is dependent on the thickness of the asphalt pavement, with lower temperatures predicted at greater depths.

The AGPT contains a function, rather than a chart, for the calculation of the WMAPT in a 100 mm thick asphalt layer (see Equation 3).

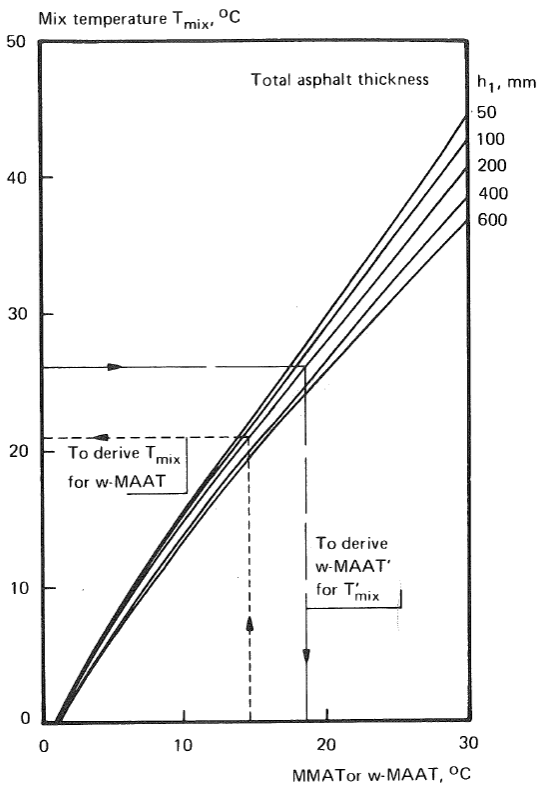
$$WMAPT = -12.4 + \frac{6.32(WMAAT)}{\ln(WMAAT)} \quad 3$$

Figure 2.1: Chart for calculation of weighting factor



Source: Shell (1978).

Figure 2.2: Chart for weighted average temperature of the asphalt mix in the pavement



Source: Shell (1978).

Note that, for pavements thicker than 100 mm, there will be a difference between the WMAPT value calculated using Equation 3 and that determined from the graph. If Equation 3 is used, the WMAPT for Brisbane is 32 °C. However, when determined using the graph, it is 32 °C for a 100 mm thick pavement, 30 °C for a 200 mm thick pavement and 29 °C for a 400 mm thick pavement.

A comparative analysis was performed using a complex stiffness modulus (E^*) master curve developed as part of an Austroads project (Austroads 2013) to determine the modulus values at 32 °C and 29 °C for a AC10 material with Class 320 bitumen. The analysis for a 400 mm thick asphalt pavement on subgrade showed that the predicted number of Equivalent Standard Axles (ESAs) to failure at 29 °C was in the order of 1.8 times larger than at 32 °C.

2.2 Mechanistic empirical design guide

The Mechanistic Empirical Design Guide (MEPDG) (NCHRP 2004) recently introduced in the USA, makes use of the fatigue prediction model developed by the Asphalt Institute (1982). The Asphalt Institute method is based on laboratory fatigue data published by Monismith et al. (1970), which was calibrated against results of the AASHO road test to predict 20% surface cracking (Asphalt Institute 1982). The Asphalt Institute model (in metric unit form) is shown in Equation 4. The relationship 'C' for the influence of binder and air void volume was developed based on work by Epps (1968) and Pell and Cooper (1975).

$$N = 18.4 C (6.167 \cdot 10^{-5} \cdot \varepsilon_t^{-3.291} |E^*|^{-0.854}) \quad 4$$

with

$$C = 10^{4.84 \left(\frac{V_b}{V_v + V_b} \right) - 0.69} \quad 5$$

where

N = number of 80 kN equivalent single axle loads

ε_t = tensile strain in the asphalt layer (mm/mm)

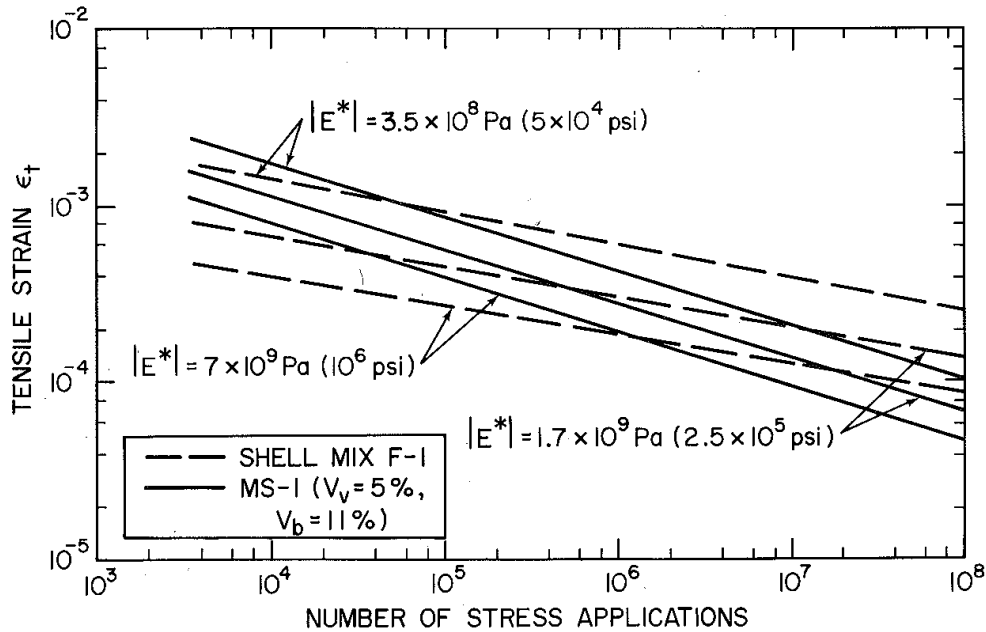
E^* = Dynamic modulus (MPa)

V_b = Effective binder volume (%)

V_v = Volume of air voids (%)

The Asphalt Institute model in its original form provided predictive results similar to the Shell equations, as shown for asphalt mixes of various stiffness values in Figure 2.3.

Figure 2.3: Comparison between fatigue relationships in Shell and MS-1 pavement design methods



Source: Asphalt Institute (1982).

As part of their inclusion in the MEPDG, the field calibration coefficients in the Asphalt Institute method were updated based on additional pavement performance data from 82 long-term pavement performance (LTPP) sections (NCHRP 2004). The final model (in US customary unit form) is shown in Equation 6.

$$N = 4.325 \cdot 10^{-3} \cdot C \cdot k'_1 \cdot \varepsilon^{-3.9492} |E^*|^{-1.281} \quad 6$$

where

- N = number of load repetitions to failure
- ε_t = tensile strain in the asphalt layer (in./in.)
- E^* = Dynamic modulus (psi)
- C = as given in Equation 5
- k'_1 = a correction factor for different asphalt layer thicknesses

For bottom-up cracking, k'_1 is obtained from Equation 7, whilst, for top-down cracking, k'_1 is obtained from Equation 8.

$$k'_1 = \frac{1}{0.000398 + \frac{0.003602}{e^{(11.02 - 3.49 \cdot h_{ac})}}} \quad 7$$

$$k'_1 = \frac{1}{0.01 + \frac{12.00}{1 + e^{(15.676 - 2.8186 \cdot h_{ac})}}}$$

8

where

h_{ac} = asphalt thickness (in.)

Using these equations and Miner's hypothesis (see Section 2.3.2), the relative damage to the pavement is calculated. This is followed by a calculation step to estimate the amount of surface cracking as a percentage of the total lane area using a separate set of calibrated equations. The full set of equations can be found in the report on NCHRP project 1–37 (NCHRP 2004).

2.2.1 Design temperature in MEPDG

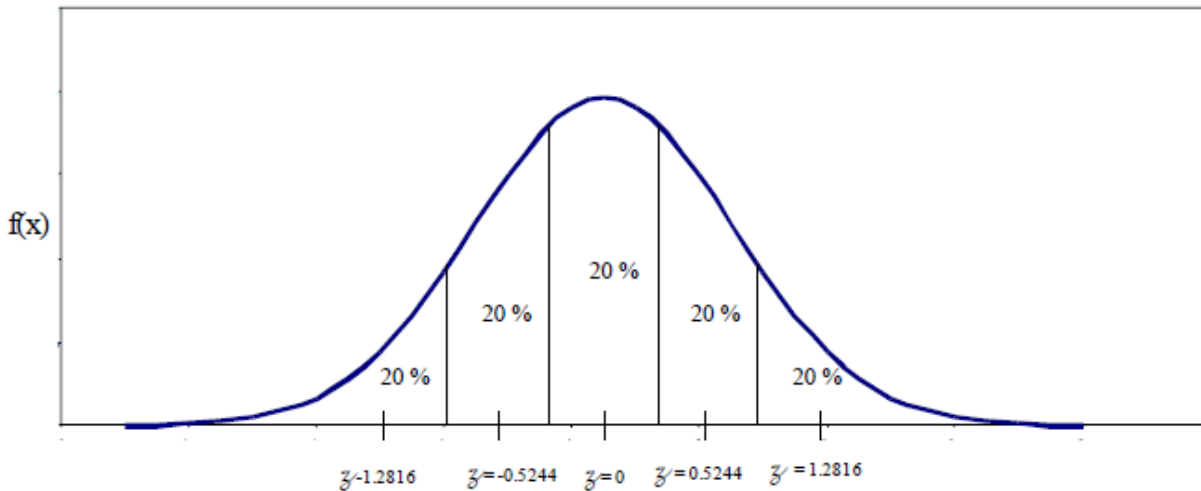
The MEPDG method requires the generation of hourly pavement temperature profiles generated using the Enhanced Integrated Climatic Model (EICM) (NCHRP 2004). The EICM has a range of inputs including weather-related data such as air temperature, precipitation, wind speed, sunshine percentage and relative humidity, as well as groundwater, drainage properties and pavement material information. The pavement temperatures are predicted using temperature data from nearby weather stations.

The user is required to enter a resilient modulus for all unbound material layers at optimal conditions, as a function of time and position. The EICM then runs within the MEPDG software. There are a number of outputs, including an environmental adjustment factor. This adjustment factor is calculated through a range of steps which determine the effects of reaching moisture equilibrium, freezing and thawing, seasonal moisture variations and changes in asphalt layer temperature over time. The environmental adjustment factor can then be multiplied by the optimal resilient modulus to give the overall resilient modulus of the unbound materials, as a function of time and position within the pavement.

Another output is the in situ pavement temperature at the mid-point of each asphalt sub-layer (with estimates of the variability), giving the hourly temperature profile for the asphalt layers.

The frequency distribution of temperatures is assumed to be normally distributed at a given time and depth over an interval (typically one month). This month is then broken into five sub-seasons, representing 20% of the frequency distribution of pavement temperatures (Figure 2.4). The pavement temperatures corresponding to the 10th, 30th, 50th, 70th and 90th percentiles within the month are each overlaid with 20% of the traffic loading in that month. The pavement response and damage accumulation is then calculated for the five resulting combinations of traffic load and temperature condition.

Figure 2.4: Temperature distribution for a given analysis period



Source: NCHRP (2004).

The MEPDG pavement response model incorporates a number of damage mechanisms to model the behaviour of the asphalt pavement under loading. The model calculates strains for all load cases of a given damage increment. The following parameters are considered in these calculations:

- pavement age (by year)
- season (by month)
- load configuration (axle type)
- load level (discrete levels in 1000-3000 lb increments, depending on the axle type)
- pavement temperature (for the dynamic modulus).

2.3 French pavement design method

The discussion in this section is based on the *French design manual for pavement structures* (Laboratoire Central des Ponts et Chaussees 1997), the French design manual for pavement structures, hypotheses and calculation data (LCPC-Setra2 n.d.) and the 2011 version of French standard NF P 98-086 *Road pavement structural design — Application to new pavement*.

2.3.1 Asphalt Base Layer

To prevent fatigue cracking, the allowable horizontal strain in the asphalt base layer $\epsilon_{t,allow}$ is calculated according to Equation 9.

$$\epsilon_{t,allow} = \epsilon_6(10^\circ\text{C}; 25\text{Hz}) \times \sqrt{\frac{E(10^\circ\text{C}; 10\text{Hz})}{E(\theta_{eq}; 10\text{Hz})} \times \left(\frac{NE}{10^6}\right)^b \times k_c \times k_r \times k_s} \quad 9$$

where

$\epsilon_6(10^\circ\text{C}; 25\text{Hz})$ = the fatigue resistance of the asphalt mix, determined at 10^6 loading cycles; in France the test is carried out according to NF EN 12697-24, Annex A at 10°C and 25 Hz

b = is the slope of the fatigue line ($-1 < b < 0$)

- $E(10^{\circ}\text{C}; 10\text{Hz})$ = stiffness of the asphalt material at 10°C and 10 Hz, tested according to NF EN 12697-26, Annex F
- $E(\theta_{eq}; 10\text{Hz})$ = stiffness of the asphalt material at the equivalent temperature θ_{eq} and 10 Hz, tested according to NF EN 12697-26, Annex F
- NE = traffic loading in equivalent standard axles
- k_c, k_r, k_s = adjustment coefficients

Coefficients k_c , k_r and k_s combined form the laboratory to field SF for the equation. The individual components of the SF are discussed below.

Coefficient k_c

The value k_c is a coefficient which adjusts the results of the computation model in line with the behaviour observed on actual pavements. The value of k_c depends on the asphalt type (Table 2.3). The value of k_c can also be used to introduce new technologies; in which case a long-term observation or accelerated loading trial is conducted and the value of k_c is derived from the comparison.

Table 2.3: Coefficient k_c , adjustment between model and in situ performance

Material	k_c value
Road base asphalt concrete (GB in French terms)	1.3
Bituminous concrete (BB in French terms)	1.1
High modulus asphalt (EME in French terms)	1.0

Source: NFP 98-086 (2011).

Coefficient k_r

The value k_r is a coefficient which adjusts the allowable strain according to the calculated risk. The value of k_r depends on the standard deviation of the thickness (S_h) and the standard deviation of the fatigue test (S_N). The value of k_r is calculated according to Equation 10.

$$k_r = 10^{-u \times b \times \delta} \quad 10$$

where

$$\delta = \sqrt{S_N^2 + \left(\frac{c \times S_h}{b}\right)^2}$$

where

- u = variable associated with the risk r (normal distribution)
- b = the slope of the fatigue line ($-1 < b < 0$)
- δ = standard deviation of the distribution of $\log N$ at failure
- S_N = standard deviation of the fatigue test
- S_h = standard deviation of the pavement thickness

c = coefficient linking the variation in strain to the random variation of the pavement thickness; with usual structures c is approximately $0.02 \frac{1}{cm}$

S_h is determined according to Table 2.4.

Table 2.4: Standard deviation of the layer thickness

Thickness of the asphalt layers (m)	$h \leq 0.10$	$0.10 < h < 0.15$	$h > 0.15$
Sh (cm)	1.0	$1+0.3x(h-10)$	2.5

Source: NFP 98-086 (2011).

Coefficient k_s

The value k_s is a reduction coefficient which takes into account the effect of a lack of uniformity in the bearing capacity of a soft soil layer (in French terms the foundation) underneath the treated layers. The value of k_s depends on the bearing capacity (surface modulus) of the formation level (Table 2.5).

Table 2.5: Coefficient k_s , adjustment to the lack of uniformity of the formation

Modulus of the soil	$E < 50 \text{ MPa}$	$50 \text{ MPa} \leq E < 80 \text{ MPa}$	$80 \text{ MPa} \leq E < 120 \text{ MPa}$	$E \geq 120 \text{ MPa}$
K_s	1/1.2	1/1.1	1/1.065	1.0

Source: NFP 98-086 (2011).

It can be seen that in the French pavement design method the SF is a combination of the risk and reliability.

2.3.2 Equivalent (design) temperature in the French pavement design method

Detailed calculation of the equivalent temperature is provided in the French design manual for pavement structures (LCPC 1997), which is discussed in this section. The equivalent temperature is defined according to Equation 11. The calculation of damage accumulation makes use of Miner's hypothesis.

$$\sum_{i=1}^n n_i \times d_i = 1 \quad 11$$

where

n_i = the number of equivalent axle passages undergone by the pavement

d_i = the elementary damage.

The elementary damage is expressed in Equation 12.

$$d_i = \frac{1}{N_i} \quad 12$$

where

d_i = the elementary damage

N_i = the number of loadings causing fatigue failure at a strain level $\varepsilon(\theta_i)$.

By combining Equations 11 and 12, Equation 13 follows.

$$\sum_{i=1}^n \frac{n_i}{N_i} = 1 \quad 13$$

Structural design is performed at a constant temperature, referred to as the equivalent temperature θ_{eq} . This temperature is such that the cumulative damage undergone by the pavement over a year, for a given temperature distribution, is equal to the damage that the pavement would undergo with the same traffic but for a constant temperature θ_{eq} (LCPC 1997). The equivalent temperature is determined by applying Miner's hypothesis (Equation 11) as referred to as in Equation 14.

$$\sum_i \frac{n_i(\theta_i)}{N_i(\theta_i)} = \frac{\sum_i n_i(\theta_i)}{N(\theta_{eq})} \quad 14$$

where

$N_i(\theta_i)$ = is the number of loadings causing failure due to fatigue for the strain level $\varepsilon(\theta_i)$

$n_i(\theta_i)$ = is the number of equivalent axles passages undergone by the pavement at a temperature (θ_i)

$N(\theta_{eq})$ = is the number of loadings causing failure due to fatigue for the strain level $\varepsilon(\theta_{eq})$

θ_{eq} is the equivalent temperature.

Equation 15 is derived from Equation 14 after re-organising the parameters.

$$\frac{1}{N(\theta_{eq})} = \frac{1}{\sum_i n_i(\theta_i)} \left[\sum_i n_i(\theta_i) \left\{ \frac{1}{N_i(\theta_i)} \right\} \right] \quad 15$$

The number of loading cycles $N_i(\theta_i)$ which causes failure can be deduced from the pavement response at a temperature $\varepsilon(\theta_i)$ and the laboratory test results $\varepsilon_6(\theta_i)$ according to Equation 16:

$$N_i(\theta_i) = \left\{ \frac{\varepsilon(\theta_i)}{\varepsilon_6(\theta_i)} \right\}^{1/b} \times 10^6 \quad 16$$

where

$\varepsilon(\theta_i)$ = pavement response at a temperature

$\varepsilon_6(\theta_i)$ = fatigue properties from laboratory test results.

The reciprocal of $N_i(\theta_i)$, as defined in Equation 16, equals, by definition, the elementary damage $d(\theta_i)$ at the strain level $\varepsilon(\theta_i)$ (Equation 17).

$$\frac{1}{N_i(\theta_i)} = d(\theta_i) = \left\{ \frac{\varepsilon_6(\theta_i)}{\varepsilon(\theta_i)} \right\}^{1/b} \times 10^{-6} \quad 17$$

Equation 18 can be derived by the combination of Equation 15 and Equation 17.

$$\frac{1}{N(\theta_{eq})} = \frac{1}{\sum_i n_i(\theta_i)} \left[\sum_i n_i(\theta_i) \left\{ \frac{\varepsilon_6(\theta_i)}{\varepsilon(\theta_i)} \right\}^{1/b} \times 10^{-6} \right] \quad 18$$

The total elementary damage at different temperatures (right side of Equation 18) is calculated; the equivalent temperature (design temperature) θ_{eq} is the temperature where the elementary damage for $\frac{1}{N(\theta_{eq})}$ equals to the total elementary damage at different temperatures.

The value of $\varepsilon_6(\theta)$ can be obtained from laboratory testing or by using the correlation Equation 19 at 10^6 loading cycles (EN 12697-24 2012).

$$\lg(N) = a + \left(\frac{1}{b}\right) * \lg(\varepsilon) \quad 19$$

where

N = number of load cycles

a = constant

b = slope of fatigue line

ε = strain (microstrain).

The temperature distribution is expressed in 5 °C intervals with the relative duration of the designated temperature shown as percentage of a year. It is believed that the duration of the temperature is an actual measure on the length of the period Table 2.6 illustrates an example used during the calculation according to the French design manual for pavement structures (LCPC 1997).

Table 2.6: Example calculation of the equivalent temperature

θ_i (°C)	-5	0	5	10	15	20	25	30
Duration (%)	10	12	18	14	18	18	8	2
ε_t (10^6) – pavement response (microstrain)	24	27	32	40	51	68	98	149
$\varepsilon_6(\theta_i)$ (10^6) - fatigue performance (microstrain)	95	95	94	92	96	100	110	121

Source: LCPC (1997).

The sum of the weighted elementary damage $d(\theta_i)$ is 0.15 in this example. The equivalent temperature is determined by interpolation, where the single elementary damage is equal to this value; this results in an equivalent pavement temperature of 18.7 °C in this example.

The above calculation for the equivalent pavement temperature is based on fundamental mechanics and considers real pavement structure responses and asphalt fatigue properties. The calculation requires detailed input on the pavement temperature distribution; when real and accurate data can be obtained for the pavement structure for a certain climatic environment, it could provide reliable input into the mechanistic pavement design.

2.4 California Mechanistic Empirical design method

The California Department of Transportation (Caltrans 2012) mechanistic empirical design method (CalME) uses an incremental-recursive approach to simulate damage accumulation in asphalt

pavements. In the CalME, fatigue damage to asphalt layers is expressed as a loss of the stiffness of the material. In each consecutive calculation step, the asphalt loses part of its stiffness due to fatigue damage. The effect of the loss in stiffness is to some extent countered by a model that predicts the gain in stiffness due to binder aging with time. Ullidtz et al. (2006a,b) provide the most detailed description of the CalME models available at present. The fatigue damage is represented by a factor, ω , which impacts directly on the value of the dynamic modulus and the modulus master curve of the material as shown in Equation 20. As a result of this formulation, the asphalt pavement loses stiffness as fatigue damage accumulates.

$$\log (E) = \delta + \frac{\alpha \times (1 - \omega)}{1 + \exp(\beta + \gamma \log (tr))} \quad 20$$

where

E = Dynamic Modulus

tr = reduced time in seconds

$\alpha, \beta, \gamma,$
and δ = experimentally determined dynamic modulus master curve constants

ω = fatigue damage calculated from Equation 21

$$\omega = A \times MN^\alpha \left(\frac{\mu\varepsilon}{200 \mu\text{strain}} \right)^\beta \times \left(\frac{E}{3000 \text{ MPa}} \right)^\gamma \times \exp(\delta \times t) \quad 21$$

where

MN = Number of load repetitions in Millions

$\mu\varepsilon$ = the tensile strain at the bottom of the asphalt layer in microstrain

$A, \alpha, \beta,$
 $\gamma,$ and δ = constants determined from four point beam controlled strain fatigue tests
(under haversine load conditions)

t = temperature in °C

Ullidtz et al. (2006a,b) provide alternatives for the fatigue model in Equation 21, which have been excluded from the summary of the method in this report. Equation 21 is calibrated against fatigue results for individual mixes tested at 10 Hz, 20 °C under haversine constant displacement loading. Users of CalME can either use default fatigue properties for mix types from the CalME database, or develop their own mix-specific models through laboratory experiments.

2.4.1 Design temperature in CalME

The CalME method follows the MEPDG method closely in some parts of the design. However, in the case of determining climatic conditions for the design, the EICM module in the MEPDG was considered too slow to make reliable simulations viable (Ullidtz et al. 2010).

As a result, Caltrans initially adopted an alternative method of modelling pavement temperatures and moisture conditions. Six climatic zones were established (which has since been expanded to nine) in which 30 years of EICM data was generated. This database allowed interpolation of

temperatures at various times and depths. However, some issues remained regarding the interpolation of results for the wide range of pavement structures possible.

A new model was developed that used a simplified method, based only on the surface temperature over the course of the day, and the temperature at depth. This calculation can output hourly temperatures at any depth for a wide array of pavement structures, and requires less data storage and a shorter computing time. However, the calculations still require a number of computational steps in order to calculate the heat transfer within the pavement structure.

The calculation steps used in the prediction of damage accumulation are described in the CalME help file (California Department of Transportation 2012). The default duration of each calculation step is 30 days, but this can be changed by the designer. The representative temperature for each calculation step is calculated based on the conditions at the day in the middle of the damage increment. Days are subdivided into five time periods and temperatures at different depths of the pavement structure are calculated. The temperature at the surface calculated by the EICM database is used as the basis for this calculation. The temperature intervals are matched with traffic load conditions from weigh-in-motion (WIM) data.

2.4.2 Shift factor in CalME

The CalME models were calibrated against the results of the WesTrack experiment and heavy vehicle simulator (HVS) data APT testing (Ullidtz et al. 2006a,b). The SF between laboratory results and field data was found to be 3 for HVS testing and between 5 and 15 for the WesTrack experiments.

The CalME software includes a function to calculate the influence of rest periods on the shift factor. The final shift factor value (SF), including the effect of rest period, is determined from the standard shift factor between laboratory and field (SFF) correct for temperature and rest period using Equation 22. The influence of the rest period on SF is dependent on the temperature through the use of the viscosity of the binder. The CalME approach in essence uses the modulus master curve concept, with its reduced time-temperature relationship to calculate the actual rest period between traffic loads. Due to this formulation, the beneficial effect of the rest period will be higher at elevated temperatures.

$$SF = \left\{ 1 + \left[\frac{Rp}{Rp_{ref}} \times \left(\frac{\eta(t_{ref})}{\eta(t)} \right)^{aT} \right]^\varphi \right\} \times SFF \quad 22$$

where

- Rp = Rest period (sec)
- t_{ref} and aT = Modulus master curve parameters
- η(t) = viscosity at temperature t
- Rp_{ref} = constant with default value of 10 sec.
- φ = constant with default value of 0.4

2.5 Predictive performance of the fatigue transfer functions

Pellinen et al. (2004) compared the predictions of various fatigue transfer functions against actual asphalt performance data from the WesTrack experiment. WesTrack is a road test facility in Nevada; different asphalt test sections were subjected to loading by four trucks, 22 hours per day over a 2.5 year period. Pellinen et al. compared the performance of the Shell models, the Asphalt Institute model (which forms the basis for the MEPDG models), a Strategic Highway Research Program (SHRP) model developed by Tayebali et al. (1992) (a predecessor of the current CalME models) and a number of other less well known models. Pellinen et al. concluded that, overall, all laboratory fatigue models provided a poor prediction of the WesTrack performance. This was even the case for a number of local models that were developed based on the WesTrack data. The SHRP model was found to correctly predict survival or failure of test sections in 50% of cases, the Asphalt Institute model in 31% of cases and the Shell model in 28% of cases. By using the recommended field shift factors for the models, the accuracy increased from 50% to 72% for the SHRP models and from 31% to 39% for the Asphalt Institute model. It needs to be noted that a correction of the prediction by the Shell models using the SFs in the SPDM was not attempted in the study.

Every fatigue prediction model evaluated by Pellinen et al. predicted the fastest accumulation of fatigue damage during the warm summer months, as this is when the highest strains occur in the pavement. The actual WesTrack data showed an opposite trend, with the fastest fatigue damage accumulating during winter. This is the main issue with the current fatigue prediction models that the present study is seeking to address.

Ullidtz et al. (2006a), when calibrating the CalME models, also noted that the problem with conventional strain-based, laboratory-based models was that they predicted damage in the form of a reduction in modulus at high temperatures, which was in contradiction to the field data. Ullidtz et al. pointed to the differences in the stress condition between the laboratory and the field to explain this difference. In the laboratory test, the first stress invariant is always tensile, whereas the first stress invariant at the bottom of an asphalt layer will change with temperature and may become compressive at high temperatures.

Mateos, Ayuso and Jauregui. (2011) and Mateos et al. (2012) used the CalME models to analyse accelerated pavement testing (APT) data from the CEDEX full-scale test in Spain. The CEDEX test track is 300 m long and is trafficked by two automatic vehicles. The CEDEX results indicated that the fatigue damage accumulates primarily at medium to low temperatures; this was consistent with other APT studies. Mateos et al. concluded that the CalME models provided an adequate prediction of the temperature effect on fatigue cracking when the temperature dependent SF for the influence of rest periods was used as described in Section 2.4.2. A fatigue prediction model for the asphalt was developed using laboratory fatigue testing. As part of the study, Mateos et al. (2011) showed that, without the use of a temperature dependent SF, the laboratory-based model would not have been successful in predicting the fatigue damage accumulation on the test track.

3 HIGH TEMPERATURE FATIGUE TESTING OF HOTMIX ASPHALT

In this section, the mechanism of fatigue damage to asphalt is discussed. A review of different methods for the characterisation of fatigue behaviour in laboratory experiments is also included.

3.1 Fatigue in asphalt

The importance of managing the onset of fatigue is increasing as higher-strength materials are being used with greater expectations of performance (Campbell 2008). The fatigue performance of metallic components at high temperatures has been the subject of exhaustive exploration. However, the characterisation of the high temperature fatigue behaviour of asphalt has received little attention (Tsai 2001). The lack of investigation may be the result of the generally accepted convention that the highest rates of fatigue damage occur at intermediate temperatures ($\approx 20\text{ }^{\circ}\text{C}$) and at high temperatures ($> 30\text{ }^{\circ}\text{C}$) the principal failure mechanism for bituminous materials is permanent deformation (Tsai 2001). The characterisation of fatigue behaviour at high temperatures can be used to validate currently-employed design methodologies in addition to distinguishing between candidate asphalt mixtures for locations where pavement temperatures are regularly in excess of $30\text{ }^{\circ}\text{C}$.

The fatigue of asphalt is a complex process involving many physics-based interactions and variable properties (Rowe 1993). Fatigue defines the damage and failure of materials subjected to repeated loading (Zhou, Fernando & Scullion 2008). Fatigue resistance defines the capacity of a material to sustain repeated loading without fracture (Tsai 2001). Three conditions are required to stimulate fatigue: adequate tensile strain, fluctuation in stress/strain state and a sufficient number of loading cycles (Campbell 2008).

Fatigue cracking of asphalt is characterised by three distinct stages: crack initiation, resulting from microstructural changes; crack propagation, resulting from the amalgamation of micro-cracks into macro-cracks; and failure, resulting from the propagation of macro-cracks through the cross-section of the structure (Pérez-Jiménez et al. 2010). As crack propagation is the dominant mode consuming most of the fatigue life, it is the subject of most fatigue performance models (Matthews, Monismith & Craus 1993).

Conventionally, fatigue cracking of asphalt has been assumed to initiate at a discontinuity on the underside of the asphalt layer where the repeated back and forth movement results in micro-crack formation followed by very slow progression until an established crack perpendicular to the principle stress is formed. More recent work has shown that fatigue cracking may also commence at the top of the pavement and propagate downward.

Higher temperatures facilitate an increased number of fatigue failure discontinuities (Pell et al. 1961). Additional loading cycles accelerate the propagation of the crack-tip to the surface. Fatigue damage manifests at the pavement surface initially as longitudinal cracks in the wheelpath, followed by the development of an interconnected crack network and finally the dislodgement of material from the surface under traffic. Fatigue cracking is also commonly referred to as crocodile cracking due to the resemblance of the cracking to the pattern on the back of the reptile. Fatigue cracking is a self-accelerating structural failure. Propagation of cracks through the surface allows moisture to enter the pavement system, weakening the underlying materials, and accelerating the deterioration of the structure (NCHRP 2004).

3.1.1 Contributing factors

In order to accurately predict fatigue performance, a comprehensive analysis is required that considers all of the elements contributing to asphalt fatigue (Zhou, Fernando & Scullion 2008).

The fatigue behaviour of an asphalt layer depends on the properties of the mix, operating environment and construction practice. Mix properties that influence fatigue performance include binder type and content, air void content, aggregate gradation, stripping potential and temperature sensitivity in addition to uniformity of properties. Environmental factors include climate, traffic loading magnitude and frequency, subsurface structural support and drainage conditions. Construction influences include compactive effort, material segregation and joint integrity.

As the environment and construction practices are often outside the influence of mix designers, the fatigue resistance of asphalt is approached through the management of material properties. The principal material properties addressed in the design of a fatigue resistant asphalt mix include binder stiffness, aggregate inter-particle friction, air void content, binder content, and voids in mineral aggregate (VMA). As the bituminous matrix bears the significant portion of the applied stresses and strains, the stiffness of the binder significantly influences the tensile capacity. Bulk material stiffness, and the resulting rate of crack propagation, is dependent upon the volume concentration of aggregate, with increased stiffness for increased aggregate volume (Pell et al. 1961). For low-stiffness mixes, or mixes exposed to high temperatures or extended loading durations, the exhibited modulus is also influenced by the type and gradation of the aggregate. Fine particle sizes are more resistant to fatigue as compared to coarser materials (Campbell 2008). The magnitude of strain required for fatigue failure at a fixed number of loading repetitions increases with increasing bitumen content. Therefore, mixes with larger volumes of bitumen provide increased fatigue life (Pell et al. 1961). Air void content significantly influences fatigue resistance as slight increases dramatically reduce fatigue life (Pell et al. 1961).

3.1.2 Temperature and strain magnitude

Temperature and tensile strain magnitude are the most significant influencers of fatigue life. Although both temperature and strain are important factors in determining fatigue performance, tensile strain magnitude is the stronger determinant with respect to fatigue life (Tsai 2001). At high temperatures and fixed strain levels, small increases in temperature result in significant increases in fatigue life due to decreased stiffness and stress. At low temperatures, significant changes in temperature produce insignificant changes in fatigue life (Pell et al. 1961). Temperature fluctuations strongly influence the tensile strains developed in a flexible pavement layer. For a fixed strain magnitude, fatigue life is greater at increased temperatures (decreased stiffness). The increased fatigue resistance results from increased strain capacity at higher temperatures. However, increased temperature also decreases material stiffness, increasing tensile strain magnitude for a fixed magnitude loading. Ultimately, the influence of temperature depends upon the interaction of rates of change for both mixture stiffness and tensile strain magnitude (Tsai 2001). In low-stress conditions, low-stiffness materials endure a greater number of cycles before fatigue failure. In high-stress conditions, high-stiffness materials exhibit the greater fatigue life (ASTM 2008).

The prediction of the fatigue life should be based upon mixture stiffness at the effective pavement temperature to account for the effects of temperature on both the dynamic stiffness and the allowable asphalt strain. The effective temperature is that at which distress development rates are similar to what would be expected from seasonal temperature variations. The effective temperature for fatigue cracking is different from other flexible pavement distresses such as permanent deformation. Therefore, it is ineffective to attempt to determine all the performance properties of an asphalt mix at a single temperature (El-Basyouny & Jeong 2009).

The establishment of the effective temperature has a significant impact on the design and evaluation of asphalt mixes. Whilst the selection of a single test temperature allows for efficient and economical evaluation of mixes (El-Basyouny & Jeong 2009), the performance of the material across the full spectrum of anticipated operating conditions may not be adequately established if only one temperature is assumed. Longer fatigue lives are obtained at high (> 30 °C) temperatures due to non-linear stiffness behaviour (Matthews et al. 1993). Pell et al. (1961) found

that the measured fatigue life was much longer at higher temperatures for a fixed strain magnitude. The apparently longer fatigue life at high temperature is a result of an extremely slow crack propagation rate resulting from low material stiffness (Pell et al. 1961). Lower temperatures facilitate increased crack propagation rates, and reduced fatigue life, due to material shrinkage and reduced strain capacity (Tsai 2001). The magnitude of initial and gradual stress reduction is also greater at higher temperatures (Pell et al. 1961). A temperature gradient exists throughout the specimen, with higher temperatures at the centre as compared to the surface (Pell et al. 1961). The variation in temperature should therefore be considered when evaluating results.

3.2 Conventional fatigue characterisation

Direct determination of fatigue behaviour is required when highly accurate performance estimates are desired, the candidate asphalt mix is only marginally suitable and/or unconventional mixes and materials are being accessed (Asphalt Research Program 1994). Considerable effort and cost is required to define the fatigue behaviour of asphalt mixes using conventional laboratory methods (Matthews et al. 1993). The available testing methods include simple flexure, supported flexure, direct axial, diametrical, triaxial, fracture mechanics and simulative tests (Matthews et al. 1993). However, the most commonly employed fatigue characterisation methods include bending beam and rotating cantilever (simple flexure), indirect tensile (diametrical) and wheel-tracking (simulative) tests. The selection of a fatigue characterisation method should be based upon sensitivity to mixture variables, replication of field loading conditions, prediction accuracy, simplicity, testing duration, implementation ease and equipment cost, in addition to reliability and reproducibility (Asphalt Research Program 1994).

3.2.1 Testing conditions

The conditions of fatigue testing – including temperature, loading duration, loading waveform, rest period and mode of loading – all strongly influence the exhibited behaviour. Laboratory testing for the purpose of developing fatigue life relationships has historically been conducted at temperatures ranging from 5 to 30 °C (Tsai 2001), although there are examples of test programs that used even higher temperatures. For example, Pickett et al. (1978) conducted tests at a maximum temperature of 43.3 °C to develop a SF for asphalt mixes containing sulphur-modified bitumen. Souliman (2012) tested beam specimens at temperatures of up to 38 °C in an attempt to characterise the fatigue endurance limit for asphalt under various conditions.

Fatigue life is also dependent to some extent on loading duration, longer life being observed at higher frequencies (Pell et al. 1961). However, Matthews et al. (1993) found that the type of loading waveform (sinusoidal, trapezoidal, triangular, etc.) had a limited influence on the results. Rest periods have an important effect on fatigue life (Matthews et al. 1993).

The two modes of asphalt fatigue testing are stress-control and strain-control. Controlled-stress testing can also be described as fixed-load testing whilst controlled-strain testing is more accurately described as fixed-deformation testing (Tsai 2001). Controlled-stress testing is preferred for thick (>150 mm thick) asphalt layers where the surface participates in the resistance to deflection (i.e. it is a structural layer). Controlled-strain testing is most commonly used in Australia and is preferred for thin (<80 mm thick) asphalt pavements that do not contribute to the resistance of applied loads (Griffin 2013).

In controlled-stress testing, the fatigue life is independent of temperature: the initiation of cracking increases overall stress and induces a stress concentration at the crack tip, facilitating rapid crack propagation and catastrophic failure. In controlled-strain testing, on the other hand, temperature plays a significant role in fatigue life: crack initiation results in an overall stress decrease and therefore a very slow rate of propagation (Pell et al. 1961).

The energy dissipated per cycle increases with additional cycles with controlled-stress testing and decreases with additional cycles in controlled-strain testing. Controlled-stress testing generally results in conservative estimates of fatigue life, while controlled-strain testing may more accurately model fatigue performance. This is because the approach considers both the crack initiation and the crack propagation phases (Matthews et al. 1993).

3.2.2 Bending beam

The majority of fatigue testing reported in the literature has been conducted using simple flexure tests. The tests involve the repeated application of stress or strain until a pre-defined failure condition is reached (Griffin 2013). The principle types of simple flexure tests are the two-point bending, four-point bending and rotating cantilever tests (Matthews et al. 1993). Two-point and four-point bending are considered to be equivalent means of characterising the fatigue behaviour of asphalt mixes (Asphalt Research Program 1994). The two-point bending test is therefore not discussed in this report.

The four-point repeated flexure test is the most commonly employed method used to evaluate the fatigue properties of asphalt mixes. The Australian Standard method is outlined in Austroads test method AG:PT/T233, *Fatigue Life of Compacted Bituminous Mixtures Subject to Repeated Flexural Bending* (Austroads 2006a). The method consists of subjecting a 390 mm long, 50 mm high and 63 mm wide prismatic beam to repeated haversine load applications at a constant strain level typically ranging between 200 and 1,000 $\mu\epsilon$ at a frequency of 10 Hz. Recent studies have shown that haversine displacement-control testing in four-point bending configurations such as specified in the AG/PT-233 protocol in effect results in a sinusoidal strain response of half the intended amplitude (Denneman 2013). This is an issue currently being addressed as part of a revision of AG:PT/T233. The standard test temperature is 20 °C. The span of a compacted asphalt beam is divided symmetrically by four clamps, with the loading applied via the inner points and the outer points restricting vertical displacement (Griffin 2013). The testing is terminated when the modulus has decreased to half the initial value.

The advantages of the four-point bending test include:

- A fundamental material property is measured directly
- stress- or strain-controlled loading
- failure is initiated in an area of uniform tensile stress free of shear
- the effects of air voids can be evaluated
- the test is reliable and repeatable with minimal specimens required
- the interpretation of the test results is straightforward (Shen & Carpenter 2007).

Additional advantages include equipment availability and powerful yet simple control and data processing software (Shen & Carpenter 2007). The limitations of the method include the intricate specimen generation and the cost and complexity of the testing apparatus. A key limitation of the test equipment for use in this study is the deformation of specimens during testing at elevated temperatures. Asphalt materials have been reported to creep and sag in the four-point bending rig at temperatures above 30 °C (Tsai 2001). However, Souliman (2012) did not report any limitations to the test method, or difficulty when undertaking fatigue testing at temperatures up to 38 °C.

3.2.3 Rotating cantilever

As just discussed, the majority of fatigue characterisation data has been generated using simple flexure tests, including the rotating cantilever method. In the rotating cantilever test, a constant bending moment, free of shear, is applied to the top of the specimen, generating maximum stress at its centre, as far as possible from the stress concentrations at the ends (Pell et al. 1961). A

necked cylindrical specimen is subjected to both stress- or strain-controlled torsional loading applied through a cable and pulley system attached to the end-fitting retaining the head of the specimen (Porter & Kennedy 1975). A uniaxial distribution of tensile and compressive stresses is generated about the vertical neutral axis, the maximum of which occurs within the necked-down portion of the specimen. Loading is applied according to a sinusoidal waveform. A standard testing method for rotating cantilever testing is not currently available. However, standard testing conditions include a loading frequency of 1 000 rpm and a temperature of 10 °C (Tangella et al. 1990). The failure state is reached when the specimen's dynamic stiffness is reduced by a predetermined amount, typically half the initial value.

The advantages of the rotating cantilever test include a long history of use, the ability to directly measure a fundamental material property, and the results can be directly input into currently-available design methodologies (Tangella et al. 1990). Additionally, the rotating cantilever test provides high productivity resulting from increased loading frequencies compared to the other fatigue characterisation methods (Porter & Kennedy 1975). The limitations of the method include only sinusoidal loading can be applied, the need for specialised equipment, the uniaxial stress state, and poor representation of in-service loading conditions (Tangella et al. 1990).

3.2.4 Indirect tensile

Repeated indirect tensile testing (ITT) can be used to characterise the fatigue properties of asphalt mixes. The test is popular within the pavement community owing to its ability to test cylindrical specimens prepared in the laboratory or cores recovered from in-service pavements with minimal modification. Additionally, the equipment required to execute the test is the same employed for indirect tensile resilient modulus characterisation. The test consists of applying a repeated controlled-stress loading following a haversine form to the vertical diametrical plane of a compacted asphalt cylinder (Griffin 2013). Specimens are considered failed when the strain increases to twice the initial value or well-established macro-cracking is apparent. An Australian standard testing method does not currently exist. However, the method outlined by the European Committee for Standardisation in *Test Methods for Hot Mix Asphalt – Part 24: Resistance to Fatigue* (2012) could be employed.

The advantages of ITT include simplicity, the required equipment is identical to resilient modulus and indirect tensile strength testing apparatus, failure is generated in an area of uniform stress, the generated biaxial stress state is more representative of in-service conditions, and testing can be conducted on both laboratory specimens and field cores (Asphalt Research Program 1994). The primary limitations of the method include the ratio of horizontal to vertical stress cannot be varied, the method significantly underestimates fatigue life, the accumulation of permanent deformation and absence of stress reversal, and the inability to conduct strain-controlled testing (Asphalt Research Program 1994). Due to the issues with permanent deformation, testing is typically conducted at a maximum temperature of 20 °C.

3.2.5 Wheel-tracking

Fatigue characterisation using wheel-tracking tests provides the best replication of in-service loading conditions (Tangella et al. 1990). Wheel tracking tests were also performed as part of the development of the SPDM (Shell 1978; Van Dijk & Visser 1977). However, the fatigue relationships in the SPDM are based on flexural beam testing.

Several scaled wheel-track devices are commercially available include the Hamburg, Model Mobile Loading Simulator (MMLS) and AUSTRACK. The method consists of repeated tracking of a loaded wheel over a compacted prism of asphalt material (Tangella et al. 1990). Failure is indicated by the development of cracking covering a predetermined portion of the loading area. A standard method for determining fatigue potential using wheel-tracking devices does not currently exist. However, the standard method outlined in Austroads test method AG:PT/T231, *Deformation*

Resistance of Asphalt Mixtures by the Wheel Tracking Test (Austroads 2006b) can be used as a guide. The asphalt prism is typically supported by a rubber mat to replicate the support provided by the underlying pavement layers (Tangella et al. 1990). The tyre contact area can be varied by adjusting either the load or the tyre pressure. The asphalt prism is typically instrumented with strain gauges, load cells and temperature sensors for the monitoring of loading conditions and the determination of crack initiation and propagation (Tangella et al. 1990). Both stress- and strain-controlled loading can be applied using the wheel-tracking device.

The advantages of the wheel-tracking test include best simulation of field loading conditions, the ability to monitor both crack initiation and crack propagation and the fact that changes in serviceability can be directly assessed (Tangella et al. 1990). In addition, it provides an accurate representation of pavement response due to the dimensional similarity principle (Bhattacharjee & Mallick 2012). Limitations include low productivity due to the speed of the loading wheel, the requirement for specialist equipment, the method does not directly measure a fundamental material property, and the measurement of fatigue behaviour may be difficult with low-stiffness mixtures (high temperature) due to the development of permanent deformation (Tangella et al. 1990).

3.2.6 Direct tensile

A recent addition to the range of available fatigue test methods is the direct tension test using the Asphalt Mixture Performance Tester (AMPT) equipment. This equipment is primarily used to determine modulus master curves for asphalt and to perform permanent deformation tests. A standard test method for a direct tension test using the equipment is currently under development (Federal Highway Administration 2013). The AMPT uniaxial direct tension test has been used in a recent comprehensive NCHRP study into fatigue endurance limits for asphalt (Witczak et al. 2013). In the study it was observed that:

The uniaxial test is more time consuming than the beam fatigue test and requires enormous attention to details. Uniaxial specimens have to be carefully glued to the loading platens and properly aligned in the loading machine in order to avoid improper or premature failure.

This is in-line with experiences with direct tension testing performed on concrete specimens. From an extensive body of work in the field of concrete technology it is known that, due to boundary conditions, eccentricities and stress concentrations, it is near to impossible to perform a true direct tension test on this material (Bazant & Planas 1997). For these reasons, and because the test is not as yet established, the direct tension fatigue test will not be considered for inclusion in this study.

3.3 High temperature fatigue characterisation

3.3.1 Four-point bending

Four-point bending fatigue tests at temperatures above 30 °C have been performed with varying degrees of success. In a comprehensive study of fatigue performance, Souliman (2012) reported on four-point bending fatigue testing at temperatures up to 38 °C with and without rest periods. A photograph of the traditional four-point bending test equipment is shown in Figure 3.1.

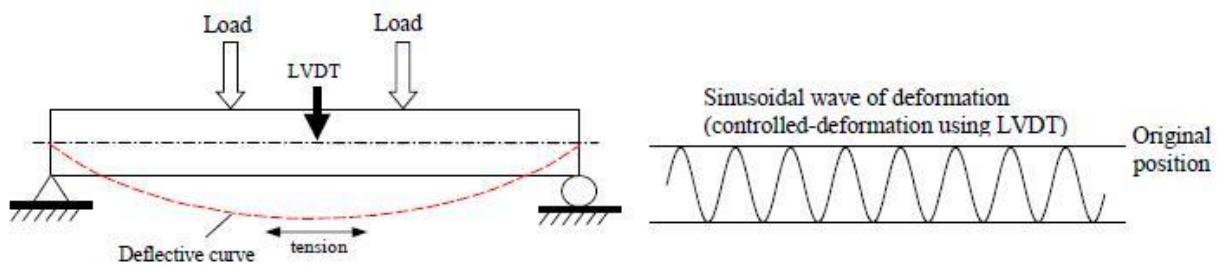
Figure 3.1: Photograph of a four point bending fatigue testing equipment



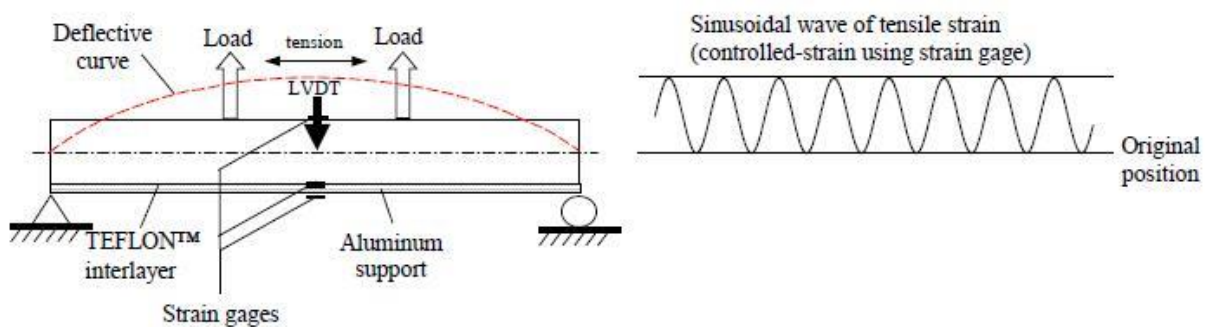
Source: Souliman (2012).

Tsai (2001), on the other hand, investigated the fatigue effects on asphalt mixes at high temperatures (30–40 °C) using a modified four-point bending apparatus to overcome issues related to high temperature flexural beam testing. A schematic diagram comparing the conventional and the modified bending test equipment setup is shown in Figure 3.2.

Figure 3.2: Schematic plots of conventional and modified flexural fatigue test setups.



(a) Conventional flexural fatigue test setup



(b) Modified flexural fatigue test setup

Source: Tsai (2003).

The modified method was based on conventional four-point bending but included a thin Teflon-coated aluminium support beneath the beam to prevent creep, displacement of the beam in the positive versus negative z-direction. Strain levels were controlled using a specimen surface-mounted strain gauge in place of a linear variable differential transducer (LVDT). The beam is deformed according to a shifted sinusoidal wave function where the peak of the wave is at the original unloaded position. Three strain gauges were employed in addition to the standard LVDTs. They were located on the upper and lower surface of the beam specimen in addition to the underside of the aluminium support. The strain gauge at the upper surface of the beam specimen was used as the control gauge. The testing program included two aggregate gradations, two air void contents (6.6 and 11.2%), two test temperatures (30 and 40 °C) and two strain levels (200 and 400 $\mu\epsilon$). A single binder content (5.7%) and a 10 Hz loading frequency were employed (Tsai 2001).

It was concluded that the conventional beam fatigue test was difficult to execute at temperatures in excess of 30 °C due to creeping and sagging of the beam specimens during installation and testing. Reliable fatigue testing data could not be obtained at temperatures above 30 °C using an unmodified four-point bending apparatus. At temperatures below 30 °C the asphalt beams retained sufficient stiffness to maintain the prismatic shape and not deform under their self-weight. Fatigue damage rate, and subsequently fatigue life, was significantly influenced and negatively correlated with the stain magnitude. It was concluded that stiffness was significantly influenced by temperature. However, the fatigue life was insensitive to changes in temperature for specimens tested at 30 and 40 °C. Additionally, the effect of temperature on fatigue life was observed to be more significant on fine-graded mixes compared to coarse-graded mixes. At high temperatures, the fatigue life was greater for fine-graded mixes compared to coarse-graded mixes.

Issues related to the modified four-point bending test for high temperatures included variations in chamber temperature and limits of maintaining strain-control with either the specimen-mounted strain gauge or traditional LVDTs (Tsai 2001). As stated earlier, however, Souliman (2012) did not report any limitations to the test method, or difficulties when undertaking fatigue testing at temperatures up to 38 °C.

In order to illustrate the fatigue behaviour of asphalt in the four-point bending test at different temperatures, Figure 3.3 shows the results for a set of tests performed by ARRB on specimens of AC10 with Class 320 binder. Tests were run in accordance with the Austroads AG:PT/T233 protocol. The data in the figure shows a trend of an increase in fatigue life with an increase in temperature for a limited dataset.

Figure 3.3: Fatigue test results at different temperatures

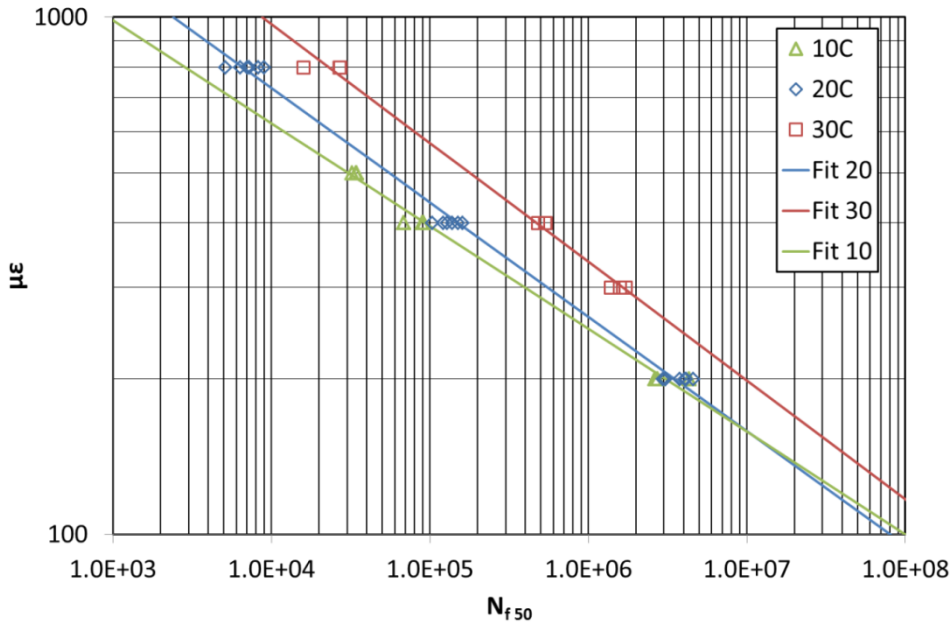
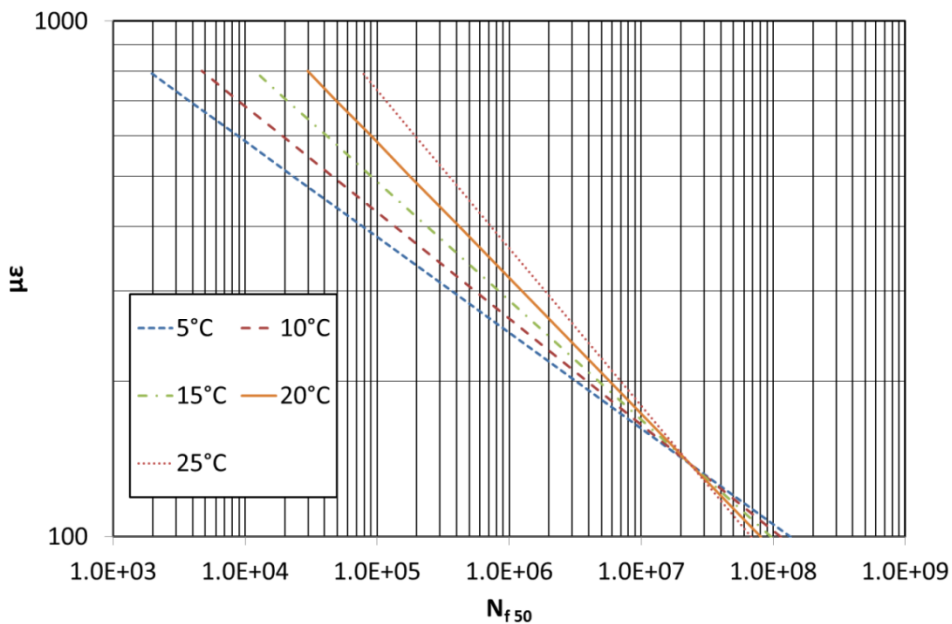


Figure 3.4 shows the relationship between temperature and fatigue performance of asphalt developed based on a large four-point bending test dataset produced by the SHRP-A-404 project run by the University of California at Berkeley (Asphalt Research Program 1994). Tests were run at low to intermediate temperatures to develop the model. Note that the trend of fatigue performance at temperature in Figure 3.4 shows a change in the slope of the fatigue line. The current AGPT fatigue model assumes the slope of the fatigue lines to be the same regardless of stiffness and therefore temperature.

Figure 3.4: Strain-fatigue relationship for asphalt at different temperatures



Source: Asphalt Research Program (1994).

3.3.2 Rotating cantilever

Pell et al. (1961) investigated the fundamental fatigue properties of bituminous mixtures and, in particular, the effects of temperature, loading duration, mix composition, void content, surface finish and rest periods. The researchers also investigated the temperature dependence of fatigue life at constant strain and material behaviour under torsion tests in a constant torsional-strain machine. Fatigue testing was accomplished using a rotating type cantilever machine. Three bituminous mixes were tested:

- a sandsheet material – 85 parts uniformly graded sand, 15 parts limestone filler and 9.5 parts 40/50 penetration bitumen with a target air void content of 3.5%
- a coarse mastic mixture – 67 parts sand, 17 parts limestone filler and 14 parts bitumen with 2.7% air voids
- a fine mastic mixture, 47 parts sand, 25 parts limestone filler and 28 parts bitumen with 1.2% air voids (Pell et al. 1961).

Testing conditions included temperatures of -20, -13.5, -9.5, -0.5, 0, 7, 20, 25, 30 and 40 °C and loading rates of 800, 1000, 1450, 2300 and 3000 rpm. Temperature control was achieved by circulating aqueous alcohol solution around refrigeration or heating elements within a constantly monitored bath.

A linear relationship was observed between log-stress and log-cycles to failure for all investigated temperatures, loading frequencies and stress levels. However, non-linearity may exist at very high stresses. The slope of the log-stress/log-cycles to failure line was independent of temperature and loading frequency. A linear relationship was observed for results plotted in log-strain/log-cycles to failure space, with slightly more scatter than the log-stress/log-cycles to failure plots. Testing time varied from five minutes for the highest stress levels (5.2 MPa) to 28 days at the lowest levels (1.6 MPa). The existence of a fatigue endurance limit was not observed, as all materials failed within 10^8 cycles. Shorter specimens were used at temperatures in excess of 25 °C to increase stability but no influence of the modified specimens on fatigue life was observed (Pell et al. 1961). Failure was according to instantaneous brittle fracture at the centre of the specimen, with the fracture plane contained in the bitumen matrix. At low temperatures (-20, -9.5 and 0 °C), the results were statistically equivalent with a constant failure slope of approximately 45°. At the higher temperatures (15, 30 and 40 °C) the failure surface was more orthogonal.

Pell et al. also found that a sharp increase in temperature preceded rapid crack propagation to failure. The internal temperature of the specimen increased during testing due to hysteresis, resulting in a reduction in material stiffness. The greater magnitude of gradual stress reduction at high temperatures was found to be a function of micro-crack development and not directly as a result of increased temperature. The authors suggested that there were two different failure mechanisms for low and high temperature fatigue. At low temperatures, macro-cracking initiated at a single nucleus which propagated rapidly through the specimen. At high temperatures, micro-cracking developed at a number of nuclei that gradually coalesced to form a macro-crack through repeated loading. Typically, fatigue failure involved a rapid initial reduction in stress, followed by a gradual decrease and then rapid failure.

In summary, crack initiation was a function of the magnitude of the tensile strain and was independent of temperature. The apparent increase in fatigue life at high temperatures was a result of a slower rate of crack propagation, tensile strain in the bitumen was the principle criterion for the initiation of cracking in asphalt materials and fatigue life was temperature dependent, with longer life observed at higher temperatures (Pell et al. 1961).

3.3.3 Indirect tensile

Artamendi, Allen and Phillips (2009) investigated the fatigue performance of asphalt mixes using the indirect tensile fatigue test. The test program included two aggregate gradations, three binder types, two temperatures (10 and 20 °C) and both aged and unaged specimens (Artamendi et al. 2009). The three dense-graded asphalt mixes were a 20 mm mix with 4.1% 40/60 penetration bitumen, a 14 mm mix with 5.3% 10/20 penetration bitumen and a 14 mm mix with 5.3% polymer modified binder (PMB). The target air void content for all of the materials was 4.0%. Material stiffness was characterised by indirect tensile stiffness modulus testing whilst fatigue characterisation was conducted using indirect tensile fatigue. The aging protocol involved five days of oven ageing at 85 °C. A photograph showing the test setup of the ITT is shown in Figure 3.1.

Figure 3.5: ITT setup



Source: Breakah (2009).

Findings of the investigation included (Artamendi et al. 2009):

- aging significantly reduced the fatigue life due to reduced ductility and adhesion
- binder film thickness had a significant influence on the sensitivity of the asphalt to changes in environmental conditions
- indirect tensile fatigue testing conducted at 20 °C rarely resulted in observable fatigue cracking after 10^6 load cycles
- alternative failure modes were generated when using the indirect tensile fatigue test including excessive permanent deformation and shear flow around the loading strip
- indirect tensile fatigue testing can only be conducted according to the controlled-stress mode of loading
- controlled-strain loading is generally adopted for pavement design purposes
- large variability in the applied load was observed at high stresses for high stiffness (low temperature) conditions

- stress evolution cannot be computed due to the measurement of permanent, not resilient, initial strain
- the influence of temperature on fatigue life is a function of binder type and content (binder film thickness)

The authors highlighted concerns regarding the suitability of indirect tensile fatigue testing to characterise the fatigue behaviour of asphalt materials.

3.3.4 Wheel-tracking

Bhattacharjee and Mallick (2012) investigated the combined effect of wheel loading and temperature on asphalt pavement fatigue behaviour in addition to the effect of temperature gradients on strain history. The fatigue performance of an asphalt material was determined using the model mobile load simulator (MMLS) 3. A photograph of a MMLS3 at the NCAT test track is shown in Figure 3.6.

Figure 3.6: MMLS3 test equipment at NCAT test track



Source: Prof. Fred Hugo.

The asphalt consisted of a dense-graded 9.5 mm NMAS aggregate with 5.9% performance graded (PG) 64–28 binder and 4 to 8% air voids. Neoprene pads and a thin steel sheet were used to provide flexible support and minimise rutting respectively. A maximum strain magnitude of $70 \mu\epsilon$ was established to maintain linear viscoelastic behaviour. The temperature, which varied between 15 and 30 °C, was controlled via an environmental chamber. The maximum temperature was limited to 30 °C to retard the development of permanent deformation in the asphalt prism (Bhattacharjee & Mallick 2012).

The findings of the investigation included back-calculated pavement modulus values decreased with increasing temperature. Linear-elastic analysis overestimated stresses and strains at low temperatures and underestimated them at high temperatures. The strain history under wheel loading was defined by three stages, including high rate of increase (primary), moderate rate of increase (secondary) and very high rate of increase (tertiary) leading up to failure. When loading according to stress-control, increased resilient strain indicates the development of damage.

Both bending beam and wheel-tracking methods indicated that the fatigue life decreases with increasing temperature, resilient strain is dependent upon the magnitude and gradient of temperature, and fatigue life is a function of temperature. The stress-controlled wheel-tracking test indicated that the relationship between resilient strain and fatigue life was temperature dependent (Bhattacharjee & Mallick 2012).

3.3.5 Comparison of methods

The four-point bending and indirect tensile testing methods are far more commonly employed for the characterisation of the fatigue properties of asphalt mixes compared to the rotating cantilever and wheel-tracking tests. In fact, standard testing methods for the rotating cantilever and wheel-tracking determination of fatigue behaviour do not currently exist.

The most common fatigue testing methods, including four-point bending and indirect tension, were evaluated to determine sensitivity to mixture variables. Of the testing methods evaluated, only the four-point bending test under strain control was able to identify differences in performance related to bitumen content (Asphalt Research Program 1994). In evaluating reliability according to coefficient of variation and variance amongst replicates, the indirect tensile testing was the most reliable, followed by the four-point bending test. Indirect tensile testing resulted in significantly increased measurements of stiffness and reduced measurements of cycles to failure compared to the four-point bending test. Fundamental differences between indirect tensile and flexural beam testing include allowing the accumulation of permanent deformation and not allowing stress reversal, generally resulting in significantly reduced fatigue life. Both the four-point bending and indirect tensile methods require intricate specimen preparation and the provision of temperature control equipment. Neither method accurately simulates the field loading conditions of asphalt pavements under traffic nor the progressive growth of cracks. However, the SHRP (Asphalt Research Program 1994) researchers selected four-point bending according to strain-control as the preferred method for evaluating the fatigue characteristics of asphalt mixes.

Matthews et al. (1993) evaluated commonly-available fatigue testing methods in order to recommend the most appropriate for defining the performance of asphalt materials. Fatigue testing methods investigated included the four-point bending and indirect tensile methods. The evaluation of test methods was based on simulation of field loading conditions, simplicity and applicability to mix and structural design inputs. The four-point bending test was found to provide a better representation of field loading conditions. The fatigue life measured according to indirect tensile loading was lower than that measured using any alternative method. Due to the accumulation of permanent deformation and lack of stress reversal, the indirect tensile fatigue testing yielded a lower fatigue life. Four-point bending received the highest ranking followed by indirect tensile testing (Matthews et al. 1993).

3.4 Using dissipated energy to predict pavement fatigue performance

In conventional fatigue testing, a certain level of stiffness reduction (typically 50%) compared to the initial stiffness of the specimen is used as the failure criterion. An alternative method, that has a long track record, although mainly for research purposes, is the use of dissipated energy as a failure criterion. There is renewed interest in dissipated energy approaches due to studies of fatigue endurance limits for asphalt. The endurance limit is a critical stress or strain level, below which fatigue damage does not accumulate and the material in theory is able to withstand an indefinite number of load repetitions.

Van Dijk and Visser (1977) introduced the concept of cumulative dissipated energy to failure as a method of predicting fatigue failure in asphalt pavements. Their work was later also incorporated into the SPDM (1978). Dissipated energy is a measure of energy lost as a result of damage to the asphalt specimen. The dissipated energy in four-point bending testing may be determined using Equation 23. This equation defines the dissipated energy as the area under the hysteresis loop.

$$D = \pi\sigma_t\epsilon_t\sin(\varphi)$$

23

where

- D = dissipated energy (J/m³)
- σ_t = tensile stress (Pa)
- ϵ_t = tensile strain (m/m)
- φ = phase angle (°)

Work in the past typically considered that all of the dissipated energy from every hysteresis loop is responsible for the damage. More recently, other researchers considered that only a portion of the dissipated energy is responsible for the actual damage. Damage only occurs when there is a change in area from one hysteresis loop to the next. Therefore, researchers proposed the use of the ratio of dissipated energy change (RDEC) as the indicator to predict the number of cycles to failure (Nf) and the endurance strain limit (Prowell et al. 2010). A typical RDEC curve can be divided into three zones:

1. initial region where damage accumulates rapidly in the material
2. plateau region where a constant RDEC is observed
3. final region where the material begins to fail and there is a rapid increase in RDEC.

Based on data collected during laboratory asphalt fatigue testing, there are a number of techniques typically used to extrapolate fatigue life. Five techniques were reported by researchers including exponential model, logarithmic model, Weibull function, three-stage Weibull function, and RDEC (Prowell et al. 2010).

Different techniques used to extrapolate fatigue life from fatigue bending testing are anticipated to give different number of cycles to failure. This is believed to be due to the difference in definition adopted in each extrapolation technique. Using WesTrack data, Daniel, Bisirri and Kim (2004) compared the number of cycles to failure obtained using different failure criteria. It was found that, in some asphalt mixes, the Dissipated Energy Ratio (DER) method gave a slightly higher number than the others. The DER is defined as change in dissipated energy over the dissipated energy in a particular load cycle ($\Delta DE/DE$).

The main advantage of the DER is in its simplicity and it is applicable for both stress-controlled and strain-controlled fatigue testing for various cyclic loading waveforms (Daniel et al. 2004). Research work using beam fatigue testing reported that this approach works well (Ghuzlan 2001). The main disadvantage of the DER approach is that it cannot be applied to complicated loading histories (i.e. it is only applicable to constant amplitude cyclic loading and requires testing to be performed at a number of amplitudes to fully characterise fatigue behaviour) (Daniel et al. 2004).

Appendix C of Prowell et al. (2010) proposed a standard practise to extrapolate the long-life beam fatigue test data using the ratio of dissipated energy change (RDEC). The method is illustrated in Figure 3.7. It is noted that, at low strain levels, extrapolation is required to determine the number of cycles to failure. A brief outline of the procedure is as follows:

1. Using the power law relationship, obtain a best-fit equation for the Dissipated Energy vs Loading Cycles (DE-LC) data.
2. Calculate the ratio of dissipated energy change (RDEC) as shown in Equation 24.

$$RDEC_a = \frac{DE_a - DE_b}{DE_a * (b - a)} \quad 24$$

where

- RDEC_a = average ratio of dissipated energy change at cycle a, compared to the next cycle b
- a,b = load cycle a and b, respectively; the typical cycle count between cycle a and b for RDEC calculation is 100, i.e., b - a=100
- DE_a,DE_b = dissipated energy (kPa) produced in load cycle a and b, respectively

3. Calculate plateau value (PV) as shown in Equation 25.

$$PV = \frac{1 - \left(1 + \frac{100}{Nf_{50}}\right)^f}{100} \quad 25$$

where

- f = slope from the regressed DE-LC curve (kPa/cycle)
- Nf₅₀ = 50% stiffness reduction failure point

4. For $|f| < 0.25$, calculate PV and Nf₅₀ as shown in Equation 26 and Equation 27.

$$PV = \frac{1 - \left(1 + \frac{100}{Nf_{50}}\right)^f}{100} \approx -\frac{f}{Nf_{50}} \quad 26$$

where

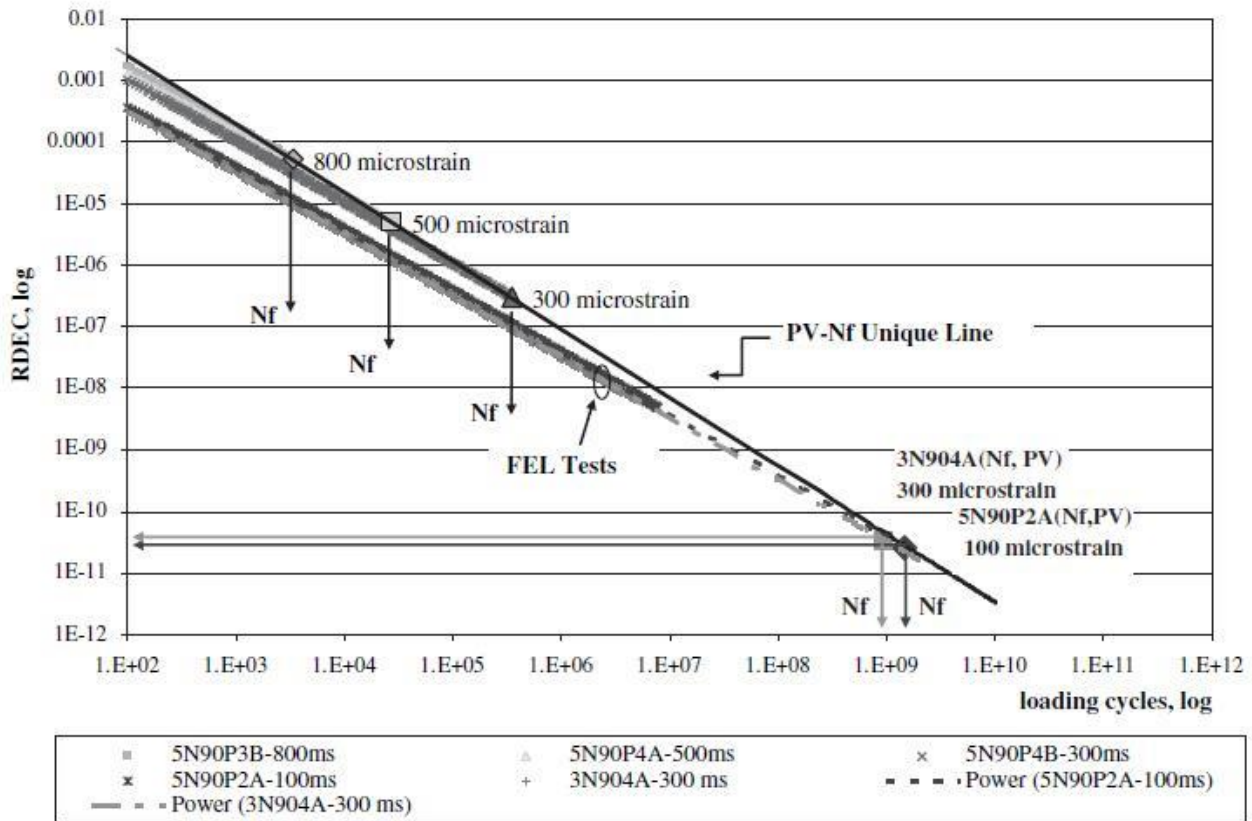
- f = slope from the regressed DE-LC curve (kPa/cycle)
- Nf₅₀ = 50% stiffness reduction failure point

$$Nf_{50} = \left(\frac{-f}{0.4428}\right)^{-9.0744} \quad 27$$

where

- f = slope from the regressed DE-LC curve (kPa/cycle)
- Nf₅₀ = 50% stiffness reduction failure point

Figure 3.7: Fatigue life prediction using RDEC approach.



Source: Prowell et al. (2010).

3.5 Methods for endurance limit estimation

The fatigue endurance limit for asphalt pavements is usually defined as the strain level, at a given temperature, below which no bottom-up fatigue damage occurs in the asphalt mix. Over the past decade a number of laboratory fatigue tests methodologies have been proposed to determine the endurance limit.

Appendix A of Prowell et al. (2010) proposed a standard practise for predicting the endurance limit of asphalt. The procedure involves undertaking beam testing at specified strain levels to confirm endurance limit behaviour. Log-log extrapolation is then used to predict the endurance limit. A brief outline of the procedure is as follows:

1. Separate test specimens into three groups. Determine the number of cycles to failure by testing at 300, 500 and 800 $\mu\epsilon$. Failure is defined as when the stiffness reaches 50% of the initial stiffness value.
2. Transform beam fatigue data by taking the log (base 10) of both the microstrain level and the cycles to failure. Then, use linear regression to determine the microstrain level which corresponds to a fatigue life of $(\log_{10} 50,000,000)$ cycles. Designate the microstrain value as y_0 . The one-sided lower 95% prediction interval can be calculated as shown in Equation 28.

$$\text{Lower Prediction Limit} = \hat{y}_o - t_\alpha s \sqrt{1 + \frac{1}{n} + \frac{(x_0 - \bar{x})^2}{S_{xx}}}$$

Where

t_α = value of t distribution for $n - 2$ degrees of freedom = 1.89458 for $n = 9$ with $\alpha = 0.05\%$

S = estimate of standard deviation from the regression analysis

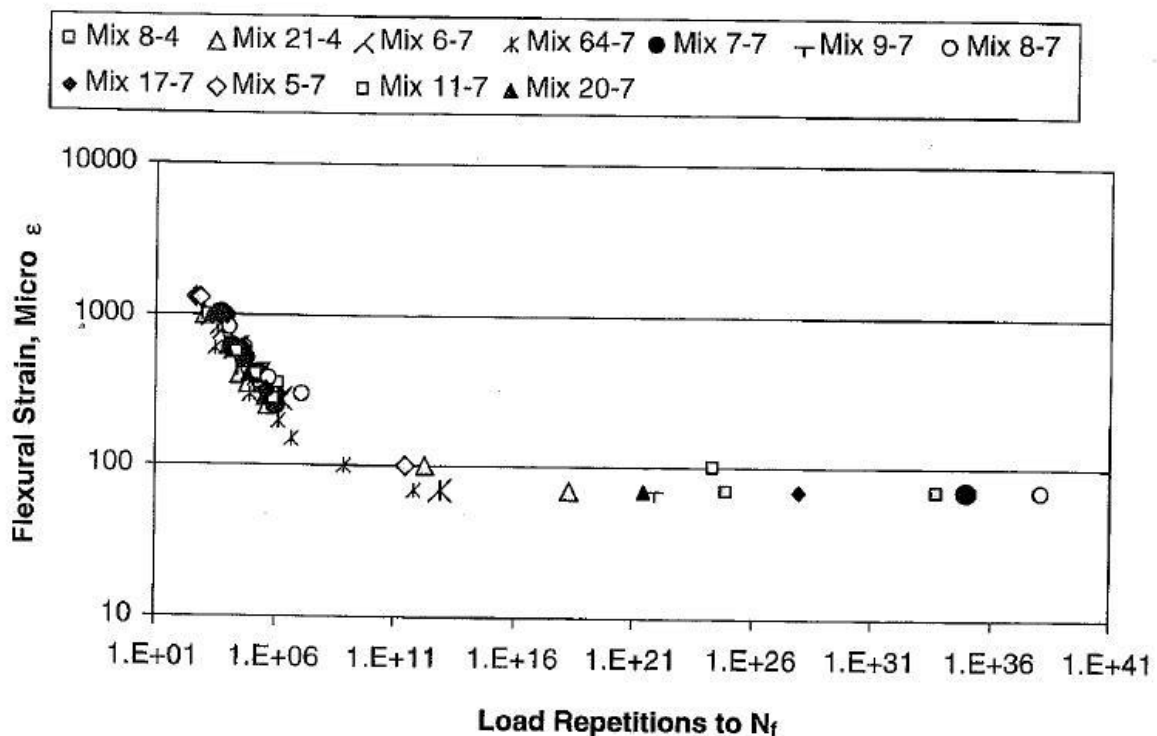
$$S_{xx} = \sum_{i=1}^n (x_i - \bar{x})^2$$

x_0 = $\log 50,000,000 = 7.69897$

\bar{x} = average of the fatigue life results from beam fatigue testing

Another example of extrapolating the result of fatigue testing to estimate the fatigue endurance limit is the work by Carpenter, Ghuzlan and Shen (2003). Two specimens were tested to 38 million and 46 million load repetitions while the remaining specimens were tested to 5 or 8 million load repetitions. The results were then extrapolated to the low-strain range as shown in Figure 3.8. The researchers indicated that the endurance limit varied with different asphalt mixes.

Figure 3.8: Traditional fatigue representation with low strain behaviour extrapolated



Source: Carpenter et al. (2003).

A number of extrapolation techniques are available to confirm the existence of the endurance limit, e.g. the single-stage or the three-stage Weibull survivor function. Based on the single-stage Weibull survivor function, the final form of the equation is shown in Equation 29.

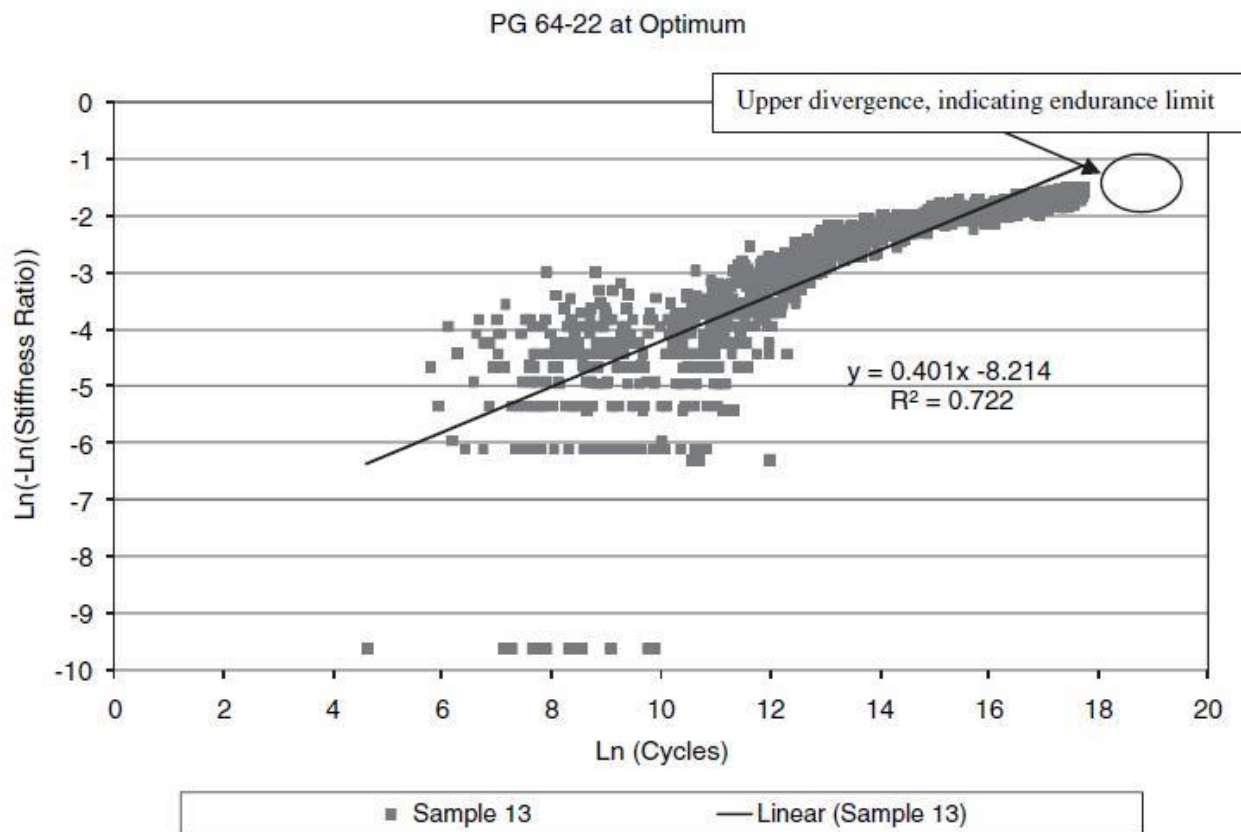
$$\ln(-\ln(SR)) = \ln(l) + \gamma \times \ln(n) \tag{29}$$

Where

- SR = stiffness ratio
- l = scale parameter (intercept)
- γ = Shape parameter (slope)

When left-hand-side of Equation 29 is plotted against the natural logarithm of the number of cycles, n , a straight line regression can be determined. Prowell et al. (2010) proposed that this could be used to confirm the endurance limit through the divergence of the test data as illustrated in the example shown in Figure 3.9.

Figure 3.9: Determination of the endurance limit using the single-stage Weibull function

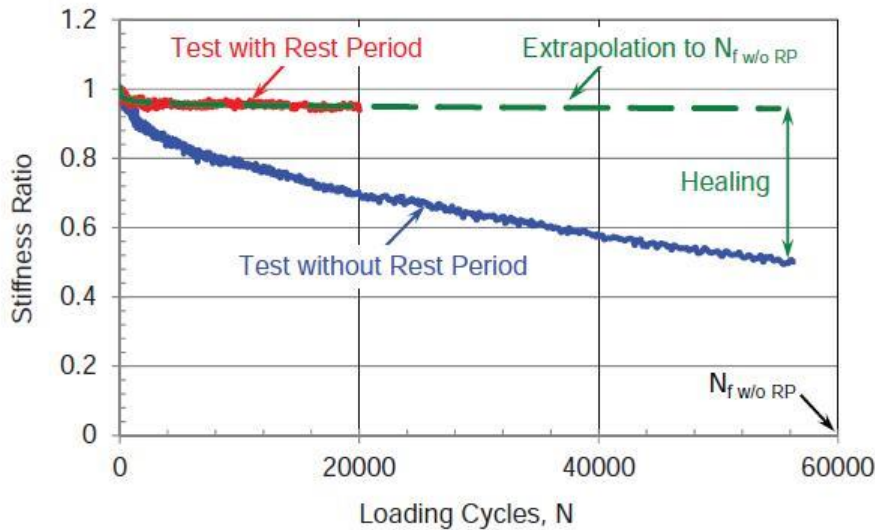


Source: Prowell (2010).

A way of determining the endurance limit for fatigue tests containing rest periods was reported by Witczak et al. (2013). The research indicated success in estimating the endurance limit based on both beam fatigue and uniaxial fatigue tests. Based on the beam fatigue test results, plots of the stiffness ratio (SR) versus log (base10) strain, the endurance limit can be determined graphically for specimens with different initial asphalt mix stiffnesses (E_0) and rest periods. The SR is defined as the ratio between the current stiffness and the initial stiffness. A typical plot of SR vs log (N) is

shown in Figure 3.10. It is noted that, in order to reduce the testing time for test with rest period, sensitivity analysis was conducted to confirm that it is adequate to use the first 20 000 cycles to extrapolate up to 200 000 cycles.

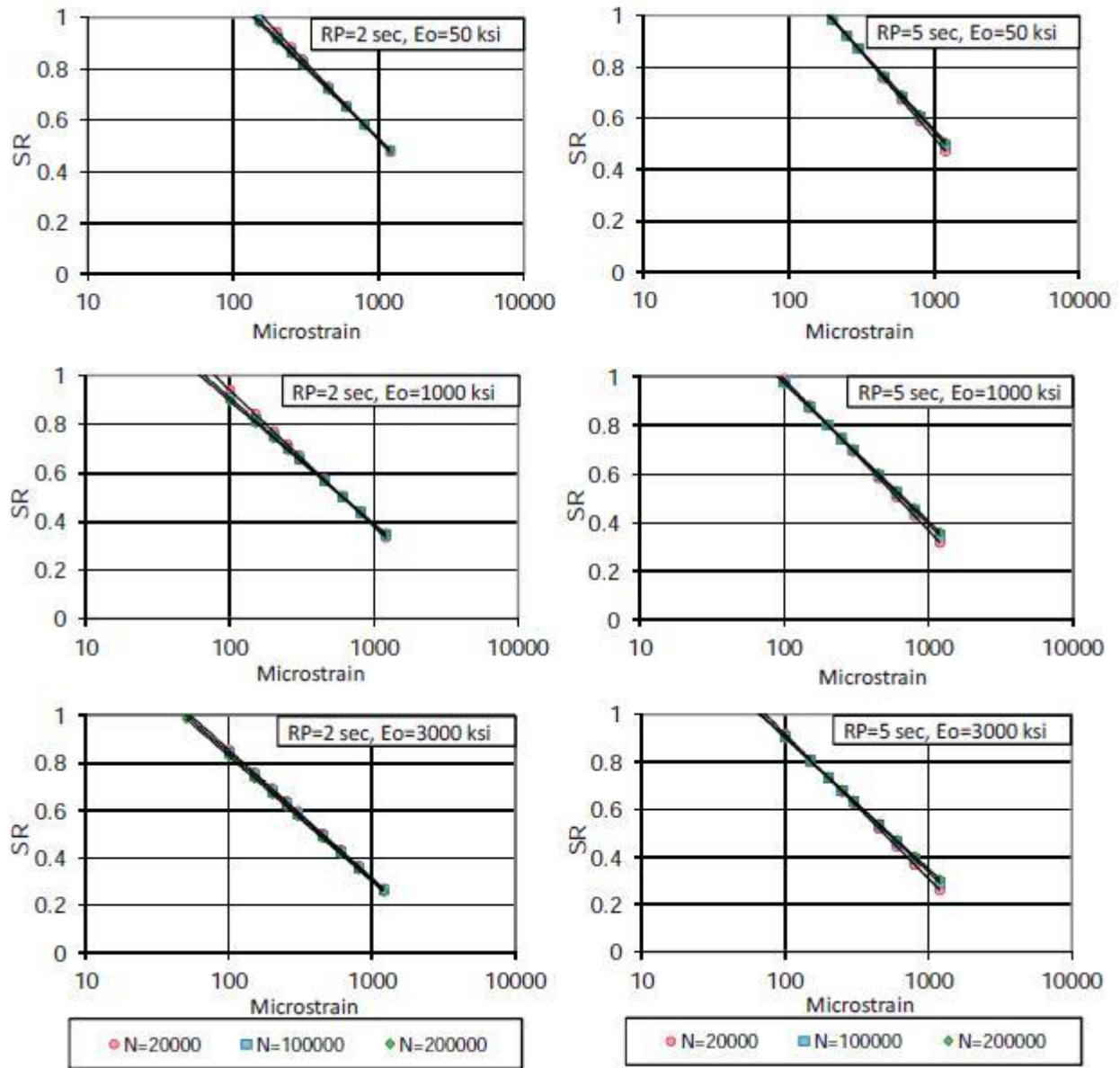
Figure 3.10: Typical extrapolation to estimate SR (with rest period) at $N_{f\ w/o\ RP}$ (PG 64–22, 40F, 4.2% AC, 4.5% Va, 200 microstrain).



Source: Witczak et al. (2013).

Based on pilot beam fatigue testing, the strain levels at each temperature were chosen so that the fatigue life was approximately 20 000 cycles at the high strain level, and approximately 100 000 cycles at the low strain level for tests without a rest period. Examples showing the determination of endurance limits from this research are illustrated in Figure 3.11. The endurance limit is the microstrain level which corresponds to a SR of 1.0 for a particular set of testing condition.

Figure 3.11: SR vs strain at different values of rest period, stiffness, and number of load repetitions.



Source: Witczak et al. (2013).

4 ACCELERATED PAVEMENT FATIGUE TESTING

Asphalt fatigue performance has been the topic of investigation in various accelerated pavement testing (APT) studies. In Australia, fatigue trials were performed in the 1990s using the Accelerated Loading Facility (ALF). The fatigue performance of two asphalt mixes was compared as part of an Austroads pilot study (Foley et al. 1998). Apart from several other APT device studies of limited scope, the influence of temperature on fatigue performance has been studied mainly on test tracks, such as the Westrack and CEDEX studies mentioned earlier in this report. In test track studies, there is no option to test at a constant temperature.

An overview of APT asphalt fatigue studies can be found in a summary report on significant findings from APT (Steyn et al. (2012)). Possibly the most extensive full-scale fatigue experiment at constant temperatures was performed by the US Federal Highway Administration (FHWA) using the ALF equipment shown in Figure 4.1. The results of this study as reported by Stuart et al. (2002) will be discussed to some detail in this section and the fatigue performance in the tests will be compared to the predictions made using pavement design models.

Figure 4.1: FHWA ALF



Source: Steyn et al. (2012).

Figure 4.2 is a photograph showing the wheel load configuration used in the study. The ALF was operated under the following operating parameters:

- Super single tyre
- Load of 53.0 kN and tire pressure of 690 kPa
- Speed of 18.5 kph
- Full wheel wander with a width of 1070 mm
- Wheelpath length of 10.0 m
- Controlled pavement temperatures of 10, 19 and 28 °C.

Figure 4.2: Super single wheel configuration in the FHWA ALF study



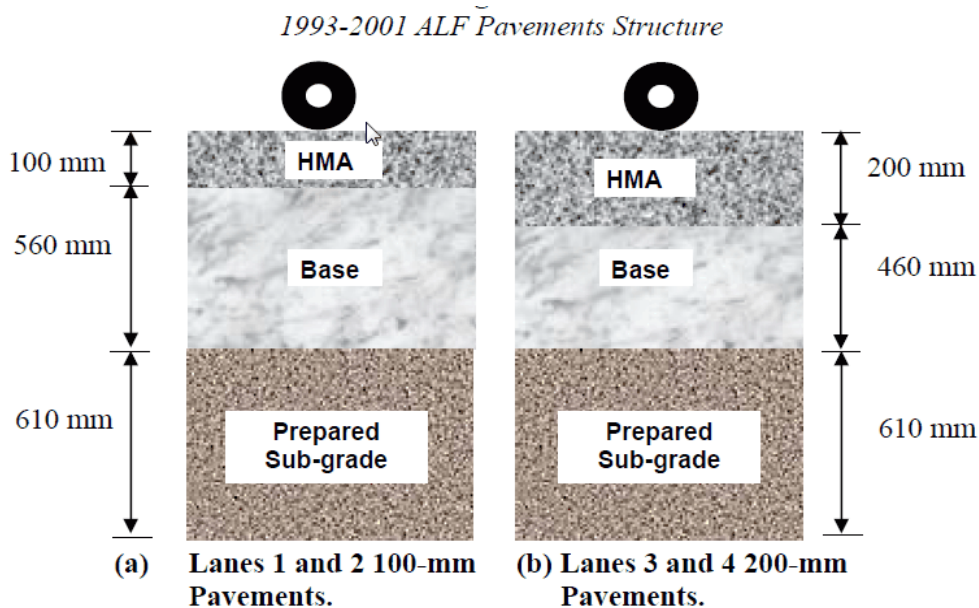
Source: Stuart et al. (2002).

4.1 FHWA ALF fatigue study

In the period from 1994 to 2000, 12 full scale pavements were tested for fatigue cracking resistance using the ALF at the Turner-Fairbank Research Centre in McLean, Virginia. The aim of the study was to validate the fatigue cracking parameter used in the Superpave performance grade binder selection system (Stuart et al. 2002).

An asphalt material with a ‘soft’ bitumen and one with a ‘hard’ bitumen were tested in the study. The pavement configuration consisted of a 100 mm asphalt layer on a 560 mm thick granular base, or 200 mm asphalt on 460 mm granular material. Fatigue experiments on these pavements were performed at controlled temperatures of 10 °C, 19 °C and 28 °C. The pavement configurations are shown in Figure 4.3.

Figure 4.3: Asphalt pavement structures tested in the FHWA ALF trial (1993–2001)



Source: Al Khateeb et al. (2008).

The pavement surfaces during trafficking were heated using infrared lamps attached to the ALF frame. For the 100 mm thick asphalt pavement layers in lanes one and two, thermocouples were used to measure the temperature at depths of 20, 50, and 100 mm. For the 200 mm thick asphalt pavement layers in lanes three and four, thermocouples were used to measure the temperature at depths of 20, 100, and 190 mm. The pavements were heated to the required pavement temperature at mid-depth because Superpave recommended that the temperature at mid-depth be used to represent the temperature of a pavement for fatigue cracking analysis. Thermocouple temperature probes were placed 50 mm outside the wheelpath.

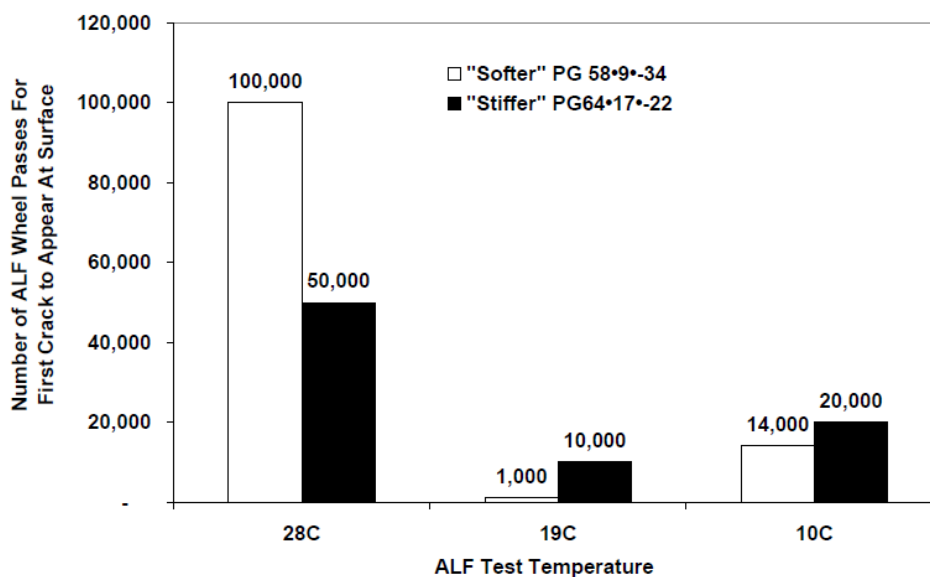
The average mid-depth pavement temperatures were 9, 18, and 29 °C for the 100 mm thick pavements and 9, 18, and 28 °C for the 200 mm thick pavements. The 95-percentile confidence limits ranged from ±2 to ±5 °C (Stuart et al. 2002).

The asphalt layer was heated over the full depth such that the average difference in temperature from the surface of the pavement to the bottom of the pavement different by a maximum of 2 °C for the 28 °C test temperature for the 100 mm thick pavement. For the 200 mm pavement, there was a difference of 3 °C at the 28 °C test temperature. This uniform condition is unlikely to be found in practice where there will be a gradient of temperature from top to bottom that varies during the diurnal cycle and seasonally.

The APT results in terms of the number of load passes for the first crack to appear at the surface in the 100 mm and 200 mm thick asphalt sections are shown in Figure 4.4 and Figure 4.5 respectively. The results indicate that, for both thicknesses and both bitumen types, there was a dip in the number of load repetitions to failure at the intermediate 19 °C temperature. The fatigue life was significantly higher at 28 °C, but at 10 °C, the fatigue performance was also better than at 19 °C.

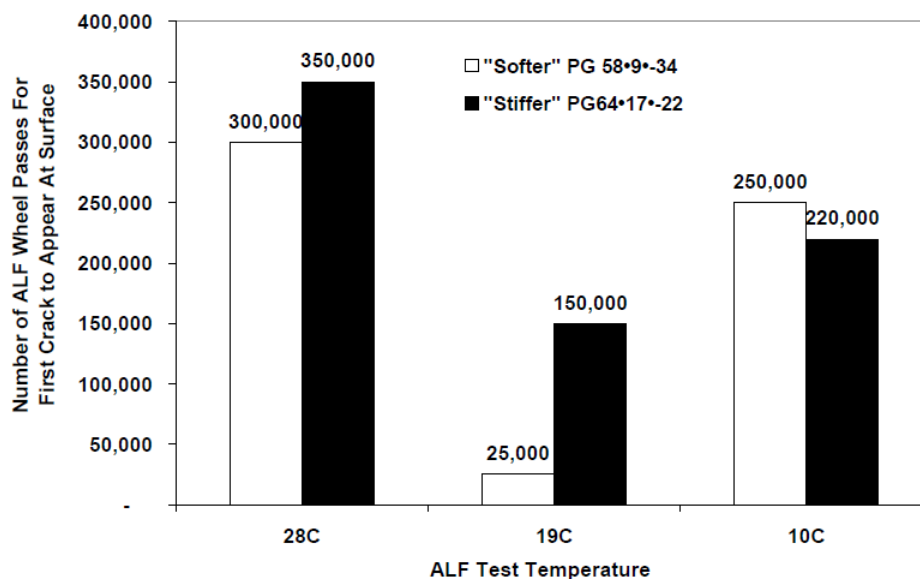
The project also sought to validate the hypothesis that softer binders provide better fatigue performance in thin layers, whereas harder binders provide better performance in thick layers. This hypothesis was only partially supported by the results.

Figure 4.4: Load passes for cracks to appear at surface of 100 mm thick asphalt sections



Source: Gibson et al. (2012).

Figure 4.5: Load passes for cracks to appear at surface of 200 mm thick asphalt sections



Source: Gibson et al. (2012).

It needs to be noted that all the pavements were constructed in 1993, and the 28 °C sections were tested first (from 1994 to 1996) the 19 °C sections were tested from 1996 to 1997 and the 10 °C section finally were tested from 1997 to 2001 (Stuart et al. 2002). The freshness of the binder at the time when the 28 °C experiments were performed may have had a positive influence on the fatigue performance of the material.

Laboratory samples of the asphalt material used in the ALF trial was also subjected to four-point bending beam testing. The laboratory fatigue data did not show the pessimum in fatigue performance at 19 °C. The best fatigue performance was obtained at 28 °C and the worst at 10 °C (Al-Khaheeb et al. 2008). This is in line with the trends of the four-point bending results shown in Figure 3.3 and Figure 3.4. The ranking of the laboratory performance of the mixes at 10 °C and 19 °C is also not necessarily in contradiction to the field results at those temperatures. Mechanistic analysis and comparison of the stress and strain condition in the unsupported laboratory beam specimens versus the supported asphalt layer in the field trials is required to further assess the relative fatigue performance.

4.2 Pavement material properties – FHWA ALF trial

The focus of the FHWA study was to evaluate the field performance of Superpave asphalt mixes under different pavement temperatures. While temperature sensors were installed in the test pavements, strain gauges were not installed underneath the asphalt layer to monitor the tensile strain during the tests. In this section, some key material properties for the asphalt, crushed rock base and subgrade are presented. Other material properties not covered here can be found in the original FHWA publication (Stuart et al. 2002).

In the study, pavements of different configurations were constructed along four lanes and each lane comprises a maximum of four test sections. Lane 1 and Lane 3 were constructed using the 'softer' binder and Lane 2 and 4 were constructed using the 'stiffer' binder.

4.2.1 Asphalt

The asphalt mixes were designed according to the Superpave specifications. Some key volumetric and aggregate density properties are shown in Table 4.1 and Table 4.2.

Table 4.1: Asphalt volumetric data extracted from FHWA ALF trial

	Volumetric information				
Lane	Asphalt Binder Content (%)	Maximum Specific Gravity	Air Voids (%)	VMA (%)	VFA (%)
Lane 1	4.7	2.686	3.2	14.3	77.6
Lane 2	4.8	2.686	2.3	13.6	83.1
Lane 3	4.8	2.678	2.6	14.1	81.6
Lane 4	4.9	2.692	2.9	14.1	79.3

Source: Stuart et al. (2002).

Table 4.2: Laboratory combined aggregate specific gravities and per cent absorption

	Combined aggregate data
Bulk dry	2.892
Bulk SSD	2.916
Apparent	2.961
% absorption	0.8

Source: Stuart et al. (2002).

The reports on the FHWA experiments showed that an asphalt binder content of between 4.7 and 4.9% (by mass) was used. Based on the volumetric data provided in the original FHWA report, the total asphalt binder content (by volume) was calculated to be between 12.2 and 12.7%.

The FHWA study has reported that samples of asphalt binders, aggregates and hydrated lime were stockpiled during construction. The materials were then used to prepare laboratory specimens for further testing. Indirect tensile tests (ITT) have been undertaken at different temperatures and results are presented in Table 4.3 below. Based on the literature review, it is unclear whether adjustments (e.g. air voids, loading speed etc.) have been applied to the reported tensile modulus values.

Table 4.3: Moduli of asphalt mixtures from the ITT

Lanes	Performance grade of binder after RTFO and PAV*	Tensile modulus (MPa)		
		10 °C	19 °C	28 °C
1 and 3	9	4,050	1,975	826
2 and 4	17	7,466	3,452	1,765

RTFO = Rolling Thin-Film Oven and PAV = Pressure Aging Vessel

Source: Al-Khateeb et al. (2008).

4.2.2 Crushed granular base

In the pavement test sections, the 100mm and 200mm asphalt layer were built over an unbound crushed aggregate base layer. The granular base material meets the VDOT 21-A specifications. Details of the construction methodology were not detailed in the referenced publications.

4.2.3 Prepared subgrade

All the test sections rested on 610 mm of prepared subgrade. The subgrade material was classified as A-4 silty soil in accordance to the AASHTO M145-91 specification. The A-4 material generally has a CBR value ranging between 5–15%. Based on the FHWA publication, it is unclear the extent of the subgrade characterisation that were undertaken. However, the FHWA report (Stuart et al. 2002) did stated that based on prior tests, the subgrade moduli were 34.5 and 68.9 MPa, respectively.

4.3 Back calculation of pavement modulus – FHWA ALF trial

Al-Khateeb et al. (2008) compared the fatigue performance of laboratory beam fatigue test with the field performance data measured during the FHWA ALF trial presented above. A direct comparison between beam fatigue cycles to failure and the ALF wheel passes were made. This was followed by a linear regression analysis on the results.

Fatigue life of asphalt depends on the applied loading strain during the fatigue testing. Since no in situ strain measurements were made at the time of the ALF trial, the researchers determined the moduli of the crushed aggregate base and subgrade by backcalculating deflection data obtained from a falling weight deflectometer (FWD). The program used for the backcalculations was BOUSDEF and the tensile strain at the bottom of the asphalt layer for each pavement was determined using the WinJULEA program. The back-calculated moduli for the crushed base and prepared subgrade are shown in Table 4.4. As the precise location of each test section was not clearly defined in the identified literatures, average moduli values have been computed across each lane. These average moduli values are then used for the analysis presented in this study.

WinJULEA is a linear elastic software utility which comes with the PCASE software (Adolf 2010). Details of the software are unknown; however, it is related to the JULEA subroutine which has been used by US Army Corps of Engineers. It is believed that the software computes elastic response parameters using a model composed of layers of linearly elastic material that is isotropic and infinite in horizontal extent.

The tensile strains at the bottom of the asphalt layer computed using WinJULEA are presented in Table 4.5.

Table 4.4: Moduli of unbound granular and prepared subgrade

Lane	Thickness (mm)		Sites	Modulus from elastic layer back analysis (MPa)			
	Asphalt pavement layer	Crushed aggregate base		E (Base)	Average E (Base)	E (Subgrade)	Average E (Subgrade)
1	100	560	1 and 2	340	321	60	51
			3 and 4	302		41	
2	100	560	1 and 2	228	215	56	51
			3 and 4	202		45	
3	200	460	1 and 2	340	321	38	34
			3 and 4	302		29	
4	200	460	1 and 2	339	411	41	35
			3 and 4	483		28	

Source: Al-Khateeb et al. (2008).

Table 4.5: Calculated tensile strains based on the back calculated moduli

Lane	Asphalt pavement layer thickness (mm)	Pavement test temperature (°C)	WinJULEA tensile strain at the bottom of asphalt layer (µε)
1	100	28	476
		19	390
		10	294
2	100	28	431
		19	332
		10	224
3	200	28	279
		19	208
		10	146
4	200	28	188
		19	142
		10	95

Source: Al-Khateeb et al. (2008).

4.4 Analysis of the FHWA ALF trial results using different methods

Details of the FHWA ALF trial between 1994 and 2001 were presented in Section 4.1. Pavement configurations and the cumulative wheel passes to reach a cumulative crack length of 50 meters are summarised in Table 4.6 below. This is different to the data presented in the previous Figure 4.4 and Figure 4.5, as the data in the Figures represents the number of load repetitions to the appearance of the first crack.

The fatigue data in Table 4.6 is presented in Figure 4.6 and Figure 4.7. It should also be noted that, for Sections 11 and 12, the test was terminated after 400 000 passes despite the end condition not being reached. This was due to difficulties in maintaining the pavement temperature of 10 °C. It is likely that these two pavements would have had the longest fatigue lives of the configurations tested.

Table 4.6: Pavement configuration for FHWA ALF trial

Section number	1	2	3	4	5	6	7	8	9	10	11	12
Temperature (°C)	28				19				10			
Asphalt thickness (mm)	100		200		100		200		100		200	
Binder grade	PG9 (soft)	PG17 (stiff)										
ALF wheel passes	200 k	160 k	320 k	460 k	4 k	39 k	75 k	410 k	25 k	50 k	400+ k	400+ k

Source: Stuart et al. (2002).

Figure 4.6: Reported number of cycles to failure (crack length of 50 m) during FHWA ALF trial (100 mm asphalt and 560 mm crushed rock section)

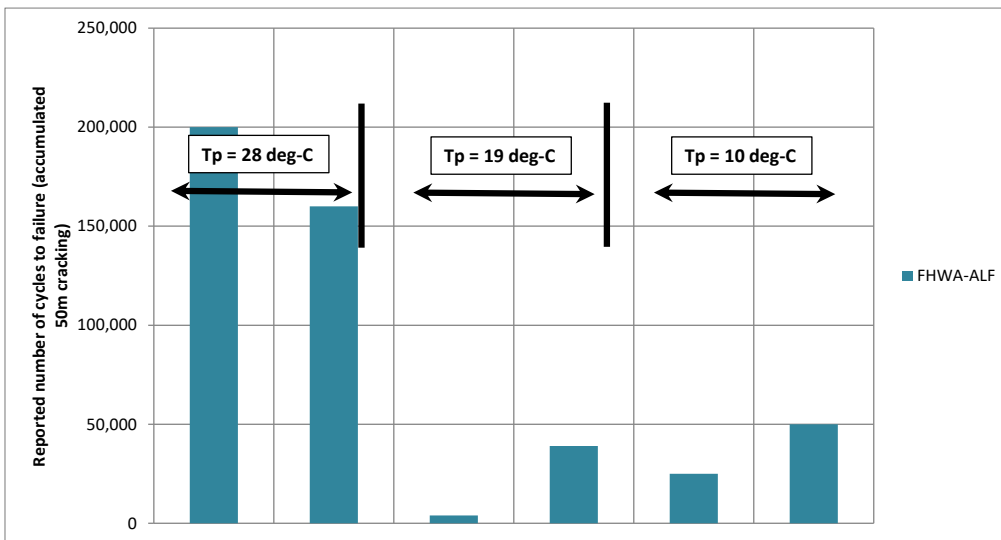
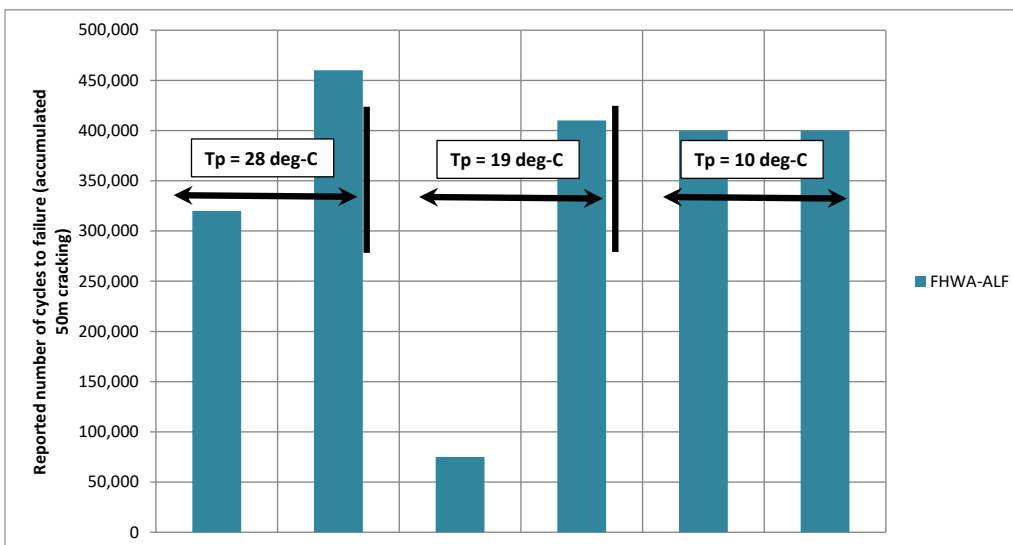


Figure 4.7: Reported number of cycles to failure (crack length of 50 m) during FHWA ALF trial (200 mm asphalt and 460 mm crushed rock section)



In this study, analyses have been undertaken to evaluate the ALF trial results in the context of common analysis procedure that have been undertaken in Australia. The two analyses conducted are listed below and are discussed further in the subsequent sections:

- Analysis A — analysis based on concepts of anisotropy, sub-layering and limiting moduli values
- Analysis B — analysis based on modelling the pavement and subgrade material with isotropic models, but no sub-layering and no limits are applied to the values obtained from the back-calculation.

The objectives of these analyses are listed as follows:

- Based on different mechanistic analysis assumptions, compare the computed tensile strains with those reported in the previous FHWA study (Al-Khateeb et al. 2008).

- Based on the Shell's fatigue equation and the computed tensile strain, predict the number of cycles to failure and compare it with the values reported by the ALF trial.

4.4.1 Analysis A

Analysis A incorporated elements of the mechanistic analysis that are typical in Australia, but are not fully compliant with the current Austroads method presented in AGPT02/12. The analysis features are listed as follows:

- Apply limit to vertical modulus of top sublayer in granular material
- Granular and subgrade materials are modelled using anisotropic models (i.e. $E_V / E_H = 2.0$)
- Apply Austroads sub-layering scheme for granular material

Table 4.7 is a summary of the parameters adopted during the analysis. In this study, in order to preserve the effect of temperature on the asphalt modulus, the modulus reported from the FHWA study has been used without further adjustments. As a result, the applicable upper limit of the granular top sublayer needs to be interpolated from AGPT02/12, as presented in Table 4.8.

Table 4.7: Summary of analysis A

Material	Source of values	Degree of anisotropy (E_V / E_H)	Sub-layering scheme	Notes
Asphalt	Indirect tensile test	1.0	No	It is unclear from the literature if any adjustment factors have been applied to the ITT results.
Granular base	Back-calculated	2.0	Yes – Austroads. Implemented by CIRCLY	Maximum value in the top sub-layer is capped according to Austroads limits under bound material. Refer Table 4.8.
Subgrade	Back-calculated	2.0	No	Prepared subgrade represents the elastic half-space. The average values reported in Table 4.4 are used.

Table 4.8: Interpolated upper limit to top sublayer of normal granular base

	100mm of overlying asphalt material										
Modulus of overlying asphalt (MPa)	826 (^)	1000	1765 (^)	1975 (^)	2000	3000	3452 (^)	4000	4050 (^)	5000	7466 (^)
Upper limit to top sublayer of normal granular base (MPa)	357 (#)	350	319 (#)	311 (#)	310	290	281 (#)	270	269 (#)	250	201 (#)
	200mm of overlying asphalt material										
Modulus of overlying asphalt (MPa)	826 (^)	1000	1765 (^)	1975 (^)	2000	3000	3452 (^)	4000	4050 (^)	5000	7466 (^)
Upper limit to top sublayer of normal granular base (MPa)	232 (#)	220	166 (#)	152 (#)	150	150	150 (#)	150	150 (#)	150	150 (#)

Note: (^) asphalt modulus values measured by ITT; (#) granular layer interpolated based on the values from Table 6.4 of AGPT02/12

Based on the methodology and material properties presented above, the strain at the bottom of the asphalt layer as well as the number of predicted cycles to failure using the Shell's equation for Analysis A are presented in Table 4.9 below.

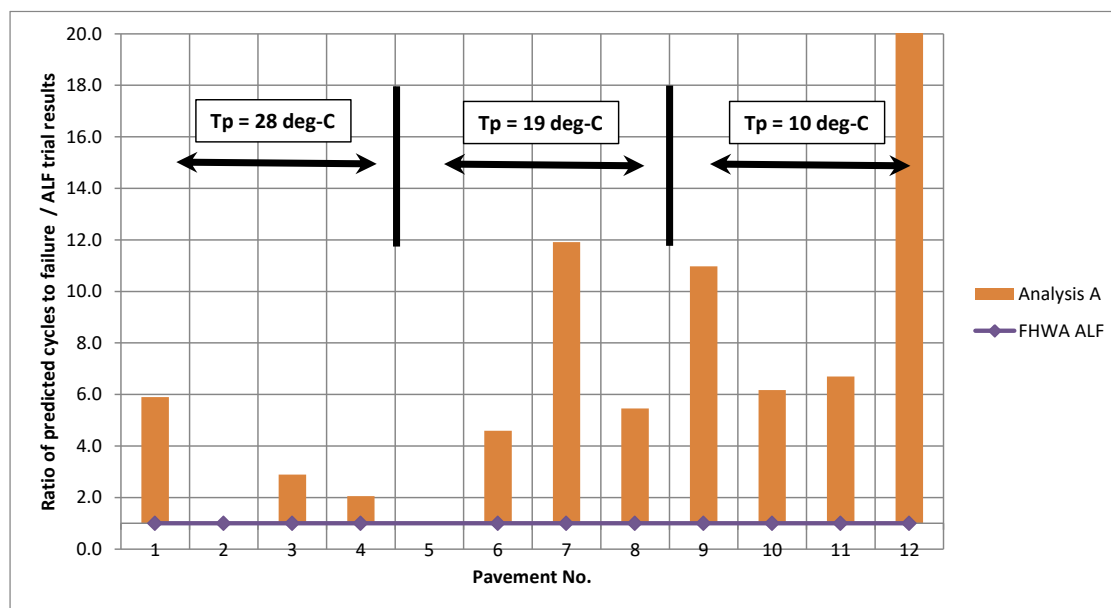
Table 4.9: Material properties used in Analysis A and the calculated tensile strain at the bottom of the asphalt layer

Analysis A											
Pavement no.	Asphalt						Granular			Subgrade Ev (MPa)	
	Thickness (mm)	E _{ASPHALT} (MPa)	V _b (%)	Strain (µm/m)	Reliability Factor	Fatigue cycles (Shell Equation)	Thickness (mm)	Sub-layer	E _{max} (MPa)		
1	100	826	12.2	433	1.00	1.18E+06	560	Yes	321	51	
2	100	1765	12.5	508	1.00	1.54E+05	560	Yes	215	51	
3	200	826	12.5	465	1.00	9.23E+05	460	Yes	232	34	
4	200	1765	12.7	357	1.00	9.44E+05	460	Yes	166	35	
5	100	1975	12.2	393	1.00	3.99E+05	560	Yes	311	51	
6	100	3452	12.5	387	1.00	1.79E+05	560	Yes	215	51	
7	200	1975	12.5	342	1.00	8.94E+05	460	Yes	152	34	
8	200	3452	12.7	236	1.00	2.24E+06	460	Yes	150	35	
9	100	4050	12.2	327	1.00	2.74E+05	560	Yes	269	51	
10	100	7466	12.5	263	1.00	3.08E+05	560	Yes	201	51	
11	200	4050	12.5	212	1.00	2.68E+06	460	Yes	150	34	
12	200	7466	12.7	134	1.00	9.45E+06	460	Yes	150	35	

Note: The total binder volume is used for the V_b value calculated above. This includes both the absorbed and effective binder.

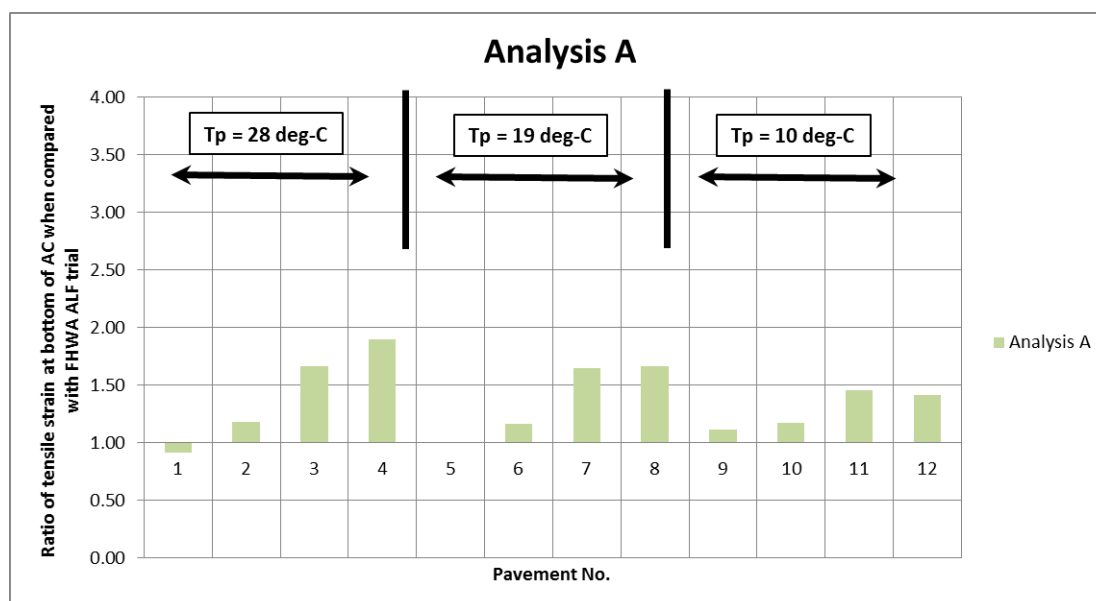
The predicted number of cycles to failure and the computed tensile strains from this analysis is presented in Figure 4.8 and Figure 4.9, respectively. Further discussions on the results are presented in Section 4.5.

Figure 4.8: Ratio between the predicted cycles to failure in Analysis A and the fatigue cycles from the FHWA ALF trial



Note: The comparison for pavement no. 5 in the FHWA ALF trial has been excluded because only 4,000 cycles to failure were reported in the ALF trial.

Figure 4.9: Ratio between the tensile strain at the bottom of asphalt obtained from Analysis A and the values reported in the research paper



Note: The comparison for pavement no. 5 in the FHWA ALF trial has been excluded because only 4,000 cycles to failure were reported in the ALF trial.
Source: Al-Khateeb et al. (2009).

4.4.2 Analysis B

Analysis A indicated that the computed strain level at the bottom of the asphalt layer has significant differences when compared with the one back-calculated from the FHWA ALF trial. In an attempt to understand the reasons for the differences in the predicted strain level between Analysis A and the one predicted from WinJULEA. Further predictions were then made by making various changes to Analysis A. It was found that similar computed strain can be determined using the details presented in Table 4.10 below. For clarity, intermediate analyses are not presented herein.

Table 4.10: Summary of analysis B

Material	Source of values	Degree of anisotropy (E_v / E_H)	Sub-layering scheme	Notes
Asphalt	Indirect tensile test	1.0	No	
Granular base	Back-calculated	1.0	No	
Subgrade	Back-calculated	1.0	No	Prepared subgrade represents the elastic half-space. The average values reported in Table 4.4 are used.

In this analysis, the computed strain from CIRCLY are compared with the values computed by WinJULEA (Al-Khatteeb et al. 2008) and presented in Table 4.11. As WinJULEA is expected to be based on isotropic model with no implementation of the sub-layering schemes, this analysis result yields the best match in the computed strain value.

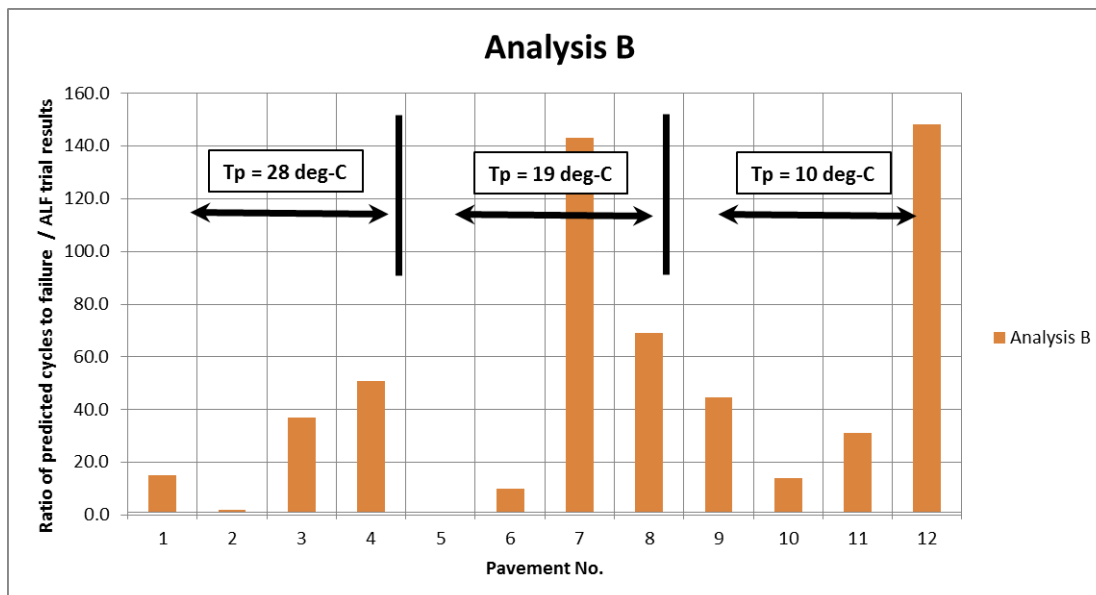
Table 4.11: Tensile strains calculated for the bottom of the asphalt layer

Pavement No.	Asphalt pavement layer thickness (mm)	Pavement test temperature (°C)	CIRCLY tensile strain at the bottom of asphalt layer (μ ϵ)	WinJULEA tensile strain at the bottom of asphalt layer (μ ϵ)
1	100	28	358 (#)	476
2	100	28	433	431
3	200	28	279	279
4	200	28	188	188
5	100	19	313 (#)	390
6	100	19	332	332
7	200	19	208	208
8	200	19	142	142
9	100	10	247 (#)	294
10	100	10	223	224
11	200	10	156 (#)	146
12	200	10	93	95

(#) Tensile strain calculated using CIRCLY using an isotropic model which shows significant difference with the WINJULEA value reported in the literature. Source: Al-Khateeb et al. (2008).

Once again, the Shell fatigue equation was used to predict the number of fatigue cycles based on the computed strain in this analysis. The results are compared with the FHWA ALF trial results and shown in Figure 4.10. It is noted that there is a much larger discrepancy between the actual field measurement and the predicted values.

Figure 4.10: Ratio between the predicted cycles to failure in analysis B and the number of cycles to failure from the FHWA ALF trial



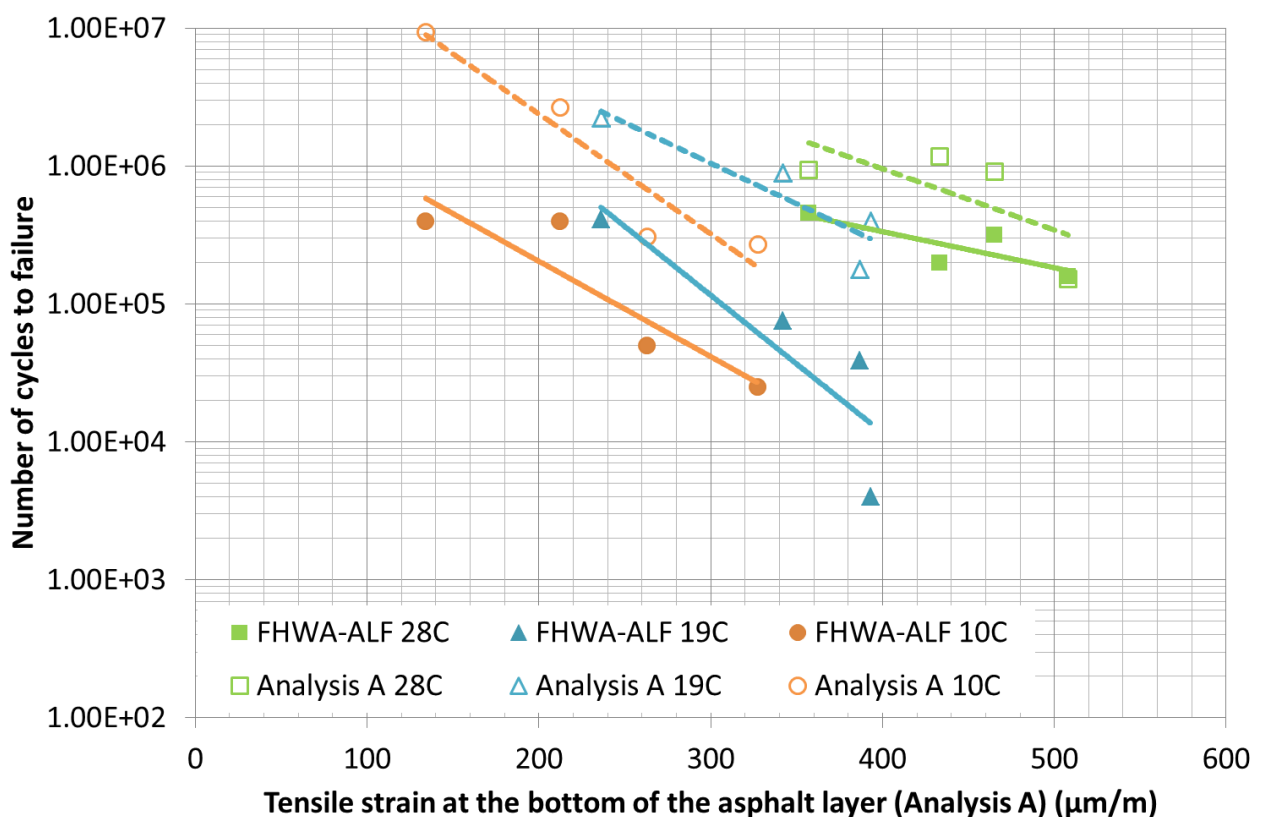
4.5 Discussion

Although the FHWA study is the most extensive APT fatigue at a constant temperatures dataset available, it only consists of 12 data points. Fatigue data is known for its high inherent scatter. The load and environmental conditions in the ALF experiment differed significantly from normal

operational pavement conditions (e.g. wander, rest periods, diurnal temperature variations). Furthermore, this study presents two sets of cycles to failure data. First set of data is the number of repetitions measured by ALF using a super single tyre at 53 kN. Second set of data are the prediction using Shell fatigue equation. Factors such as load equivalency and shift factors between the laboratory and field measurements have not been explicitly addressed. Therefore, a difference between the APT results and the prediction by the Austroads fatigue model should be expected. Nevertheless, the analysis in this section has identified some trends that invite further investigation.

The Austroads fatigue model predicts a higher number of cycles to failure than recorded in the ALF experiments at all temperatures. However, the difference between predicted and actual is much greater at temperatures of 10 °C and 19 °C than at 28 °C. This effect is summarised in Figure 4.11, where the continuous lines are the results of the ALF experiments at the various temperatures and strain conditions and the dotted lines the predicted life of the asphalt from Analysis A. If it is accepted that the model is accurate for the prediction of fatigue in full-scale pavements at the lower temperatures (20 °C is the reference temperature for the Shell models), then it may be underestimating the load repetitions to failure at high temperatures.

Figure 4.11: Comparison of the computed number of cycles to failure (Analysis A – AGPT method) and the number of cycles to failure determined from FHWA ALF trial



The modelled strain condition in the pavement depends to a significant extent on the analysis procedure used. In general, the strain computed by the FHWA researchers is lower than the other methods. This difference can be explained by the fact that the FHWA trial used an isotropic model; it also did not use sub-layering to reduce the modulus value within the granular layer as would typically take place in the Austroads method. In general, the Analysis A assumptions in terms of the modulus of granular material in combination with sub-layering of granular layers and anisotropy result in higher tensile strains. Figure 4.12 and Figure 4.13 presented graphically the maximum horizontal strain condition computed in the two analyses presented in this report.

Figure 4.12: Comparison of the calculated tensile strain at the bottom of the asphalt layer between analysis A and FHWA ALF trial

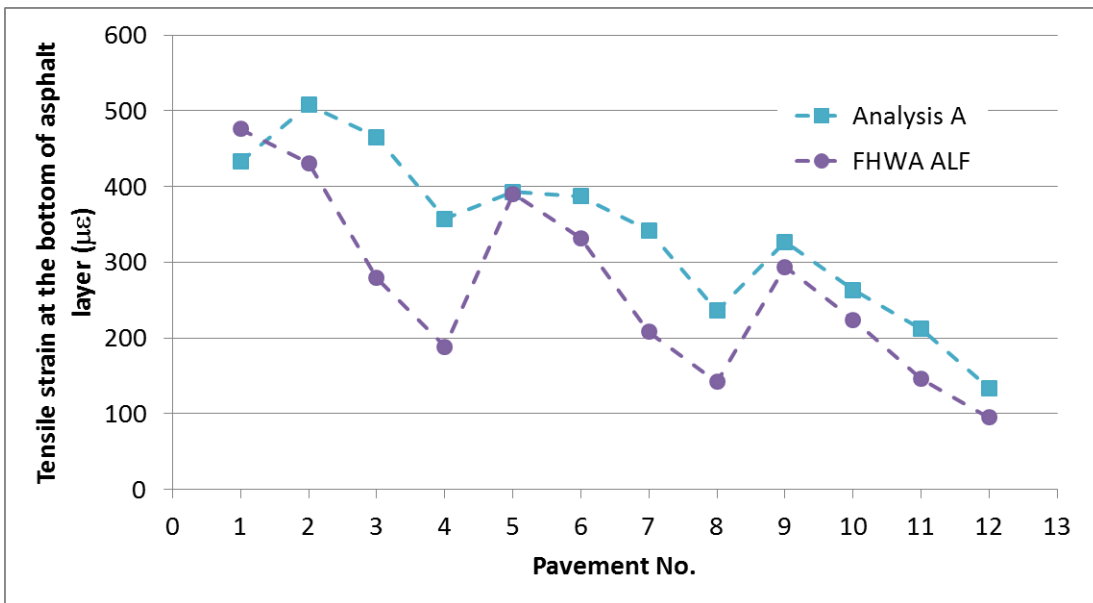
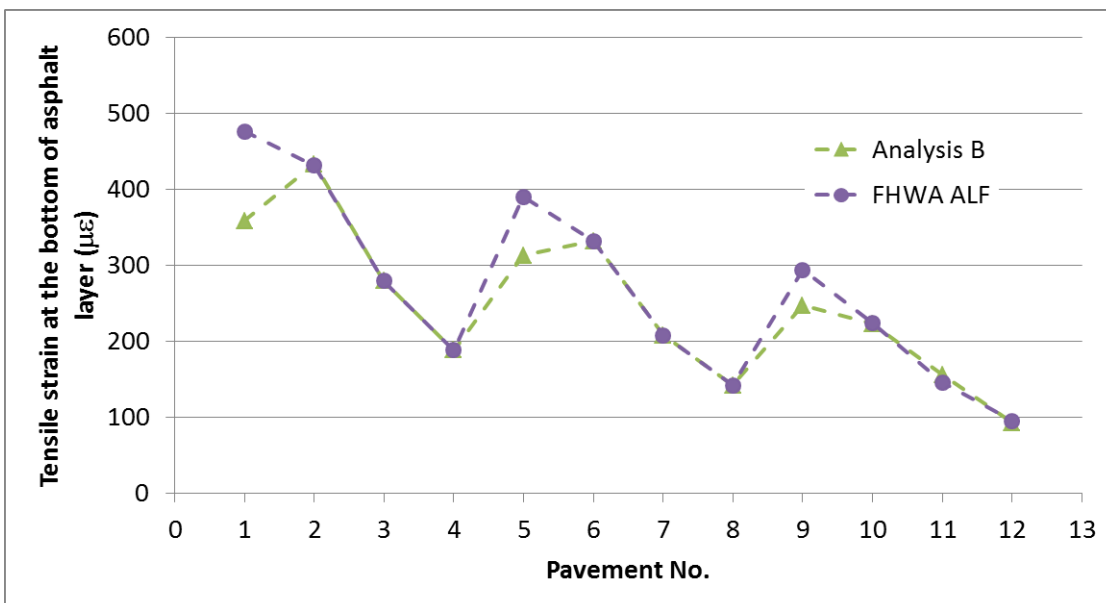


Figure 4.13: Comparison of the calculated tensile strain at the bottom of the asphalt layer between analysis B and FHWA ALF trial



5 HEALING AND REST PERIODS

One of the phenomena that has been linked to the differing asphalt fatigue behaviour with temperature is crack healing. The concept of healing taking place in asphalt between load cycles is not new, having been reported since at least the late 1960s (e.g. Bazin and Saunier (1967); Van Dijk and Visser (1977)). It is also mentioned in the SPDM (Shell 1978). These studies discussed how rest periods between load applications resulted in longer fatigue lives. Among other things, it was shown that when direct tensile specimens are completely broken they can be healed to a significant extent by putting the halves back into contact. Bazin and Saunier (1967) found that the amount of healing was strongly dependent on temperature. At the highest test temperature used in the study (25 °C), up to 90% of the initial tensile strength was recovered after three days of healing. It should be noted that the binder used in the asphalt (180/220 Pen grade) was very soft by modern standards. Healing was shown to occur in specimens damaged in both monotonic and cyclic testing.

The effect of healing and temperature was, at least to a certain extent, already included in the SPDM (1978). The SPDM states that, due to the effects of healing and intermittent loading (i.e. each loading cycle being followed by a rest period), the fatigue life in the field should be taken to be a factor of 2–10 times greater than laboratory results.

5.1 Damage and healing mechanisms

Limited information is available in the literature regarding the actual mechanism of healing in asphalt. In an extensive study by the FHWA (2001), knowledge on healing in polymers was extrapolated to describe the likely healing processes in asphalt. When two asphalt surfaces are brought into contact, a junction between them will gradually develop due to adhesion and diffusion. The rate of the healing process is dependent on the temperature and the viscosity of the material. The FHWA healing study confirmed the occurrence of healing of asphalt under both laboratory and field conditions.

It is generally accepted that fatigue damage in asphalt pavements is due to the growth, or accumulation, of cracks due to traffic loading or environmental stressing, such as temperature change. Cracking was originally considered to be initiated at the bottom of the asphalt layer but in more recent times, surface-initiated cracking has been observed and extensively studied (Matsuno & Nishizawa 1992; Nunn 1997; Uhlmeier et al. 2000). In the FHWA (2001) study of micro-damage healing in asphalt and asphalt, fatigue was described as a two-stage process:

1. micro-crack growth and healing
2. macro-crack growth and healing.

The fatigue service life of asphalt is controlled by two competing mechanisms: damage and healing. During a rest period, which is a period when the applied traffic loading is removed, followed by a period of no load, relaxation of stresses (or recovery) and physical healing of the micro-cracks occur simultaneously (Kim, Whitmoyer & Little 1994).

From a property measurement viewpoint, the healing capacity of asphalt is usually described in terms of the recovery of mechanical properties (e.g. stiffness) and increase in the number of loading cycles to failure (Qiu et al. 2012a). From a physical viewpoint, healing has been described as a three-stage process (Phillips 1998):

1. the closure of micro-cracks due to wetting (i.e. adhesion of previously separated surfaces)
2. the closure of macro-cracks due to consolidating stresses and binder flow
3. the recovery of mechanical properties due to the diffusion of asphaltene structures (asphaltenes are the largest molecules present in bitumen and associate as clusters).

5.2 Interaction between rest periods and healing

Rest periods between load applications are introduced in laboratory fatigue tests to simulate loading and non-loading periods of vehicular traffic. Whilst it is difficult to establish realistic loading times and rest periods between the passage of vehicle axles, as an approximation, researchers have introduced, in the laboratory, rest periods ranging from one to 100 times the loading time. Rest periods permit healing or relaxation of accumulated stresses and damage in the asphalt. Thus laboratory fatigue tests which incorporate rest periods can be used to obtain information about the extent of the healing process and the likely increase in field fatigue life which will occur because of this.

Rest periods between successive loadings increase the fatigue life in both controlled displacement and controlled force modes in laboratory tests, irrespective of specimen geometry or loading conditions. Rest periods can be introduced either by intermittent loading or by discontinuous loading, as described below (Bonnaure, Huibers & Boonders 1982; de la Roche et al. 1994; Souliman 2012):

- intermittent loading – each loading cycle is followed by a rest period, which is a multiple of the duration of the loading cycle, or
- discontinuous loading – continuous loading for a certain period of time followed by a rest period, during which the test specimen is kept under the test conditions (temperature in particular) but under a no-load situation.

Intermittent loading conditions are considered to be closer to in-service conditions. Souliman (2012) reported that intermittent loading had lesser impact on the fatigue life of asphalt mixes due to the healing process.

5.2.1 Asphalt properties which affect healing

The primary factors which control crack closure and thus healing in asphalt are the flow properties of the binder and the period of time available for healing to occur. Binder flow will depend on the viscosity of the binder and the prevailing temperature conditions. To a lesser extent, the chemical properties of the binder will affect healing through their effect on diffusion and adhesion.

In a particular asphalt mix at a particular location, these primary properties will be controlled by a number of secondary factors:

- binder viscosity will depend on:
 - initial binder grade
 - degree of hardening due to oxidation
 - presence of additives, such as polymers, which may affect viscous flow
- temperature:
 - temperature distribution throughout the day, and throughout the year
- rest periods:
 - in the field, traffic flow throughout the day-night cycle, and the proportion of combination vehicles with a high number of axles may be important factors affecting healing times
- mix type, which influences:
 - binder film thickness
 - binder flow through the effect of filler particle size and concentration

- void content which affects binder hardening rate
- binder chemical properties:
 - not normally specified or known but dependant on binder grade, source of crude oil and bitumen manufacturing process.

5.3 Consideration of healing parameters in asphalt pavement design

In order to include the effect of the asphalt healing process in a design procedure, it is desirable to have quantitative information regarding: each of the main factors which affect healing and the relationship between the factor and the degree of healing or change in fatigue life. To obtain such information from the research studies which have been conducted on healing, it is necessary that all factors in a study, except the one being investigated, are held constant, or that a multifactorial experiment was designed so that the effect of each of the contributing factors could be isolated.

A review of the literature indicated that such information was not available. All the studies so far identified included more than one variable, and the generally small data sets meant it was difficult to isolate the effect of a single variable. Furthermore, in some cases quantitative relationships were not obtained; rather, factors were ranked in their effect on healing.

However, it may be possible to estimate the effects of the main variables on healing and thus fatigue life by utilising information from a number of studies. This may be sufficient to allow an improved estimate of fatigue life to be developed.

In a number of the healing studies reported, binder specimens only were used, rather than asphalt specimens. This has been justified on the basis that observation of asphalt cores taken from damaged roads, or inspection of laboratory specimens tested in fatigue, show that fracture mostly occurs within the bitumen (or mastic) film (Hammoum et al. 2002).

5.3.1 Rest periods

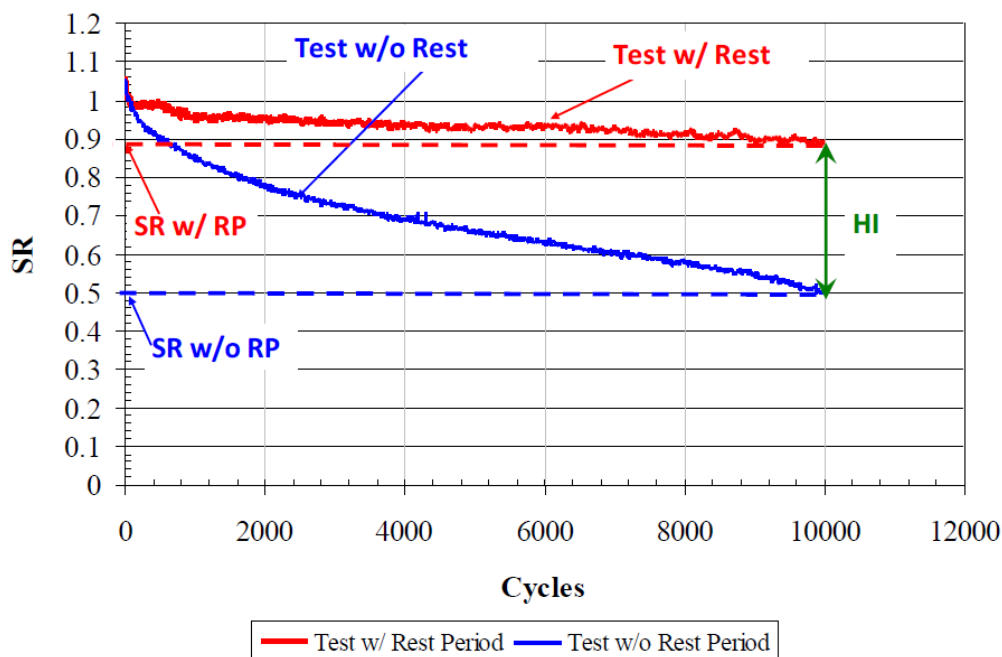
A considerable amount of work has been done over the last 40 years on the effect of rest periods during fatigue testing of asphalt (e.g. Bonnaure, Huibers & Boonders 1982; Raithby & Sterling 1970; Raithby & Sterling 1972; Van Dijk & Visser 1977). Findings from the literature indicated that the introduction of rest periods during fatigue testing resulted in longer fatigue life. However, the results from different researchers cannot be directly compared due to differences in mix composition and loading conditions.

More recently, Souliman (2012) conducted, an extensive investigation to evaluate the fatigue response of asphalt using four-point bending testing. This study was referred to in Section 3.5 in the discussion on the determination of a fatigue endurance limit. The study involved six factors: binder type, binder content, air voids, test temperature, rest period and applied strain. A full factorial design (432 beam tests) was conducted to evaluate all possible interacting factors.

Souliman defined the Healing index (HI) as 'the difference between the SR for the test with and without rest period at the number of cycles to failure for the test without rest period ($N_{f w/w RP}$) (Figure 5.1). It was concluded that there was no additional benefit in healing after a particular rest period duration (10 s and 5 s produced similar results).

Souliman developed a complex model for calculating the endurance limit of asphalt. The asphalt Endurance Limit (A-EL) is the repeated asphalt flexural strain level, below which asphalt damage is not cumulative. Thus, an asphalt layer experiencing strain levels less than the A-EL should not fail due to fatigue. The model could also predict the number of cycles to failure at any rest period and stiffness combination if the model is extrapolated outside the data range.

Figure 5.1: Example of effect of loading cycle (with and without rest period) on SR



Source: Souliman (2012).

5.3.2 Optimum rest period duration

The rest period duration to produce optimum healing, often expressed as a load-to-rest period (LRP) ratio, has been studied by various researchers over the last four decades (e.g. Bonnaure et al. 1982, Molenaar 1984, Robertus 1993, Van Dijk & Visser 1977; Verstraeten, Veverka & Francken 1982). However, findings on the optimum LRP ratio varied for different investigators, depending, as they did, on binder properties, asphalt mix type and loading conditions.

An example of this type of study is the work of Bonnaure et al. (1982) who conducted laboratory fatigue tests using three-point bending of rectangular beams (230 mm x 30 mm x 20 mm) under sinusoidal loading at 40 Hz, three temperatures (5 °C, 20 °C, 25 °C) with rest periods of 0, 3, 5, 10 and 25 times the loading periods. Two penetration grades of bitumen (45/60 and 80/100 Pen) were examined in a typical dense-graded asphalt used for wearing courses in the Netherlands.

It was concluded that rest periods had a beneficial effect on fatigue life, with the benefit reaching a maximum at about 25 times the loading cycle. Increases in test temperature increased the beneficial effect, as did the use of softer binders.

As indicated above, other researchers have quoted different optimum LRP ratios. For example, Verstraeten et al. (1982) suggested a ratio of 10 to 15, Molenaar (1984) a ratio of 1.7, and Van Dijk and Visser (1977) a ratio of 1.5.

5.3.3 Rest period duration and temperature

An asphalt beam-on-elastic-foundation (BOEF) test setup, as shown in Figure 5.2, was used to study the self-healing capacity of asphalt mixtures (Qiu et al. 2012b). The Dutch asphalt was composed of 70/100 penetration grade bitumen, 6.5% bitumen content and 4% air voids. A load crack opening displacement (COD) curve was used to characterise the self-healing capability of the monotonic response with a loading-healing-reloading procedure (i.e. the beam was first subjected to loading until the pre-defined crack length was attained, followed by a rest period, and

lastly reloading). A factorial design of three crack levels (0.2 mm, 0.6 mm and 0.9 mm), two healing periods (3 hours and 24 hours) and two healing temperatures (5 °C and 24 °C) was used.

Figure 5.3 presents an example of loading-healing-reloading response of an asphalt BOEF test designed at a crack level of 0.9 mm, rest period of 3 hours and a healing temperature of 5 °C. It was found that the crack length decreased rapidly at the commencement of the unloading process and that the recovery plateaued after approximately 60 minutes for an initial crack length of 0.9 mm. It was reported that the visible crack (0.9 mm) closed autonomously and completely after unloading.

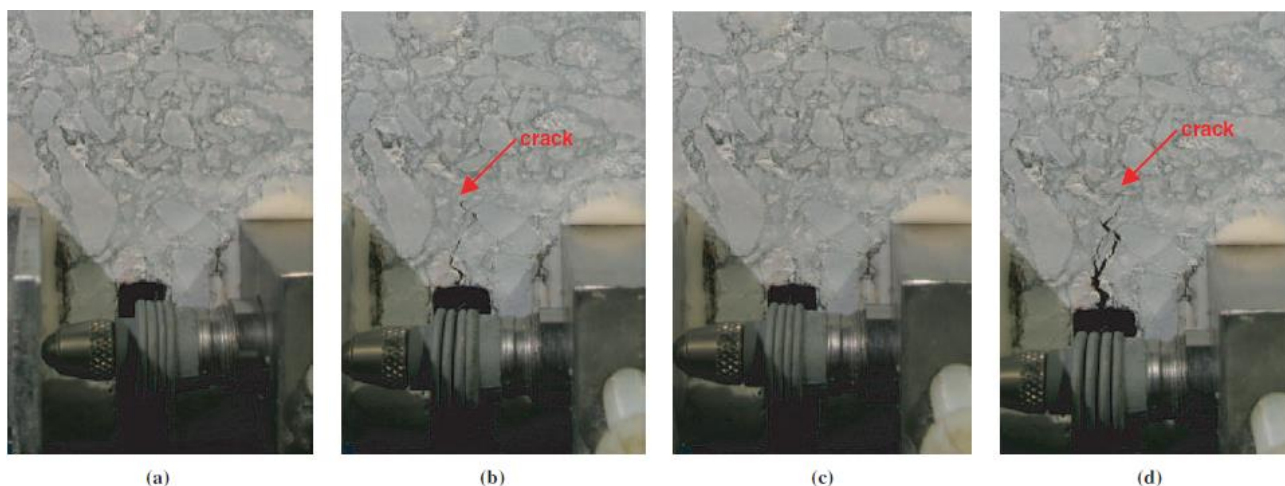
The percentage of healing in the asphalt beam was measured using dynamic loading and a stiffness modulus before and after a period of healing calculated. The self-healing capability increased with both the healing temperature and healing time. The results indicated that the effect of healing temperature was more dominant than healing time.

Figure 5.2: BOEF setup



Source: Qiu et al. (2012b).

Figure 5.3: Example of crack (crack level of 0.9 mm) formation and closure with 3 h rest period at 5 °C: (a) before loading; (b) loading until crack of 0.9 mm achieved; (c) unloading; (d) reloading unit crack of 1.5 mm.



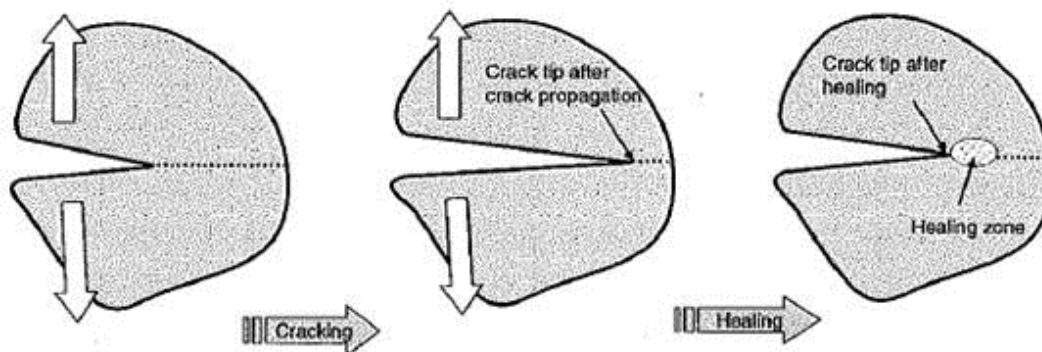
Source: Qiu et al. (2012a).

Using the same experimental arrangement of BOEF, Qiu and co-workers developed the concept of a cohesive zone model (CZM) based on non-linear fracture mechanics (Qiu et al. 2012b). In the CZM, the healing process was considered as a reverse of cracking, with the healing process improving cohesive strength (in the binder phase) of the healing zone, and hence moving the crack tip back towards its pre-cracking position (Figure 5.4).

A symmetric monotonic load was applied with loading-unloading-healing-reloading cycles. Increased reloading curves were observed for increasing healing time and healing temperature.

The authors concluded that healing behaviour under the simulated loading conditions was directly related to a decreasing crack length as a crack repairing (i.e. self-healing) process.

Figure 5.4: Hypothesis of cracking and healing process: cohesive zone model (CZM)



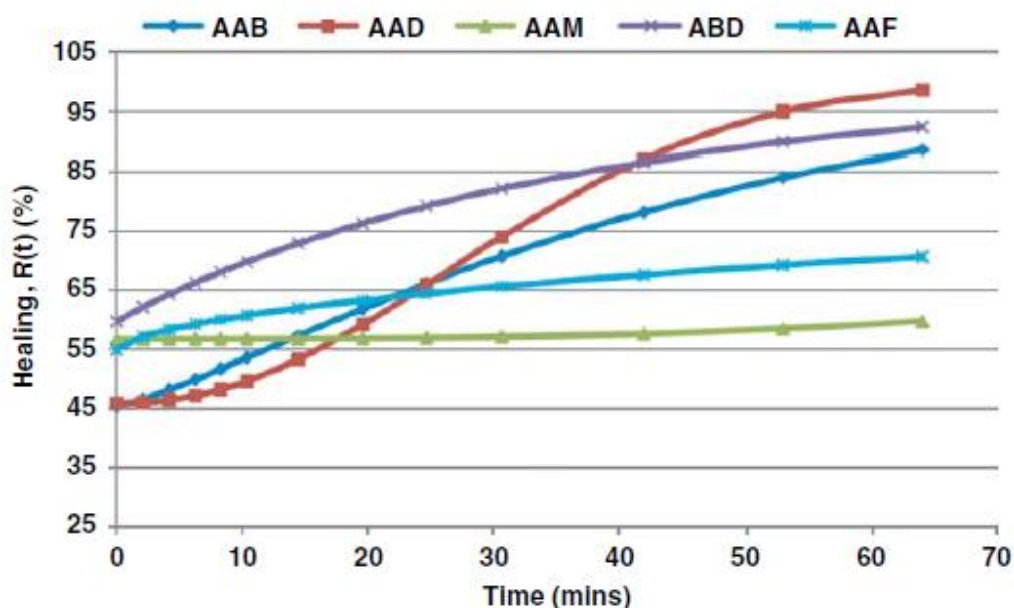
Source: Qiu et al. (2012a).

5.3.4 Binder type and healing time

Two studies by Little and co-workers looked at the effect that different binders and different rest periods had on the healing of binder specimens. In the first study (Bommavaram, Bhasin & Little 2009), selected SHRP binders were used neat (i.e. un-aged and unmodified). Bommavaram et al. outlined a three-stage healing process where the first stage, wetting of the two faces of a nanocrack, was represented by a wetting distribution function. The second and third stages, namely strength gain caused by interfacial cohesion and inter-diffusion of molecules between the wetted surfaces, were represented by an intrinsic healing function. The model was developed for polymers and may not be directly applicable to bitumen, so modified forms of the supporting mathematical functions were used.

The test procedure involved Dynamic Shear Rheometer (DSR) measurements on initially-separated specimens of the same binder which were brought together. The intrinsic healing function, $R(t)$, was calculated using the values of the complex modulus (G^*) over time. Figure 5.5 shows the change in the intrinsic healing function of the five binders tested with time of contact (or healing).

Figure 5.5: Changes of the intrinsic healing function (R(t)) with time for five SHRP binders (denoted as AAB, AAD, AAM, ABD and AAF) tested in DSR at 25 °C, 10 rad/s and constant strain amplitude of 0.001%



Source: Bommavaram, Bhasin and Little (2009).

Binders AAD, ABD and AAB showed a marked increase in intrinsic healing function of over 85% in 65 minutes. In contrast, binder AAM remained almost constant at around 57%. While it appears that binder type (and thus viscosity) had an effect on healing, the effect is complex.

5.3.5 Binder ageing and temperature

In a second study, Bhasin, Palvadi & Little (2011), used a similar test arrangement to that described in Section 5.3.4. Testing was conducted on three binders which had each been artificially aged by two standard procedures. The test materials were three performance grade binders (PG 64-22, PG 70-22 and PG 76-22) that were subjected to two ageing treatments: short-term aging using the rolling thin film oven test (RTFO) and long-term aging using the pressure aging vessel (PAV). The percentage healing of these binders was then measured using a DSR at three temperatures (10 °C, 15 °C, 20 °C). The findings are summarised in Table 5.1.

Table 5.1: Effect of healing on three binders as affected by ageing (RTFO and PAV) and temperature

Binder	Ageing	Healing (%)				
		10 °C	15 °C	20 °C	25 °C	30 °C
PG 64-22	RTFO	78.4	86.8	95.4	-	-
	PAV	-	-	74.6	86.2	91.7
PG 70-22	RTFO	77.6	81.7	83.6	93.6	-
	PAV	-	-	71.7	76.7	82.1
PG 76-22	RTFO	-	56.3	67.5	86.1	-
	PAV	-	-	60	68.4	72.5

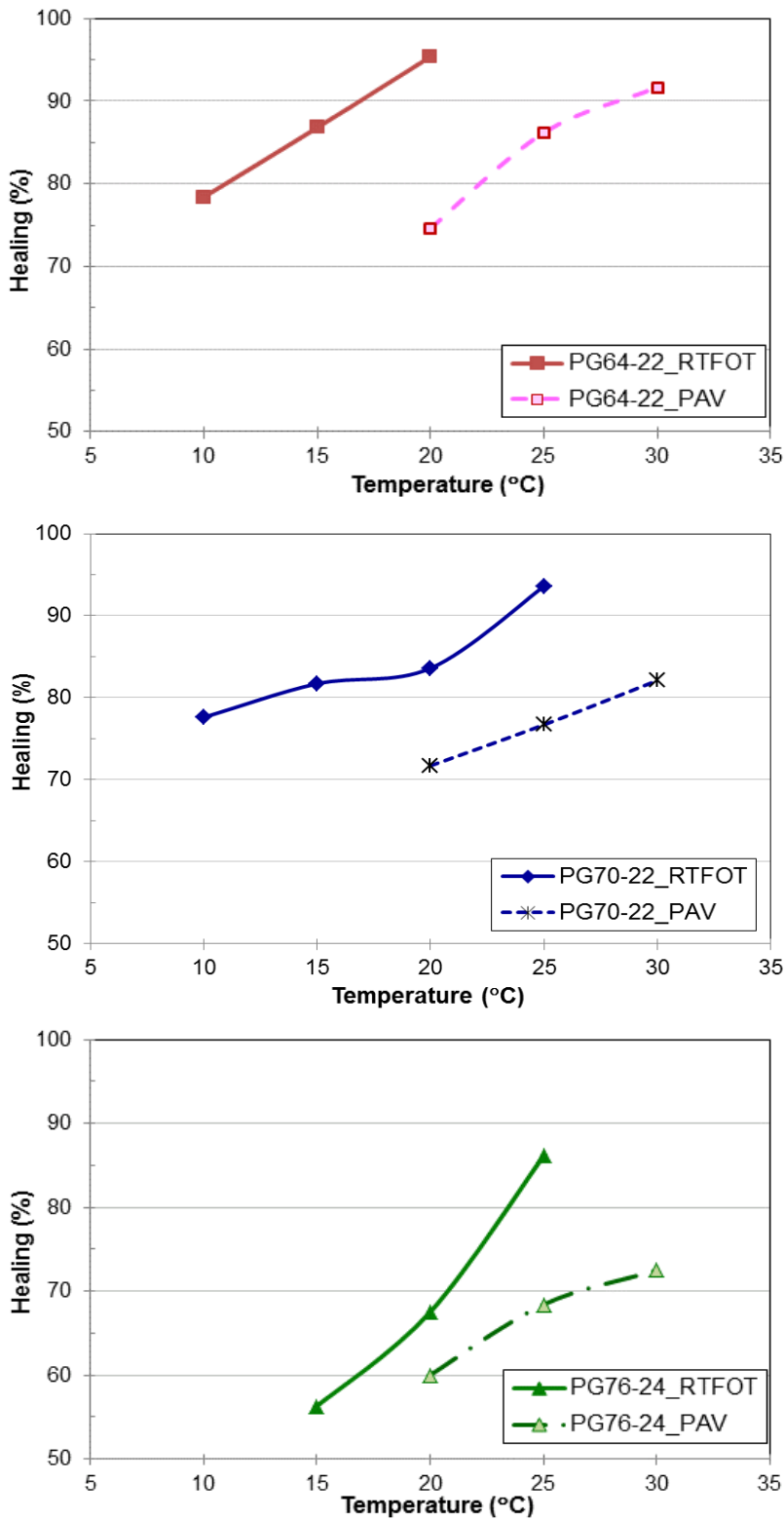
Source: Adapted from Bhasin, Palvadi and Little (2011).

Figure 5.6 and Figure 5.7 present the effect of ageing conditions (RTFO vs PAV) on healing, utilising findings extracted from In a second study, Bhasin, Palvadi & Little (2011), used a similar test arrangement to that described in Section 5.3.4. Testing was conducted on three binders which had each been artificially aged by two standard procedures. The test materials were three

performance grade binders (PG 64-22, PG 70-22 and PG 76-22) that were subjected to two ageing treatments: short-term aging using the rolling thin film oven test (RTFO) and long-term aging using the pressure aging vessel (PAV). The percentage healing of these binders was then measured using a DSR at three temperatures (10 °C, 15 °C, 20 °C). The findings are summarised in Table 5.1. Some key observations are as follows:

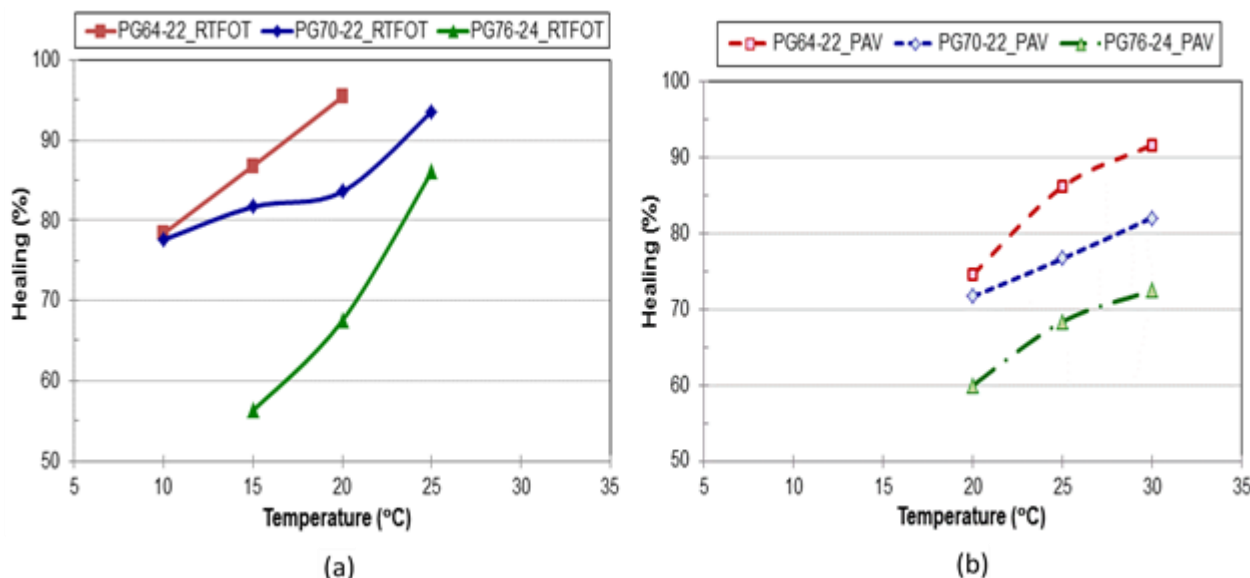
- The binders subjected to RTFO treatment consistently recorded a much higher percentage healing than those treated in the PAV. Since PAV treatment causes more severe hardening than the RTFO treatment, this indicates that an increase in viscosity results in less healing.
- For the three binders studied, the softer the binder grade, the greater the percentage healing (Figure 5.7).
- Healing capacity increases substantially with increasing temperature.

Figure 5.6: Comparison of the effect of healing (%) on three binders (PG 64-22, PG 70-22 and PG 76-22) as affected by two ageing conditions (RTFO and PAV) and temperature



Source: Adapted from Bhasin, Palvadi and Little (2011).

Figure 5.7: Effect of healing (%) on three binders (PG 64-22, PG 70-22 and PG 76-22) as affected by temperature and two ageing conditions: (a) RTFO; (b) PAV



Source: adapted from Bhasin, Palvadi and Little (2011).

5.3.6 Binder ageing and rest period duration and number

Stimilli et al. (2012) studied the effect of healing on the fatigue law parameters of bitumen. Testing consisted of strain-controlled time sweeps in a DSR with a single rest period inserted at a specified damage level. Nine neat and modified binders were tested. Healing testing was conducted at multiple age levels and strains.

Healing was defined as the extension in fatigue life resulting from rest, including contributions from viscoelasticity, thixotropy (time-dependent, reversible decrease in viscosity with loading) and crack closure. The majority of tests were conducted with a single, long rest period.

Four binders from the LTPP were tested at three age levels: unaged, RTFO aged and PAV aged. A further set of tests studied the effect of rest on the relationship between fatigue and life using five binders: two base binders without modification and with either one or two levels of styrene butadiene styrene (SBS) modification. All these binders were RTFO treated before testing.

It was found that significant recovery in $|G^*|. \sin \delta$ (the fatigue parameter used in the performance grading of binders in the USA) was observed when rest periods were included in strain-controlled cyclic testing of binders. The rates of damage accumulation before and after a single rest period were similar. Thus the relationship between fatigue life and strain (the A and B parameters in the commonly used binder fatigue relationship $(N = A.\gamma^B)$) was not significantly affected by inclusion of a single rest period.

Testing results from one binder indicated that an increase in the number of rest periods from one to ten resulted in a change in the fatigue law parameter but not a change in parameter B. Increasing the number of rest periods was more significant for healing than increasing the duration of the rest time. The greatest benefit from rest occurred at the start of the period. Increasing the rest period duration beyond 30 minutes did not appear to lead to significant fatigue life gain.

5.3.7 Damage level at rest period introduction

Palvadi et al. (2012) developed a method to characterise the healing in an asphalt composite (fine aggregate matrix or FAM) as a function of the level of damage prior to the rest period, and the

duration of the rest period. The method, which was based on viscoelastic continuum damage theory, was used to evaluate the healing of four different FAM mixes using a DSR.

The results showed that, as expected, when rest periods were introduced at similar levels of damage, longer rest periods resulted in a greater amount of healing. Also, a greater amount of healing was achieved when rest periods were introduced at lower levels of damage in the specimen. The results suggested that complete healing may not be possible after a certain level of damage.

5.3.8 Effect of temperature on surface crack healing

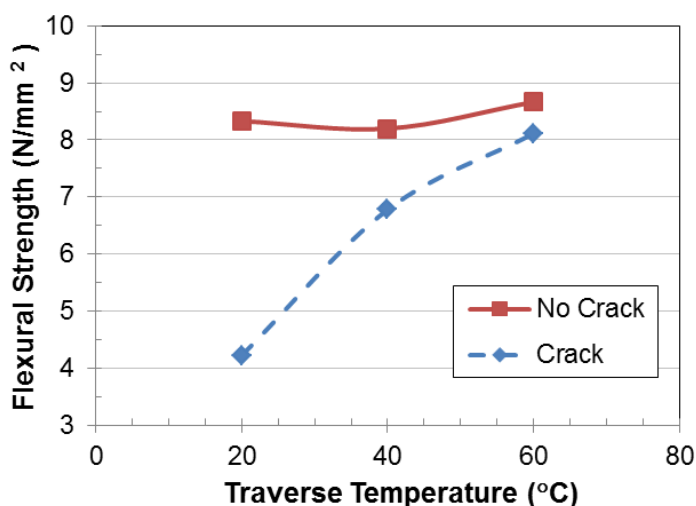
Uchida et al. (2002) observed that surface cracking can be initiated by micro-cracks due to traffic loading at high temperature in the summer. Kneading and rearrangement of the aggregates due to the rolling action of vehicle tyres can cause rebonding of the surfaces of the micro-cracks, providing the binder is sufficiently adhesive. They conducted a series of tests to examine the healing of asphalt binders with various degrees of ageing, healing temperature and loading times.

To evaluate the healing characteristics of asphalt mixes, cracks were induced in wheel-tracking slabs by bending the specimen over a steel bar inserted underneath the slab. The cracks were closed by reverting the slab to its original shape.

The slabs were then traversed by a rolling wheel which was intended to simulate the kneading action of vehicle tyres which was presumed to cause healing. Strip specimens were cut from the slab for flexural strength testing at 5 °C.

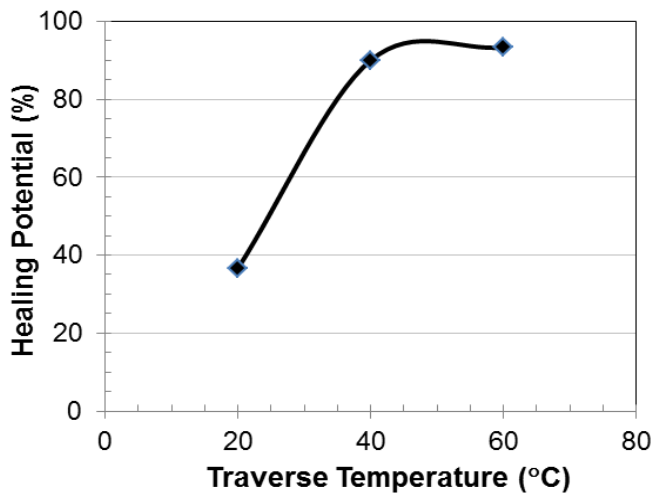
The effect of traverse temperature on the flexural strength of asphalt specimens is presented in Figure 5.8. The flexural strength of the cracked specimens increased two-fold, from approximately 4 N/mm² at 20 °C to 8 N/mm² at 60 °C. It can be seen that, at 60°C, the flexural strength had almost recovered to the level of the uncracked specimen.

Figure 5.8: Effect of traverse temperature on flexural strength of asphalt test specimen



Source: adapted from Uchida et al. (2002).

Figure 5.9: Effect of traverse temperature on healing of asphalt test specimen at outdoor exposure of one month

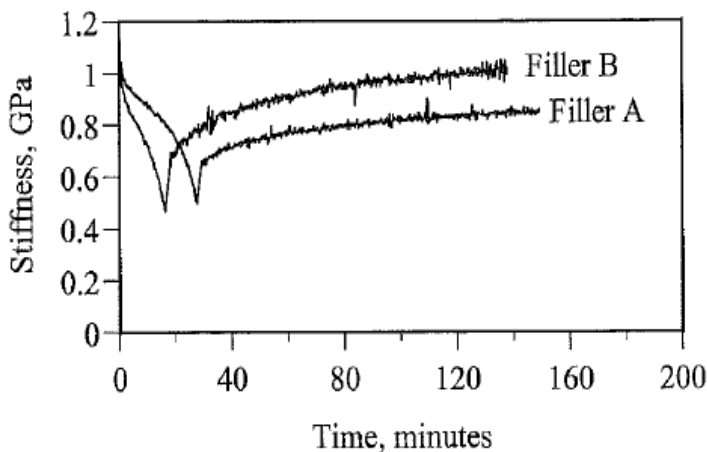


Source: adapted from Uchida et al. (2002).

5.3.9 Effect of filler size

In a study to evaluate the effect of finely-dispersed fillers on healing in asphalt binders and asphalt mixes, Smith and Hesp (2000) defined healing as the percentage recovery of original stiffness over a 2 hour rest period at 10 °C. The specimens were first subjected to applied strain of 0.3% in a DSR until the stiffness reduced to half of its original value. The strain was then reduced to 0.003% (small enough to not to cause any further damage) and recovery of stiffness was measured over a 2 hour period. The results (see Figure 5.10) showed that asphalt mastics with coarse filler (filler B) healed at a substantially faster rate than those with fine filler (filler A).

Figure 5.10: Typical effect of two fillers on stiffness recovery for asphalt specimen over two-hour rest period



Source: Smith et al (2000).

6 PROPOSED RESEARCH PROGRAM

In this section, a research program is proposed to develop improved models for the prediction of fatigue in asphalt under climatic conditions in Queensland.

6.1 Research findings

The objectives of the first year of this multi-year study were to:

- Review the literature and assemble available published data on the laboratory characterisation of the fatigue of asphalt mixes at elevated temperatures and the results of field trials, including accelerated loading trials.
- Assess the suitability of the laboratory beam fatigue test for fatigue testing at high temperatures ($> 30^{\circ}\text{C}$).
- Assess the influence of the rest period on healing at high temperatures.
- Identify possible alternative laboratory test methods.
- Assess the outcomes of the US Federal Highway Administration (FHWA) accelerated loading trial conducted at temperatures of 4, 19 and 28°C .
- Develop hypotheses on how the fatigue prediction models could be improved, with the hypotheses to be tested in an experimental program in subsequent years of this study.
- Recommend a test method for laboratory fatigue characterisation and assess whether an accelerated loading trial on Queensland mixes is required.
- Prepare a status report, including the proposed program for year two.

The literature survey confirmed the need to improve the models for the prediction of fatigue in asphalt pavements at elevated temperatures. Current fatigue models predict the fastest accumulation of fatigue damage at higher temperatures, while field data shows that most fatigue damage accumulates in cooler winter months. The analysis of the FHWA ALF study also indicated that the current Austroads fatigue prediction model may be more conservative at elevated temperatures compared to low and medium temperatures.

Currently, the four-point bending test is the standard test for the characterisation of the fatigue performance of asphalt mixes in Australia. The literature review found that the four-point bending test is a suitable test method to characterise the fatigue behaviour of asphalt over a range of temperatures, although there were mixed reports on the suitability of the tests at temperatures over 30°C . No alternative method was identified that provides significant advantages over the four-point bending test. The proposed test program will therefore be based on four-point bending testing.

A number of different methods to characterise fatigue performance in the four-point bending test were identified, and it is proposed to further explore some of these methodologies as part of the laboratory component of this study.

The literature review indicated that the low rate of fatigue damage accumulation in asphalt at high temperatures observed in the field and in the laboratory may be due to a number of factors, including slower crack growth due to lower stresses and stiffness and healing. Healing is a function of the number and duration of rest periods (number may be more significant than duration, with greatest benefit occurring at the start of the rest period), the viscosity of binder and temperature.

Of the constituents of an asphalt mix, the rate of healing would appear to be predominantly determined by binder properties rather than aggregate properties. This is probably the reason that

much recent research has focussed on studying the healing phenomenon in DSR tests, although the healing of asphalt mixes is also still being actively investigated. Currently, there is no established standard method to characterise the influence of rest periods and healing for use in pavement design models. One of the main challenges is that fracture propagation in asphalt under cyclic loading can at this stage not be readily described by current fracture mechanics models. The development of such a method would require a fundamental research program and it would be unlikely to yield results that would be implementable in the short to medium term.

6.2 Hypothesis

Based on the literature review, it is expected that improvements to the models for the prediction of fatigue in asphalt pavements in Queensland can be achieved through the following steps:

1. Improving the characterisation of pavement temperature by replacing the current definition of the WMAPT by correcting it for the variation of temperature with depth and investigating the use of a statistical temperature distribution in the pavement, rather than a single value.
2. Characterising the fatigue behaviour of typical Queensland mixes at different temperatures using four-point bending fatigue tests and using this data to develop temperature-dependent fatigue models for Queensland mixes.
3. Characterising the effect of rest periods on fatigue performance in laboratory tests and developing a temperature and rest period-dependent component to the fatigue prediction models.
4. Investigating possible improvements to the shift function between laboratory and field fatigue performance.

6.3 Methodology

An experimental plan is proposed to test the hypothesis. It is expected that Step 1 will be addressed as part of a separate project funded under the Austroads program (project TT1826: Improved design procedures for asphalt pavements). The design procedures for asphalt pavements in Queensland can be updated based on the outcomes of the Austroads study.

Step 2 and Step 3 will be addressed in a laboratory program, which is described in Section 6.3.1 and Section 6.3.2. The proposed experimental program work under this study will consist of two phases:

- Phase I: two concepts will be tested:
 - whether flexural fatigue testing can be run up to high temperatures
 - whether a fatigue endurance limit can be identified using the procedures from NCHRP report 762
- Phase II: the final experimental matrix will be extended to include multiple mix designs.

Completion of Steps 2 and 3 would yield the following:

- a database of complex modulus master curves based on flexural testing for typical Queensland mixes, which can be used to determine the modulus of the material at any combination of load frequency and temperature
- improved laboratory models for the prediction of fatigue at elevated temperatures developed for Queensland asphalt mixes, with the aim to replace the current fatigue prediction models
- a method to account for the effect of healing and rest periods in the fatigue prediction models.

Step 4 is the most challenging and requires calibration against field data, which is currently not available for Australia. It is recommended that work be initially aimed at replacing the current laboratory-based fatigue prediction models and, in doing so, increasing the reliability of the models.

It is expected that the outcomes of Steps 2 and 3 can lead to significant reductions in asphalt pavement thicknesses in Queensland. At the same time, field validation sections are to be identified where the mixes tested in the laboratory study are actually being used. These sections would need to be monitored under a LTPP component of the NACOE agreement. The intention would be to address any issues in the laboratory to field SF in the medium to long term based on the LTPP data.

6.3.1 Phase I: Improved characterisation of fatigue at different temperatures: proof of concept

The purpose of the initial phase of testing is to validate the selected test procedures and ensure that the test results provide the data that is required to develop improved fatigue models. Tests will be performed on specimens produced from a single mix design. A DG 20 mm mix design with Class 600 bitumen was selected for this purpose. The mix design is the same as that used for the control section for the EME2 trial in Whinstanes.

Fatigue testing

Fatigue tests will be run at the following temperatures: 10, 20, 30 and 40 °C. A set of 18 specimens will be tested per temperature. The tests will be run in sinusoidal displacement loading mode at a load frequency of 10 Hz. A minimum of three strain levels will be utilised in the test such that the number of cycles will be at least 100 000 (1.0E+5) at the highest strain level and a maximum of 20 000 000 (2.0E+7) at the lowest strain level. Testing will be terminated once the stiffness of the specimen reduces to 50% of the initial stiffness. Apart from the number of cycles to 50% stiffness reduction, dissipated energy will also be recorded in the tests. A fatigue function will be fitted to the set of results obtained at each temperature, using the model form shown in Equation 30.

$$\ln(N_{fat}) = a + b \ln(\varepsilon_{\mu}) \quad 30$$

where

- N_{fat} = Number of cycles to 50% stiffness reduction
- a, b = constants determined from a set of fatigue test results
- ε_{μ} = strain in $\mu\text{m}/\text{m}$

As part of Phase I, it will be investigated whether the model form in Equation 31 can be fitted against the fatigue at temperature data. This model has been used in the past to express fatigue test results at different temperatures (CROW 2010) as a function of the modulus of asphalt is shown as Equation 31.

$$\ln(N_f) = c_1 \cdot \ln^3(E) + c_2 \cdot \ln^2(E) + c_3 \cdot \ln(E) + c_4 + c_5 \cdot \ln(\epsilon) \quad 31$$

where

N_{fat} = Number of load cycles to 50% reduction in modulus

E = Modulus of the asphalt (MPa)

ϵ_μ = strain in $\mu\text{m/m}$

c_1 - c_5 = regression coefficients

The computation procedures presented in Section 3.4 will be used to determine the fatigue life and endurance limit in the normal-strain and low-strain range.

Complex modulus master curve

As part of Phase I complex modulus temperature and frequency sweeps will be performed as well. At each temperature, modulus tests will be performed on at least five specimens at 0.1, 0.5, 1, 3, 5, 10, 15 and 20 Hz, to develop complex modulus master curves.

Endurance limit and rest period

As part of Phase I, a limited number of tests will be run to explore the influence of rest period and healing on fatigue results. The test matrix will include results to validate work performed under: NCHRP Report 762: Laboratory validation of an endurance limit for asphalt pavements. The endurance limit will be determined using the methods presented in Section 3.5.

Checking test compliance

One of the key aims of Phase 1 is to see if the test method can determine the fatigue life of asphalt mixes at elevated temperature (i.e. above the traditional 30 °C upper limit). It is hypothesised that the modified fatigue bending setup presented by Tsai (2001) may not be necessary. The concern that specimens creep at higher temperature will be monitored to investigate if any anomalies occur in the reported fatigue curve at different temperatures as well as the shape and phase lag of the sinusoidal loading waveform. Waveform distortion or non-linear behaviour of the fatigue curve may suggest specimens creep at elevated temperatures when the current experimental setup is used.

Linearity tests will be performed at each temperature. This test consists of measuring the complex modulus at a fixed frequency for an increasing range of strains (or stresses) and determining the value of the strain at which the modulus is no longer constant (commences to decrease). If the modulus commences to decrease, then the test is not compliant at the chosen test condition.

6.3.2 Phase 2: testing for general model development

The test matrix for Phase 1 of the pilot study is summarised in Table 6.1. After Phase 1 of the pilot study, the test matrix will be expanded to include different asphalt mixes used in Queensland.

Table 6.1: Preliminary test matrix

			Phase I				Phase II (tentative)							
Asphalt mix			DG20 (DG20HM/13/981)				DG14		DG14		DG20		DG20	
Binder type			C600				EME2		A5S		C320		M1000	
Binder content (%)			4.7				tbc		tbc		tbc		tbc	
Target air voids (%)			5%				5%		5%		5%		5%	
Temperature	Strain Level	Rest Period (s)	Modulus	Fatigue	Modulus	Fatigue	Modulus	Fatigue	Modulus	Fatigue	Modulus	Fatigue		
10 °C	Low	0		6		6		6		6		6		
		1												
		5												
		10												
	Medium	0	5	6	5	6	5	6	5	6	5	6		
		1		6										
		5		3										
		10		3										
	High	0		6		6		6		6		6		
		1												
		5												
		10												
20 °C	Low	0		6		6		6		6		6		
		1												
		5												
		10												
	Medium	0	5	6	5	6	5	6	5	6	5	6		
		1												
		5												
		10												
	High	0		6		6		6		6		6		
		1												
		5												
		10												
30 °C	Low	0		6		6		6		6		6		
		1												
		5												
		10												
	Medium	0	5	6	5	6	5	6	5	6	5	6		
		1		6										
		5		3										
		10		3										
	High	0		6		6		6		6		6		
		1												
		5												

Asphalt mix			Phase I		Phase II (tentative)								
			DG20 (DG20HM/13/981)		DG14		DG14		DG20		DG20		
40 °C	Low	10											
		0		6		6		6		6		6	
		1											
		5											
	Medium	10											
		0	5	6	5	6	5	6	5	6	5	6	
		1											
		5											
	High	10											
		0		6		6		6		6		6	
		1											
		5											
			10										
			Sub-Total	96		72		72		72		72	
			Total	384									

REFERENCES

- Adolf, M 2010, User Manual of PCASE 2.09, US Army Corps of Engineers, Vicksburg MS, USA.
- Al-Khaheeb, G, Stuart, K, Mogawer, W & Gibson, N 2008, 'Fatigue performance: asphalt binders versus mixtures versus full-scale pavements', *Canadian Journal of Transportation*, vol. 2, no. 1, pp. 21.
- Artamendi, I, Allen, B & Phillips, P 2009, 'Influence of temperature and aging on laboratory fatigue performance of asphalt mixtures', in Loizos, A, Partl, MN, Scarpas, T & Al-Qadi, IL (eds), *Advanced testing and characterisation of bituminous materials*, CRC Press, Boca Raton, Florida, USA, chapter 19.
- Asphalt Institute 1982, *Research and development of the Asphalt Institute's thickness design manual (MS-1) ninth edition*, research report no. RR-82-2, Asphalt Institute, College Park, Maryland, USA.
- Asphalt Research Program 1994, *Fatigue response of asphalt-aggregate mixes*, report no. SHRP-A-404, Strategic Highway Research Program (SHRP), Washington, DC, USA.
- Austrroads 2006b, *Fatigue Life of Compacted Bituminous Mixtures Subject to Repeated Flexural Bending*, Austrroads test method AG:PT/T233.
- Austrroads 2006a, *Deformation Resistance of Asphalt Mixtures by the Wheel Tracking Test*, Austrroads Test Method AG:PT/T231.
- Austrroads 2008 *Technical basis of Austrroads pavement design guide*, AP-T98/08 Austrroads, Sydney, NSW
- Austrroads 2012, *Guide to pavement technology. part 2: pavement structural design*, 3rd edn, Austrroads Sydney, NSW.
- Austrroads 2013, Improved Design Procedures for Asphalt Pavements: Pavement temperature and load frequency estimation AP-T248-13, Austrroads Sydney.
- Bazant, Z & Planas, J 1997, *Fracture and size effect in concrete and other quasi-brittle materials*, CRC Press, Boca Raton, Florida, USA.
- Bazin, P & Saunier, J 1967, 'Deformability, fatigue and healing properties of asphalt mixes', *Proceedings: second international conference on the structural design of asphalt pavements*, Ann Arbor, Michigan, International Society for Asphalt Pavements, Lino Lakes, MN, USA, pp. 553-69.
- Bhasin, A, Palvadi, S & Little, DN 2011, 'Influence of aging and temperature on intrinsic healing of asphalt binders', *Transportation Research Record*, no. 2207, pp. 70-8.
- Bhattacharjee, S & Mallick, RB 2012, Effect of temperature on fatigue performance of hot mix asphalt tested under model mobile load simulator, *International Journal of Pavement Engineering*, vol. 13, no. 2, pp. 166–80.
- Breakah, TM 2009, 'Stochastic finite element analysis of moisture damage in hot mix asphalt', Ph.D. dissertation, Department of Civil Engineering, Iowa State University.
- Bommavaram, RR, Bhasin, A & Little, DN 2009, 'Determining intrinsic healing properties of asphalt binders: role of dynamic shear rheometer', *Transportation Research Record*, no. 2126, pp. 47-54.
- Bonnaure, FP, Huibers, AHJJ & Boonders, A 1982, 'A laboratory investigation of the influence of rest periods on fatigue characteristics of bituminous mixes', *Journal of the Association of Asphalt Paving Technologists*, vol. 51, pp. 104-28.
- California Department of Transportation 2012, 'CalMe v1.05-20120224 help file', Caltrans, Los Angeles, USA.
- Campbell, FC (ed) 2008, *Fatigue elements of metallurgy and engineering alloys*, ASM International, Materials Park, OH, USA.
- Carpenter, SH, Ghuzlan, KA, Shen, S 2003, 'Fatigue endurance limit for highway and airport pavements', *Transportation Research Record*, Volume 1832, pp. 131-38.
- CROW, 2010, *Publicatie 285: Asfalt in weg- en Waterbouw* (in Dutch), CROW Ede.

- Daniel, JS, Bisirri, W & Kim, YR, 2004, 'Fatigue evaluation of asphalt mixtures using dissipated energy and viscoelastic continuum damage approaches', *Association of Asphalt Paving Technologists Technical Sessions, 2004, Baton Rouge, LA, USA*, Association of Asphalt Paving Technologists MN USA, 29pp.
- de la Roche, C, Odeon, H, Simoncelli, JP & Spornol, A 1994, 'Study of the fatigue of asphalt mixes using the circular test track of the Laboratoire Central des Ponts et Chaussées in Nantes, France', *Transportation Research Record*, no. 1436, pp. 17-27.
- Denneman, E 2013, 'Review of AG/PT-233 fatigue test protocol and its link to structural pavement design', *AAPA International flexible pavements conference, 15th, 2013, Brisbane, Queensland, Australia*, Australian Asphalt Pavement Association (AAPA), Toowong, QLD, 11 pp.
- El-Basyouny, M & Jeong, MG 2009, 'Effective temperature for analysis of permanent deformation and fatigue distress on asphalt mixtures', *Transportation Research Record*, no. 2127, pp. 155-63.
- EN 12697-24-2012, Bituminous mixtures: test methods for hot mix asphalt: part 24: Resistance to fatigue.
- EN 12697-26-2012, Bituminous mixtures: test methods for hot mix asphalt: part 26: Stiffness
- Epps, J 1968, 'Influence of mixture variables on the flexural fatigue and tensile properties of asphalt concrete', PhD thesis, University of California, Berkeley, USA.
- European Committee for Standardisation (CEN) 2012, *Bituminous mixtures: test methods for hot mix asphalt: part 24: resistance to fatigue*, EN 12697-24-2012, CEN, Brussels, Belgium.
- Federal Highway Administration 2001, *Microdamage healing in asphalt and asphalt concrete: volume I: microdamage and microdamage healing, project summary report*, FHWA-RD-98-141, FHWA, McLean, Virginia, USA.
- Federal Highway Administration 2013, *Tech brief: asphalt mixture performance tester (AMPT)*, FHWA-HIF-13-005, FHWA, Washington, DC, USA.
- Foley, G, Sharp, K, Baburamani, PS, Johnson-Clarke, J & Fossey, D 1998, 'A pilot study of the fatigue performance of two asphalt mixes under field and laboratory conditions', APRG 98/01, ARRB Transport Research, Vermont South, Vic.
- Ghuzlan, K. 2001, 'Fatigue damage analysis in asphalt concrete mixtures based upon dissipated energy concepts', Ph.D. dissertation, University of Illinois at Urbana-Champaign.
- Gerritsen, A & Koole, R 1987, 'Seven years' experience with the structural aspects of the Shell Pavement Design Manual', *Proceedings of the sixth international conference on structural design of asphalt pavements: volume 1*, University of Michigan, Ann Arbor, Michigan, USA, pp. 94-106.
- Gibson, N, Qi, X, Shenoy, A, Al-Khateeb, G, Kutay, E, Andriescu, A, Stuart, K, Youtcheff, J & Harman, T 2012, *Performance testing for superpave and structural validation*, report no. FHWA-HRT-11-045, Federal Highway Administration, McLean, Virginia, USA.
- Griffin, J 2013, 'Asphalt fatigue testing', contract report, ARRB Group Vermont South, Vic.
- Jameson, G 1999, 'An assessment of the need to incorporate shift factors for predicting the fatigue life of asphalt', APRG 99/43 (RE), ARRB Transport Research, Vermont South, Vic.
- Kim, YR, Whitmoyer, SL & Little, DN 1994, 'Healing in asphalt concrete pavements: is it real?' *Transportation Research Record*, no. 1454, pp. 89-96.
- Laboratoire Central des Ponts et Chaussées 1997, *French design manual for pavement structures*, LCPC, Paris, France.
- LCPC-Setra 1998, Réseau routier national, Catalogue des structures types de chaussées de calcul, LCPC-Setra, Hypotheses et données de calcul (in French language).
- Mateos, A, Ayuso, J & Jauregui, B 2011, 'Shift factors for asphalt fatigue from full-scale testing', *Transportation Research Record*, no. 2225, pp. 128-36.
- Mateos, A, Ayuso, J, Cadavid, B, & Marron, J 2012, 'Lessons learned from the application of the CalME asphalt fatigue model to experimental data from CEDEX test track', in Jones, D, Harvey, J, Mateos, A & Al-Qadi, IL (eds), *Advances in pavement design through full scale accelerated pavement testing*, CRC Press, Boca Raton, Florida, USA, pp. 483-92.

- Matsuno, S & Nishizawa T 1992, 'Mechanism of longitudinal surface cracking in asphalt pavement', *International conference on asphalt pavements, 7th, 1992, Nottingham, UK*, International Society for Asphalt Pavements, Austin, Texas, USA, pp. 277-91.
- Matthews, JM, Monismith, CL & Craus, J 1993, 'Investigation of laboratory fatigue testing procedures for asphalt aggregate mixtures', *Journal of Transportation Engineering*, vol. 119, no. 4, pp. 634–54.
- Molenaar, AAA 1984, 'Fatigue and reflection cracking due to traffic loads', *Proceedings of the Association of Asphalt Paving Technologists*, vol. 53, pp. 440-74 .
- Monismith, C, Epps, J, Kasianchuk, D & McLean, D 1970, 'Asphalt mixture behaviour in repeated flexure', report no. TE 70-5, University of California, Berkeley, USA.
- National Cooperative Highway Research Program 2004, *Guide for mechanistic-empirical design of new and rehabilitated pavement structures*, NCHRP 1-37A, Transportation Research Board, Washington, DC, USA.
- NFP 98-086–2011, Road pavement structural design – Application to new pavements (French language).
- Nunn, M 1997, 'Long-life flexible roads', *International conference on asphalt pavements, 8th, 1997, Seattle, Washington*, University of Washington, Seattle, USA, vol. 1, pp. 3-16.
- Palvadi, S & Bhasin A 2012, 'Method to quantify healing in asphalt composites using continuum damage approach', *Transportation Research Record*, no. 2296, pp. 86-96.
- Pell, P & Cooper, K 1975, 'The effect of testing and mix variables on the fatigue performance of bituminous materials', *Journal of the Association of Asphalt Pavement Technologists*, vol. 44, pp. 1-37.
- Pell, PS, McCarthy, PF & Gardner, RR 1961, 'Fatigue of bitumen and bituminous mixes', *International Journal of Mechanical Sciences*, vol. 3, no. 4, pp. 247–8.
- Pellinen, T, Christensen, D, Rowe, G & Sharrock, M 2004, 'Fatigue-transfer functions: how do they compare?' *Transportation Research Record*, no. 1896, pp. 77-87.
- Pérez-Jiménez, F, Valdes, G, Miro, R, Martinez, A & Botella, R 2010, 'Fénix test: development of a new test procedure for evaluating cracking resistance in bituminous mixtures', *Transportation Research Record*, no. 2181, pp. 36–43.
- Phillips, MC 1998, 'Multi-Step models for fatigue and healing, and binder properties involved in healing', *Proceedings of Eurobitume workshop on performance related properties for bituminous binders*, Luxembourg, paper no. 115.
- Pickett, D, Saylak, D, Lytton, R, Conger, M, Newcomb, D & Schapery, RA 1978, *Extension and replacement of asphalt cement with sulphur*, FHWA-RD-78-95, Federal Highway Administration, Washington, DC, USA.
- Porter, BW & Kennedy, TW 1975, *Comparison of fatigue test methods for asphalt materials*, research report 183-4, Texas Highway Department, University of Texas, Austin, TX, USA.
- Prowell, BD, Brown, RE, Anderson, RM, Daniel, JS, Quintus, HV, Shen, S, Carpenter, SH, Bhattacharjee, S & Maghsoodloo, S, 2010, *Validating the fatigue endurance limit for hot mix asphalt*, NCHRP Report 646, National Cooperative Highway Research Program, DC, USA.
- Qiu J, Molenaar AAA, Van de Ven, MFC & Wu, S 2012b, 'Development of autonomous setup for evaluating self-healing capability of asphalt mixtures', *Transportation Research Record*, no. 2296, pp. 15-23.
- Qiu, J, Van de Ven, MFC, Schlangen, E, Wu, S & Molenaar, AAA 2012a, 'Cracking and healing modelling of asphalt mixtures', *Rilem international conference on cracking in pavements, 7th, 2012, Delft, Netherlands*, Springer, Heidelberg, Germany, pp. 1135-44.
- Raithby, KD & Sterling, AB 1970, 'The effect of rest periods on the fatigue performance of hot-rolled asphalt under repeated loading', *Journal of Association of Asphalt Paving Technologist*, vol. 39, pp. 134-52.
- Raithby, KD & Sterling, AB 1972, *Some effects of loading history on the fatigue performance of rolled asphalt*, TRRL laboratory report LR496, Transport and Road Research Laboratory, Crowthorne, UK.
- Robertus, C 1993, 'Shell multigrade bitumen: a binder for high stability asphalts', *Eurobitume Congress, 5th, Stockholm, Sweden*, Congress Secretariat, Stockholm, Sweden, vol. 1A, pp. 161-5.

- Rowe, GW 1993, 'Performance of asphalt mixtures in the trapezoidal fatigue test', *Journal of the Association of Asphalt Paving Technologists*, vol. 62, pp. 344-84.
- Shell International Petroleum Company 1978, *Shell pavement design manual: asphalt pavements and overlays for road traffic*, Shell International Petroleum, London, UK.
- Shen, S & Carpenter, SH 2007, *Dissipated energy concepts for HMA performance: fatigue and healing*, Advanced Transportation Research and Engineering Laboratory, University of Illinois at Urbana-Champaign, Urbana, IL, USA.
- Smith, B & Hesp, SAM 2000, 'Crack pinning in asphalt mastic and concrete: effect of rest periods and polymer modifiers on the fatigue life', *Eurasphalt and Eurobitume Congress, 2nd, 2000, Barcelona, Spain*, Foundation Eurasphalt, Breukelen, The Netherlands, pp. 539-46 (book 2).
- Souliman, M 2012, 'Integrated predictive model for healing and fatigue endurance limit for asphalt concrete', PhD thesis, Arizona State University, USA.
- Steyn, W 2012, *Significant findings from full scale accelerated pavement testing*, NCHRP synthesis 433, Transportation Research Board, Washington, DC, USA.
- Stimilli, A, Hintz, C, Li, Z, Velasquez, R & Bahia, HU 2012, 'Effect of healing on fatigue law parameters of asphalt binders', *Transportation Research Record*, no. 2293, pp. 96-105.
- Stuart, K, Mogawer, W & Romero, P 2002, *Validation of the Superpave asphalt binder fatigue cracking parameter using an accelerated loading facility*, FHWA-RD-01-093, Federal Highway Administration, McLean, Virginia, USA.
- Tangella, SCSR, Craus, J, Deacon, JA & Monismith, CL 1990, *Summary report on fatigue response of asphalt mixtures*, report SHRP-A/IR-90-011, Strategic Highway Research Program, Washington, DC, USA.
- Tayebali, A, Deacon, J, Coplantz, J, Harvey, J & Monismith, C 1992, 'Fatigue response of asphalt aggregate mixes: part I: test method selection', SHRP-A-404, Strategic Highway Research Program, Washington, DC, USA.
- Tsai, BW 2001, *High temperature fatigue and fatigue damage process of aggregate-asphalt mixes*, PhD thesis, University of California, Berkeley, USA.
- Uchida, K, Kurokawa, T, Himeno, K & Nishizawa, T 2002, 'Healing characteristics of asphalt mixture under high temperature conditions', *International conference on asphalt pavements, 9th, 2002, Copenhagen, Denmark*, The Danish Road Directorate, Ministry of Transport, Denmark, pp. 1:5-5.
- Uhlmeier, JS, Willoughby, K, Pierce, LM & Mahoney, JP 2000, 'Top-down cracking in Washington state asphalt concrete wearing courses', *Transportation Research Record*, no. 1730, pp. 110-6.
- Ullidtz, P, Harvey, J, Tsai, B-W & Monismith, C 2006a, *Calibration of CalME models using WesTrack performance data*, research report no. UCPRC-RR2006-14, University of California Pavement Research Center, Berkeley, CA, USA.
- Ullidtz, P, Harvey, J, Tsai, B-W & Monismith, C 2006b, *Calibration of incremental-recursive flexible damage models in CalME using HVS experiments*, research report no. UCPRC-RR-2005-06, University of California Pavement Research Center, Berkeley, CA, USA.
- Ullidtz, P, Harvey, J, Basheer, I, Jones, D, Wu, R, Lea, J & Lu, Q 2010, 'CalME: a new mechanistic-empirical design program for flexible pavement rehabilitation', *Proceedings of the Transportation Research Board 2010 annual meeting*, Washington DC, USA, 18 pp.
- Van Dijk, W & Visser, W 1977, 'The energy approach to fatigue for pavement design', *Asphalt Paving Technology*, vol. 46, pp. 1-39.
- Verstraeten, J, Veverka, V & Francken 1982, 'Rational and practical designs of asphalt pavements to avoid cracking and rutting', *Proceedings of the fifth international conference on structural design of asphalt pavements*, vol. 1, pp. 45-58.
- Witczak, M, Mamlouk, M, Souliman, M & Zeiada, W 2013, *Laboratory validation of endurance limit for asphalt pavements*, NCHRP report 762, Transportation Research Board, Washington, DC, USA.

Zhou, F, Fernando, E & Scullion, T 2008, *A review of performance models and test procedures with recommendations for use in the Texas M-E design program*, technical report FHWA/TX-08/0-5798-1, Texas Department of Transportation, Austin, Texas, USA.